

**Neurogenesis, Growth and Integration of Local Nerve Cells in a
Multisensory Compartment in the Central Brain of Mature Insects.
A Light and Electron Microscopic Study of the Mushroom Bodies
in the Cricket *Gryllus bimaculatus***

Dissertation

zur Erlangung des Doktorgrades
der Mathematisch-Naturwissenschaftlichen Fakultäten
der Georg-August-Universität zu Göttingen

vorgelegt von
Ashraf Mohamed Ali Mashaly
aus Kairo / Ägypten

Göttingen 2004

D7

Referent: Prof. Dr. Friedrich-Wilhelm Schürmann

Korreferent: Prof. Dr. Reinhold Hustert

Tag der mündlichen Prüfung: 04.11.2004

Contents

Abbreviations

1. Introduction	1
2. Material and Methods	9
2.1. Animals	9
2.2. Preparation procedures for fixation	9
2.3. Fixations	9
2.4. Light microscopy	10
2.4.1. Phalloidin f-actin staining	10
2.4.2. Propidium iodide staining	10
2.4.3. Immunocytochemical methods	10
2.4.3.1. Antibodies	10
2.4.3.1.1. Anti-phospho histone H3	11
2.4.3.1.2. Anti- α -tubulin	11
2.4.3.1.3. Anti-synapsin I	11
2.4.3.1.4. Anti-GABA	11
2.4.3.1.5. Anti-5-HT	11
2.4.3.2. Secondary fluorescent antibodies	12
2.4.4. Serial vibratome sectioning	12
2.5. Conventional electron microscopy	12
2.5.1. Sectioning	12
2.5.2. Contrasting	13
2.5.2.1. Uranyl acetate	13
2.5.2.2. Lead citrate	13
2.6. Microscopy	13
2.6.1. Light microscopy	13
2.6.2. Conventional electron microscopy	14
2.7. Digital image processing	14
2.8. Procedures for quantitative study	16
2.8.1. Differences in fibre profiles	16
2.8.2. Determination of tubules in fibre profiles	17
2.8.3. Counting of synapses and mitochondria	17

3. Results	19
3.1. The structure of the MBs: compartments, cell types, synaptic connectivity	19
3.2. Sprouting KCs in the MBs	22
3.2.1. F-actin in MBs	22
3.2.2. Pericaryal layer	23
3.2.3. Calyx	24
3.2.4. Stalk	25
3.2.5. Lobes	25
3.3. Tubulin in the MBs	26
3.3.1. Pericaryal layer	26
3.3.2. Calyx	26
3.3.3. Stalk	27
3.3.4. Lobes	27
3.4. Synaptic areas related to MB compartments and neurones	27
3.4.1. Synapsin distribution	28
3.4.1.1. Calyces	28
3.4.1.2. Stalk and lobes	29
3.4.2. Extrinsic MB GABA-fibres	29
3.4.2.1. Calyces	30
3.4.2.2. Stalk and lobes	30
3.4.3. Extrinsic 5-HT neurones	30
3.4.3.1. Calyces	31
3.4.3.2. Stalk and lobes	31
3.5. Glial cells in the MBs	31
3.6. Ultrastructure of MBs	32
3.6.1. Pericaryal cortex	33
3.6.2. Calyx	34
3.6.3. Stalk and lobes	35
3.6.4. KC fibre classes: profiles associated with organelles and synaptic sites	36
3.7. Degeneration in the MBs	39

4. Discussion	40
4.1. Synaptic connectivity in the MBs	41
4.2. The addition of newly formed KCs into the MBs of mature brains: morphological characters	44
4.2.1. The sprouting KC cluster	44
4.2.2. Actin in developing KCs	45
4.2.3. Tubulin expression	47
4.3. Synaptic complexes in MB compartments related to KC neurones of different age	49
4.3.1. Synapsin distribution	49
4.3.2. Extrinsic fibres in relation to growing KCs	50
4.4. Growing KCs and ultrastructural characters	51
4.5. Glial cells, growth and degeneration processes	52
5. Summary	56
6. References	59
7. Appendix of figures	77

Acknowledgements

Curriculum Vitae

Abbreviations

5-HT	5-hydroxytryptamine (indolamine serotonin)
a	anterior
α	alpha lobe of mushroom body
Al	alpha lobe of mushroom body
β	beta lobe of mushroom body
BL	beta lobe of mushroom body
Brdu	5-bromo-2-deoxyuridine
BSA	bovine serum albumin
CA	anterior calyx
Cb	central body
CB	central bridge
CP	posterior calyx
Cy2	green fluorochrome, carbocyanine
Cy3	red fluorochrome, indocarbocyanine
deg	degeneration
d	dorsal
eF	extrinsic fibre
ER	endoplasmic reticulum
EX	extracellular processes
F-actin	filamentous actin
G-actin	globular actin
GA	glutaraldehyde
GABA	gamma amino buteric acid
Gc	glial cell
iAct	inner antenno-cerebral tract
KC	Kenyon cell
LSM	laser scan microscopy
MB	mushroom body
N	nucleus
NGS	normal goat serum
P	stalk
p	posterior

PBS	phosphate buffered saline
PCD	programmed cell death
PFA	paraformaldehyde
PL	pericaryal layer
PN	projection neuron
SKC	sprouting Kenyon cells
TEM	transmission electron microscopy
v	ventral

1. Introduction

Mature brains have been considered widely to be completely unable to produce new neurones during all phases of adult life, and older reports on the neurogenesis of neurones in functional networks have been either ignored or taken as rare exceptions until recently (Ito and Hotta, 1992; Fahrbach et al., 1995; Malun, 1998; Farris et al., 1999). The making of neurones and neuronal networks has therefore been studied in premature vertebrate and invertebrate animals, in order to find general principles for neuron augmentation, fibre growth, path finding and synaptogenesis (for a review, see Cayre et al., 2002). In the last two decades compelling evidence has been found that neural stem cells do belong to the normal equipment in adult brains of many vertebrate and invertebrate species, adding newly formed neurones throughout life (Cayre et al., 2002).

Secondary neurogenesis in mature brains is generally not randomly distributed or installed in many brain regions, but confined to some areas and neuron types (Altman and Das, 1965; Cayre et al., 1994; Eriksson et al., 1998; Harzsch et al., 1999). Addition or replacement of neurones into a functional network, which organizes electrical activity to properly exert behaviours to cope with the environment of an animal, is one basis for neuroplasticity. It is also seen in fibre growth, synaptic modulation and changes in molecular inventory of mature, fully developed neurones that are not able to produce further cell divisions (Cayre et al., 1996; Scotto Lomassese et al., 2000). Neuroplasticity is understood as interdependent structural and functional dynamics of neurones in developmental and mature stages of the animal's life (Tucker et al., 2004). A number of factors ranging from complex environmental conditions to single molecules are involved in the expression of neuroplasticity (Kemperman and Gage, 1999; Van Praag et al., 1999; Meinertzhagen, 2001).

Interestingly, morphological changes, including gross alterations or the refinement of specialized structures in neurones have been repeatedly reported in peripheral and central brain areas with neurones and synaptic circuits specifically

serving for integration of sensory inputs (Scotto Lomassese et al., 2003) and/or in systems considered to be specialized in learning and memory (Gould et al., 1999; Harzsch et al., 1999; Sandeman and Sandeman, 2000; Schmidt, 2001). For example, as early as in 1977 Kaplan and Hinds described the development of newly emerged cells after mitosis in the olfactory bulb and dentate gyrus of the rat brain by autoradiographic and electron microscopic studies, proving a hypothesis of Altman (1962) raised from studies of other areas in the rodent brain. The forming of newly emerging neurones throughout adult life has so far been demonstrated for a considerable number of examples in the brains of fish, reptiles and birds, often in areas for visual integration (Johns and Easter, 1977; Raymond and Easter, 1983; Chetverukhin and Polenov, 1993).

Adult neurogenesis and cell proliferation exists in invertebrates too, comparatively well investigated in arthropod brains (Cayre et al., 2002). Neurogenesis throughout adult life has been shown for decapod crustaceans (Harzsch et al., 1999; Sandeman and Sandeman, 2000). Prominent cell proliferation forming local neurones is located in the brain olfactory and accessory lobes, neuropil centres for sensory input from the antennules. The amount of cell divisions quantified from BRDU-labelling is correlated with environmental conditions, which were experimentally impoverished or enriched and followed by negative or positive effects, respectively (Sandeman and Sandeman, 2000).

Mitotic activity in nervous systems of mature insects has been pointed out by the previously often overlooked detailed studies of Johansson (1957) and Panov (1960) using classical histological methods (for a review, see Pipa, 1973), later on confirmed and intensely investigated by Cayre et al. (1994; 1996), especially in crickets. Panov found cell divisions in adult orthopteroid insects. Grasshoppers, crickets and cockroaches are hemimetabolous insects which develop the brain and its compartments in a sequential manner, so that in the late instars the complete architecture of the brain neuropil is found before final imaginal hatching.

Post larval and pupal growth is found as well in holometabolous insect nervous systems, undergoing complete metamorphosis. This has been detected for

the mushroom bodies (MBs) of beetles (Rossbach, 1962). A remarkable positive allometric increase of MBs differing from other brain regions has been revealed by volumetric determinations and cell counts in young imagines of the rove beetle *Aleochoa* during the first twenty days after eclosion (Bieber and Fuldner, 1979). The dramatic augmentation of the neuropil volume – more than 71 % - is based on the proliferation of persisting neuroblasts, giving birth to local interneurons, the so-called Kenyon cells (KCs). The number of KCs increases from 1632 (day 1 of imago) to 2797 (day 20).

Persistence of MB neuroblasts and neurogenesis in mature imagines of holometabolous insects is considered to be rare, because it was not found in a number of well investigated other forms, among them bees and the fruit fly *Drosophila*. In hemimetabolous insect brains, proliferation of neurones in adults may be more widespread (Cayre et al., 2002), but the scarcity of studies in the large kingdom of insects does not allow us to put forward a firm generalizing statement. Especially findings that some species classified as closely related from systematics show differences with respect to imaginal neurogenesis.

In hemimetabolous insects of the groups of Gryllidae, Mantidae, and Heteroptera (Cayre et al. 1994; 1996), neuroblasts produce neurones during imaginal life either in early life, e.g. the cockroach *Diploptera punctata* for 8 days (Gu et al., 1999), or continuously throughout the whole life, as shown for the house cricket *Acheta domesticus*. In this species, the addition of newly generated KCs in adults has been estimated to make up 20% of these local intrinsic MB cells in 50 day old imagines (Malaterre et al., 2002) in a total of about 50000 KCs in one MB (Schürmann, 1987). Neuroblasts may not only produce neurones but also glial cells in MBs of imagines as shown for the grasshopper *Locusta migratoria* and the cockroach *Periplaneta americana* (see Cayre et al., 1996). Glial cells were discriminated from neurones by cell type specific markers.

Interestingly, in all cases intensely studied, massive proliferation of neurones after larval hatching in adults is located in the MBs (corpora pedunculata), and the neurogenesis from neuroblasts via ganglion mother cells is here confined to a special

class of neuron types, the globule cells, now termed KCs (see Kenyon, 1896; Strausfeld, 1976). These unique local interneurons have been documented in numerous studies on different insect orders since the detection of the MBs in the protocerebral part of the bee brain by Dujardin (1850). A brief outline of the common architecture the MB structures in insects is therefore given here (for comparison of insect groups, see reviews by Schürmann, 1987; Strausfeld et al., 1998; Farris and Sinakevitch, 2003). Details of the MB structure, including new findings in the species *Gryllus bimaculatus* investigated in this study are given below (see results section). MBs comprise two symmetrically arranged neuropils of characteristic shape in the protocerebral brain hemispheres. Each unilateral corpus pedunculatum consists of a peripheral layer of KC somata with scarcely developed pericaryal cytoplasm (neurons gathered in a cup shaped cortex). These intrinsic local interneurons form a neuropil typically subdivided in well-defined compartments: the proximal calyx, followed by a columnar stalk (peduncle), which distally bifurcates into columnar α - and β -lobes (now often termed vertical and medial lobes). These compartments are further sub structured into subcompartments in a species-specific manner. Form and position of MBs varies in the taxonomic groups. The most accentuated subdivisions of MBs seen in delicately ordered strata of the lobes are established in the voluminous MBs of cockroaches and bees (Strausfeld and Li, 1999). A more simple organization of the MB neuropil of crickets has been documented by use of Golgi techniques (Schürmann, 1973; 1987), and later confirmed by experimental marking of MB cell types (Malaterre et al., 2002; Frambach and Schürmann, 2004). The form and positioning of cricket MBs resembles the tiny MBs in *Drosophila* (Yasuyama et al., 2002). The shape of MBs, though differing in the diverse insect forms, is governed by the orderly arranged KC fibres, and apparently not very much influenced by a smaller number of relay neurons of different types, the extrinsic neurons with cell bodies outside the MBs, connecting them with other brain areas (for reviews, see Schürmann, 1987; Homberg, 1994; Strausfeld et al., 1998). KCs, forming 3 and more types, display distinct fibre bundles with more or less parallel axonal fibres to be traced from the proximal calyces through the stalk to the distal tips of the lobes. The largest number of KCs has been reported for the cockroach *Periplaneta* (a total of about 400000) by Neder (1959), similar to worker honeybees (a total of 340000; Witthöft, 1967), both forms endorsed with voluminous MBs. Gross outlines of

synaptic circuitry in MBs have been given for the cricket MBs and found similarly established for other insect forms systematically not closely related by electron microscopy (Schürmann, 1974). These concern main sites of input, crosstalk and output between extrinsic and intrinsic fibres. Thus the known structural and ultrastructural characters, intensely investigated in many details in cricket MBs, are a solid basis for the present study. Size and the simple strong structural geometry ease a systematic study at all levels of the cricket MBs by light and electron microscopy.

A detailed knowledge of the MB structure is the indispensable basis for understanding functional roles of MBs. These are briefly reported here. There is compelling evidence for a special higher role of the MBs in the hierarchy of neuropils in multimodal sensory integration. This was earlier shown for the cricket *Acheta* by intracellular recordings and combined iontophoretic staining (Schildberger, 1981; 1983; 1984; for a review see Schürmann, 1987) and for bees (Erber et al., 1987).

The prominent chemosensory input to MBs has stimulated a search for modes of information processing and given insights into general mechanisms of filtering olfactory signals relevant to executing selected behaviours (Stopfer et al., 2003). Space, time and cell specific activation of input to the calyces of *Drosophila* MBs has been recently visualised (Fiala et al., 2002) in the boutons of olfactory projection neurones (Yasuyama et al., 2002). Furthermore, MBs are useful favourite model neuropils which are crucially involved in different types of learning and memory (Heisenberg et al., 1995; Zars et al., 2000). The relevance of MBs in organizing and triggering behaviours was first proposed by ablation and stimulation studies in bees, ants, cockroaches and crickets (Neder, 1959; Huber, 1960; Vowles, 1964; for a review see Erber et al., 1987). MBs of fruit flies are now intensely studied neuropils of high interest, based on genetic dissection experiments in the context of behavioural performances (Heisenberg, 1998; Zars et al., 2000).

As mentioned above, MBs of crickets are the only ones provided with massive adult neurogenesis of a single cell class, in this respect different from the other model animals. Due to this feature, together with a relative structural simplicity, cricket MBs appear especially well suited to study the sequential morphological steps leading to

the integration of added KCs into a functional network. These events comprise mitosis, forming and outgrowth of fibres, path and space finding, establishment of dendritic branches and of collaterals, synapse formation and maturation, transmitter equipment and other molecular dynamic changes. These dynamic structural changes have been studied in other systems of vertebrates and invertebrates as well, including *in vivo* and *in vitro* approaches (cell and tissue culture) (Altman and Das, 1965; Johns and Easter, 1977; Kaplan and Hinds, 1977; Raymond and Easter, 1983; Chetverukhin and Polenov, 1993; Eriksson et al., 1998; Harzsch et al., 1999), also testing growth inductive factors (Scotto Lomassese et al., 2002; Farris and Sinakevitch, 2003). These studies should therefore lead to comparisons with the MBs, a system which allows access to hundreds of identifiable local neurones condensed in small neuropil volume, developing to their ultimate mature form under constant completely natural conditions, not experimentally triggered by selected factors.

The studies presented here using adult crickets of the species *Gryllus bimaculatus* are devoted to morphological aspects of newly added and sprouting KCs which are meant to find their synaptic partners in the functional MB system. The MB system is already present and obligatory functional in larval stages. In contrast to KCs, the extrinsic MB relay neurones are already all existent in the late larvae. They cannot be added by cell divisions of persisting stem cells in adult brains, but must underlie structural plasticity in adult individuals when synapsing with newly added KCs in the neuropil compartments. Moreover, structural association of developing neurones with glial cells could be important, as these non-neural cells might be used for fibre path finding, regeneration and degeneration in space delivering processes (Rakic, 1971; 1972; Boyan et al., 1995; Xiong and Montell, 1995).

Cellular contents, structural design and synaptic circuitry of MBs have been given for *Acheta domesticus* (Schürmann, 1971; 1972; 1973; 1974), but not for the closely related species *Gryllus bimaculatus*, except for some preliminary studies (Mashaly et al., 2003; Frambach et al., 2004). Synaptic equipment requires electron microscopy, because high-resolution light microscopic visualisation of synaptic sites by highly specific markers is not sufficient, and is often misleading for reliable proof of

synapses in the dense fibre meshwork of neuropils (Yasuyama et al., 2003). Therefore, a description of synaptic endorsement in *Gryllus bimaculatus* is first given, including newly detected details on synaptic connectivity in some MB compartments. The site, amount and formation of new KCs, the growth and invasion of their fibres into the calyx, thereafter into the stalk up to the distal ends of the lobes is presented. This raises the question as to whether the placement of new fibres in space is achieved in an orderly manner throughout life, or whether age specific alterations lead to disorder or volume changes. Therefore, individuals of different ages were investigated. Sequential addition of thousands of new fibres could cause space problems, if free extracellular space were not be reserved in adult MBs or compensatory mechanisms of decline of neuropil (degeneration) did not exist. Both possibilities were therefore examined.

Growing fibres form at their tips growth cones subjected to continuous molecular and structural alterations (Knobel et al., 1999), such as elongation at axonal endings and at collateral branches. This was inspected in the calyces and in parts of the stalks and lobes. Growth and synapse formation, elements of neuronal plasticity, require the formation and temporal use of a wide range of molecules present and organisation of these delicate and tiny structures (for review, see Harris, 1999; Matus, 2000; Huntley et al., 2002). Among these molecules, which can be visualized by specific markers for light and electron microscopy, f-actin is crucial for cell growth and pre- and postsynaptic dynamics (Colicos et al., 2001; Huntley et al., 2002). Microtubules are organelles indispensable for fibre elongation and axonal transport. Their distribution in MBs was investigated by immunocytochemistry in order to find differences in developing and mature KC fibres. Synapsin proteins are associated with synaptic vesicles, forming pools in presynaptic boutons (Huttner et al., 1983; De Camilli et al., 1993). Synapsins also interact with actin, microtubules and spectrin (De Camilli et al., 1990; Greengrad et al., 1993), and anti-synapsin antibodies were therefore used in this study to explore synaptic sites in neuropil areas and neurones stained by transmitter immunocytochemistry. Markers for these molecules and for mitotic events were employed in this study to describe their emergence and distribution in the MBs. Conventional electron microscopy, still the only reliable technique to directly visualize and ensure the existence of synapses and

other membrane specializations, provided an insight into their occurrence in the equipment of developing fibres with organelles. A brief communication of parts of the study on the growing process of newly added KCs has been published (Mashaly et al., 2003).

2. Material and Methods

2.1. Animals

Male and female crickets of the species *Gryllus bimaculatus* De Geer reared in the institute's breeding colony were maintained under photoperiods (12h light / 12h dark cycle), at 27-30 °C and 55% relative humidity. Larval insects and of the adult stage aged 1 week, 2 weeks and two months were taken for light and electron microscopy. A total of 89 brains was used for light microscopic studies and 15 brains (age 7 days) for the electron microscopic study.

2.2. Preparation procedures for fixation

Crickets were first immobilised, generally by cooling at 4°C. The whole head was then separated from the body, pinned down dorsal side up in a wax dish. A window was opened between the compound eyes in the head capsule and the brain was immersed in fixative. Brains were subsequently carefully dissected from the head capsule and transferred immediately in cold, fresh fixative (10°C).

2.3. Fixations

For light microscopy, the fixative solutions were used according to the requirements of the staining experiments (see table 1).

Table 1	
F-actin, tubulin, synapsin, 5-HT	4% paraformaldehyde (PFA) in 0.1M phosphate buffer
Anti-phospho histone H3, propidium iodide	4% PFA in phosphate buffered saline (PBS)
GABA	1.5% glutaraldehyde (GA) in 0.1M phosphate buffer

For conventional electron microscopy, a primary fixative with 1% PFA and 2.5% GA in 0.1M phosphate buffer for 24h on ice, followed by osmication in 2% osmium tetroxide in 0.1M phosphate buffer for 1.5h was applied.

2.4. Light microscopy

2.4.1. Phalloidin f-actin staining

To localize f-actin, fluorescence coupled phalloidin (MOBITEC, Molecular Probes USA) was used (for staining procedures see Wulf et al., 1979; Rössler et al., 2002)

2.4.2. Propidium iodide staining

Propidium iodide has been widely used as a fluorescent stain for DNA in fixed cells (Sasaki et al., 1987). In the present study propidium iodide was employed to investigate the glia distribution in the cricket MBs (for staining procedures see Devaud et al., 2001).

2.4.3. Immunocytochemical methods

2.4.3.1. Antibodies

Primary antibody concentrations and manufactures are listed in table 2.

Primary anti-body	Dilution	Sources
Anti-phospho histone H3 (rabbit)	1:200	Upstate Biotechnology, USA
α -Tubulin (mouse)	1:1000	Sigma, Saint Louis, Missouri, USA
Anti-GABA (rabbit)	1:500, 1:1000	Incstar Cooperation, Stillwater, MN, USA
Anti-synapsin I (mouse)	1:1000	Buchner/ Hofbauer, Würzburg
Serotonin (5-HT, rabbit)	1:1000	Incstar, USA

2.4.3.1.1. Anti-phospho histone H3

Polyclonal serum raised in rabbit against phosphorylated histone H3 (for staining procedures see Harzsch et al., 1999) was used to stain the mitotic cells in the MB pericaryal layer. This antibody detects mitotic cells (Mahadevan et al., 1991; Chadee et al., 1995; Ajiro et al., 1996).

2.4.3.1.2. Anti- α -tubulin

The monoclonal antibody raised in mouse against acetylated tubulin was used to detect acetylated α -tubulin in the developing and mature KCs. The antibody has been used to detect acetylated α -tubulin in many organisms: protista, plants, invertebrates and vertebrates (LeDizet and Piperno, 1991).

2.4.3.1.3. Anti-synapsin I

The monoclonal antibody raised in mouse against *Drosophila* synapsin I (SYNORF1) (Klagges et al., 1996) was used to visualize presynaptic sites in the cricket MBs. Specificity of the antiserum was tested by Western blot analysis of syn gene product in transformed *Escherichia coli* strains, in the head homogenates of the fruit fly (Klagges et al., 1996) and in the spider *Cupiennius salei* (Fabian-Fine et al., 1999).

2.4.3.1.4. Anti-GABA

Monoclonal anti-GABA raised in rabbit against GABA coupled to BSA with glutaraldehyde was used for the localization of GABA in the cricket MBs (for procedures and specificity controls see Fabian-Fine et al., 1999).

2.4.3.1.5. Anti-5-HT

The polyclonal antibody raised in rabbit against serotonin conjugated to bovine serum albumin was used to localize the serotonin in the cricket MBs (for procedures and specificity controls see Strambi et al., 1989).

2.4.3.2. Secondary fluorescence antibodies

Secondary fluorescent antibodies are listed in table 3.

Secondary anti-body	Dilution	Sources
Cy3 goat anti rabbit	1:200	Rockland, Gilbertville, PA, USA
Cy3 anti-mouse	1:100	Jackson, Dianova, Hamburg
Cy2 anti-rabbit	1:100	Rockland, Gilbertville, PA, USA

2.4.4. Serial vibratome sectioning

After fixation brains were washed with PBS and embedded in 5% low melting point agarose. Embedding of the specimens was performed at 50°C and subsequently the agarose blocks were cooled to allow further gelling. After trimming and mounting, the blocks were sectioned into serial vibratome slices (thickness 30–60 µm) with vibratome (LEICA VT 1000 S) in frontal, horizontal and sagittal planes. The preparations were washed again with PBS and, after treatments according to the different experiments, mounted on glass slides for microscopy. For embedding medium PBS/ glycerin mixture (v:v/1:1) was used.

2.5. Conventional electron microscopy

The ultrastructure of cricket MBs was studied by conventional transmission electron microscopy (TEM) (for methods see Robinson et al., 1985) in order to compare results with immuno-light microscopy.

2.5.1. Sectioning

Whole brains were embedded in Araldite and the blocks were sectioned with ultramicrotome (Reichert Jung Ultracut E) into 0.5-1 µm semithin or 50-60 nm ultrathin sections.

Semithin sections were obtained with a glass knife. To recognise different brain regions, semithin sections were stained with toluidine blue for light microscopy inspection. Ultrathin sections were taken with a diamond knife.

2.5.2. Contrasting

2.5.2.1. Uranyl acetate

Block staining with uranyl acetate was performed during dehydration. The saturated solution of uranyl acetate in 70% ethanol was freshly prepared and applied for 30 min.

Alternatively, ultrathin sections were contrasted with aqueous solution of uranyl acetate for 1-2 min (Robinson et al., 1985).

2.5.2.2. Lead citrate

Ultrathin sections were contrasted with lead citrate according to Reynolds (1963) for 1-2 min. After staining, grids were washed several times with double-distilled water.

2.6. Microscopy

2.6.1. Light microscopy

Vibratome sections were examined with a fluorescence microscope (Axioskop, Zeiss) with the appropriate fluorescence optics: Zeiss plan Neofluar 10x/ 0,3; 20x/ 0.5; and 40x/ 0.75. Images were taken with a digital CCD camera (Diagnostic Instruments Inc., Spot 32), with a resolution of 1300*1035 pixel. The following filter combinations were used for fluorescence microscopy: for green fluorescence (excitation: BP 450-490 nm, beam splitter: FT 510 nm, emission: BP 515-565 nm) or for red fluorescence (excitation: BP 546/12, beam splitter: FT 580, emission: LP 590).

Double stained preparations were photographed separately for each fluorescence, and subsequently merged to a single image by UTHSCSA Image Tool software.

Detailed analysis of the fluorescent preparations was accomplished with a confocal microscope (LSM 510, Zeiss, objective Zeiss plan - Neofluar 40x/ 1.3 oil). Single optical sections as well as series of optical sections were taken from a vibratome section. The optical section thickness was in the range of 0.5 to 0.9 μm . An excitation wavelength of 543 nm was used for red fluorescence with a long pass filter 560, and an excitation wave length of 488 nm in connection with a band pass filter 505-550 was used for green fluorescence. Monochrome digital images were taken up in the 8-bit mode. During transformation of the monochrome raw images into colour images, the colour channels were selected according to the wavelength of the fluorescence colouring materials: texas-red, tetramethylrhodamine and Cy3 \rightarrow red channel, alexa 488 and Cy2 \rightarrow green channel.

2.6.2. Conventional electron microscopy

Ultrathin sections were photographed at primary magnifications ranging from 2,500-20,000 with TEM (Zeiss EM 10B or Zeiss CEM 902A) and analysed. Defined MB parts were photographed to obtain montages of selected areas used for measurements and counts. EM negative or positive were scanned (scanner Epson perfection 2450 photo) at high resolution (800 or 1200 dpi).

2.7. Digital image processing

Treatment of pictures and data evaluation for the conventional and confocal fluorescence microscopy and electron microscopy were made with the programs Adobe Photoshop 7.0.1, Corel Photopaint 8.0 and UTHSCSA Image Tool 2.0.

To improve subjective visual impression in the different images types, the contrast and brightness were raised. In addition the stretch function in UTHSCSA

Image Tool 2.0 program was used. This function spreads the brightness in the image linearly on the available range (with 8 bit grey images 0-255).

To optimise the contrast of a stack of laser microscope images, some special additional scripts (Dr. Gras, Göttingen) within the program environment of UTHSCSA Image Tool 2.0 were used. The following steps were carried out:

- 1- A set of images was exported from the LSM510 program to the UTHSCSA Image Tool 2.0 program (modified) and arranged in a sequential image stack.
- 2- The image stack was processed for colour separation to obtain two new stacks of green and red images.
- 3- The image with the best resolution of intensities was selected as a reference separately from each stack (green and red).
- 4- The cumulative histogram of intensities of every image in the respective stack was modified to match as closely as possible the intensity distribution of the reference image (implemented as script in Image Tool; Dr. Gras; Göttingen; unpublished). This non linear correction of brightness loss in focus series obtained by confocal microscopy is justified for objects which can be expected to contain a rather homogeneous distribution of fluorophores at least on a coarse structural level.
- 5- A further Image Tool script (Dr. Gras) was used to combine the intensity-corrected stacks as red and green channels to finally create a 24 bit RGB colour image stack with the blue channel set to \emptyset .

Pictures were arranged and labelled using Adobe Indesign 2.0.1 program. Some plates were printed using an EPSON stylus photo ex printer.

2.8. Procedures for quantitative study

2.8.1. Difference in the fibre profiles

To differentiate between the fibre profiles of different KC classes, special scripts (Dr. Gras, Göttingen) within the program environment of UTHSCSA Image Tool 2.0 were used and the following steps were performed:

- 1- Electron micrographs (10000x) showing cross sectioned axons at different area from the outer layer to the central bundle of the stalk and alpha lobe were taken.
- 2- Scanning of negatives was done using the scanner Epson perfection 2450 photo (resolution: 1200 dpi). Images were processed with Adobe Photoshop 7.0.1 program.
- 3- The scanned image was analysed for the size of the cell membrane.
- 4- The contrast was increased in a non-linear manner depending on the lowest and highest intensities within the $n \times n$ neighbourhood of every pixel ($n = 31, 51, 71$). This means that regions of high contrast in the original image remain unmodified while regions of low contrast are subjected to an intensity stretch, the amount of which is selected by the program operator.
- 5- To determine cell membrane shape and integrity, the original image as well as the contrast improved image were separately transformed to binary images (black/ white only) by threshold operation to separate membrane and plasma regions. Standard dilation and erosion operations served to close gaps and to smooth the borderlines of objects in the binary images. The pixels which made up the semi-automatically detected membranes were finally coloured in shades of red within the original image or within the contrast-enhanced image. At this stage of processing the image contains many disconnected cell membranes so that two or more fibre profiles appear as one object.
- 6- The image was then manipulated using Corel Photopaint 8.0 program so that the gaps between disconnected cell membranes were filled by straight red lines.

- 7- The manually corrected colour image was transferred back to Image Tool, where another script was used to extract all pixels with a red intensity $> \emptyset$ and to generate a binary image showing only those pixels while plasma area appears black.
- 8- The Image Tool functions for object analysis were used to determine numbers and the areas of the sectioned fibre profiles.
- 9- Measured surface areas were classified into different size groups using the classification command of Image Tool. A colour-coded figure representing the different groups of the cell surface areas was obtained.
- 10- Mean and standard error of the mean of the areas were determined and plotted using Microcal Origin 6.0 program.

2.8.2. Determination of tubules in fibre profiles

The analysis is based on the same electron micrographs used in 2.8.1 to study the difference in the fibre profiles in the stalk.

- 1- & 2- were employed as in 2.8.1.
- 3- Image Tool 2.0 program was used to improve the images by reducing the pixel noise with 3*3 median filter or mean filter (3*3, 5*5).
- 4- Images were enlarged twice (for the better viewing of tubules) and printed. The numbers of tubules in every profile with defined section area (μm^2) were counted. We excluded those profiles from counting, which did not fully occupy the square selected.
- 5- Mean and standard error of tubules were counted and plotted using Microcal Origin 6.0 program.

2.8.3. Counting of synapses and mitochondria

To study the distribution difference of synapses and mitochondria in the MBs parts, the following steps were used.

- 1- Electron micrographs (4000x) showing cross sectioned axons were taken at adjacent areas from the outer layer to the central bundle.

- 2- Electron micrographs for montages were taken at different MBs levels (e.g. medial of the calyx; beginning, medial and basis of the stalk; medial and basis of the alpha lobe and medial of the beta lobe, horizontal sections).
- 3- Negatives scanned by Epson perfection 2450 photo (resolution: 1200 dpi) were processed with Adobe Photoshop 7.0.1 program. We analysed samples of micrographs (defined squares from montages of micrographs) for all regions of the MBs.
- 4- UTHSCSA Image Tool 2.0 program was used to improve the images by reducing the pixel noise with 3*3 median filter or mean filter (3*3, 5*5 pixels).
- 5- Images were enlarged twice and printed, then the number of synapses and mitochondria were counted. We did not count the synapses and mitochondria which were not completely inside the image squares ($9\mu\text{m}^2$).
- 6- Numbers of synapses and mitochondria were counted and plotted using Microcal Origin 6.0 program.

3. Results

The investigation was focussed on structural features of growing neurones in the MBs of adult brains. These neurones emerge from ganglion mother cells displaying mitotic activity, directed fibre outgrowth, and they are considered to become structurally integrated into a mature functional network of synapsing elements of diverse classes of neurones. These neuron classes fall into two main categories: local interneurones of KC types and extrinsic relay interneurones (synonym proction neurones). All neuron classes show a specific distribution in the MB compartments. The only newly added, sprouting neurones in the imaginal cricket brain are local MB KCs.

By use of different markers for molecules involved in growth and in the establishment of synapses, the growing KCs are compared to more mature or fully developed MB neurones, using immuno-light microscopy, fluorescence microscopy and TEM. For understanding the sophisticated MB architecture, a short description of this protocerebral neuropil is given first. New findings of this study on the structure of MBs, complementing former investigations are also reported in this section.

3.1. The structure of the MBs: compartments, cell types, synaptic connectivity

The paired MBs of the cricket represent a dense neuropil in the protocerebral brain. This central neuropil with obvious geometrically ordered components is made up of extrinsic relay neurones and intrinsic local neurones (KCs). The extrinsic neurones connect the MBs with other brain neuropils and with MB compartments (Schürmann, 1973; Honegger and Schürmann, 1975; Schildberger, 1983; Strausfeld et al., 1998). The KCs are tiny Y-shaped local interneurones with small pericarya (so called globule cells) in the peripheral cortex (pericaryal layer) of the MBs, with their fibres restricted to this neuropil. The parallel arrangement of thousands of KC fibres mainly determines the form of the MBs. The neuropil of the MBs is composed of four major compartments, from proximal to distal regions of the KCs: bipartite calyces (calyx anterior and posterior), a columnar stalk, and the columnar α - and β -lobes. In

the genus *Acheta* and *Gryllus* three major KC types (KC I, II, III) are distinguished according to their dendritic form, size and position of somata and axon bundles (Schürmann, 1973). For the MBs of *Gryllus bimaculatus* the following length of the columnar neuropil compartments, determined by the KC fibre bundles, were measured: stalk 190 μm , alpha lobe 110 μm , beta lobe 40 μm .

KC I and II somata form a frontal cup-shaped pericaryal layer, anterior to the somata layer of KCIII neurones. The KC I and II fibres are restricted to the anterior calyx, whereas KCIII elements form the posterior calyx. The KC axonal fibres form compact bundles traversing the calyces and stalk to end in the alpha- and beta lobes (Fig. 1) (Schürmann et al., 2000). The KCs in crickets thus represent non-isomorphous subpopulations of local intrinsic neurones, not only to be discerned by Golgi impregnations, but also characterized by expression factors revealed by genetic studies (Yang et al., 1995; Crittenden et al., 1998; Sinakevitch et al., 2001).

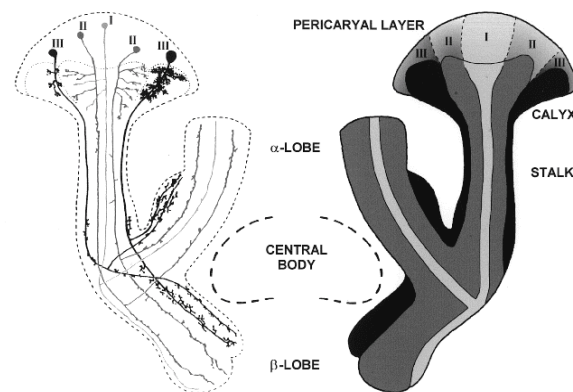


Fig. 1: Diagram of MBs (horizontal view, after Schürmann et al., 2000) in the house cricket brain, with Kenyon cell types I-III (left) as determined from Golgi-impregnations. Their somata are clustered into three groups and their axons, arranged in parallel, form discrete fibre bundles (right).

The calyces are the regions of KC dendrites. KC I and II dendrites are restricted to the anterior calyx. The dendrites radiate from the central mass of axonal fibres arranged in parallel, to form dendritic spines synapsing with extrinsic neurones in a marginal shell-like zone. The most prominent extrinsic neurones are iACT cholinergic projection neurones, forming idendeted boutons. These boutons are

consistently presynaptic and coupled to the KC dendrites in a divergent mode (Frambach et al., 2004).

The KC III dendrites in the bulbous posterior calyx (also named accessory calyx, Weiss, 1981) receive extrinsic fibre input from other tracts as well, supplying the posterior calyx with patterns of presynaptic boutons as well. The analysis of synaptic wiring of KC III elements is not within the scope of this study. The calyces are considered to represent the main regions where KCs receive synaptic inputs of various sensory signals by extrinsic neurones. Other extrinsic elements project from other parts of the brain into the calyces. They have been detected by single cell iontophoresis and electrophysiology (Schildberger, 1983; 1984; Schürmann, 1987), by Golgi impregnations (Schürmann, 1973; 1974), and by transmitter immunocytochemistry (Schürmann, 1987; Frambach et al., 2004). Cholinergic and other extrinsic cell types represent a minority of neurones in comparison to intrinsic KCs.

GABAergic arborizations with tiny boutons (2-4 μm) in the anterior and posterior calyces form basket-like networks surrounding the large cholinergic boutons (Fig. 12A). These GABA elements are interpreted to synapse with KC dendrites. In addition blebbed fibres in the anterior calyx core region are arranged along the radially projecting KC dendrite fibre bundles, corresponding to hot spots of synapsin-like immunocytochemistry (Fig. 8A). These new findings of this study suggest a synaptic coupling of GABA elements to KC fibres distant from their dendritic tips as well. The dense network of GABA fibres is similarly organized in the anterior and posterior calyx.

Serotonergic fibres in the MB form a network in all its compartments, but not as dense as GABA elements. In the anterior calyx, 5-HT fibres appear to be confined to the outer parts of the synaptic glomerular layer (marginal calyx portions; Fig. 13A). The serotonergic fibres show tiny boutons, as stated for GABA-elements. A presynaptic nature is also suggested, but remains to be demonstrated by immunoelectron microscopy.

MB stalks, α - and β -lobes are considered to represent main output regions, though electron microscopy revealed input synapses in the lobes and other modes of synaptic coupling as well (Schürmann, 1972; 1973). In the stalks and lobes, KC axons usually have only short side branches or blebs, to form presynaptic contacts with extrinsic neurones which project to various areas in the superior and inferior protocerebrum (Schürmann, 1973; 1974; Schildberger, 1983; Frambach et al., 2004).

The view of the calyces as main input stations and the distant stalk and lobes as main sites of output and other forms of synaptic coupling (Schürmann, 1987) is generally adapted to the MBs of other insect species. The connectivity of most extrinsic neurones outside the MBs is mostly unknown and cannot be simply derived from light microscopy (Yasuyama et al., 2003).

3.2. Sprouting KCs in the MBs

The source and site of the newly added KCs and their sprouting fibres in mature brains had to be discriminated from structurally developed neurones at the light and electron microscopic level in all MB compartments: the pericaryal layer, the calyx, stalk and alpha- and beta-lobes. At the light microscopical level, the demonstration of newly formed cells was achieved by marking mitotic events, and by employing f-actin-phalloidin staining, performed on single or double stained vibratome sections of complete section series.

3.2.1. F-actin in MBs

Differences in phalloidin staining intensity and distribution reflect neuron type specific equipment with actin. In the MBs and in surrounding neuropils f-actin is typically found at synaptic complexes, e.g. in antennal lobe glomeruli, in MB calycal microglomeruli and in fibre groups of KCs, related to the developmental state and age (Fig. 2C). In *Gryllus bimaculatus*, the three populations of KCs could be clearly discriminated by their f-actin staining with phalloidin. Type KC I neurones represent the youngest cells. Fibre bundles of these neurones showed the most intense phalloidin staining. Type KC II fibres surrounding the central bundle of growing KC I

fibres show a faint phalloidin staining. Type KC III neurones representing the oldest KCs display a high phalloidin staining in dendritic tips and lack phalloidin staining in fibres free of synaptic connectivity (Figs. 2E, F).

The forming of new neurones in mature brains is only stated for KCs throughout the cricket's life (compare Cayre et al., 1994; 1996), and there in the MB portion with KC I and II elements with dendrites in the anterior calyx receiving input from the antennal lobe via the iACT tract of projection neurones. The antennal lobes are primary brain neuropils, crucially involved in the integration of olfactory information.

3.2.2. Pericaryal layer

To discriminate the proliferative cluster in the MB cortex we used the anti-phospho histone H3 mitosis marker. In Figure (2D), the positive staining of the central core of the MB pericaryal cortex indicated a conic cluster of about 100 growing KC somata, stemming from persisting neuroblasts present throughout adult life, located in the centre of the anterior MB pericaryal cortex. The marginal cluster of stained mitotic large somata of ovoid shape is encapsulated by a shell of small weakly stained KC somata. The immunostaining marks the large nucleoli. The mitotic somata and surrounding older KC somata are depicted by osmic acid and toluidine blue staining in semithin sections as well (Figs. 2A, B).

Mitotic and older surrounding KCs are intensely marked by fluorescent phalloidin, outstanding against neighbouring KC somata. The young growing somata give rise to a compact stained fibre bundle, descending into the central anterior calyx. Older KC somata groups form small f-actin fibre bundles, descending to the calycal fibre column too, in the circumference of the central core of the sprouting fibre bundle (Fig. 3A). The position of these fibre bundles of KC II elements is considered to reflect their age: distal fibre bundles are interpreted to represent most ancient KCII neurones, whereas KC fibres are younger in proximity to the central core KCI fibre bundle.

The structural image of sprouting KCs during adulthood, forming the massive central bundle with f-actin is similarly encountered in last instar larvae (Figs. 3B,C). These larval KCs in the cricket MBs persist through metamorphosis of these hemimetabolous insects.

3.2.3. Calyx

As described, the group of proliferating neuroblasts gives birth to new KC interneurons which progressively differentiate and migrate to the periphery of the pericaryal cortices. The fibres grow to produce their calyx neuropil contribution.

The central core fibre bundle (type KC I) traverses the calyx and continuously forms the central core of the stalk. Weakly stained type II cells surround the central core fibres, together forming a compact axial cylinder throughout the entire anterior calyx. The calycal fibre column also holds small scattered dots of intense phalloidin fluorescence in areas occupied by KCII fibres. These dots could not be allocated to extrinsic or intrinsic fibres by laser scan microscopy.

The f-actin rich central fibre bundle forms dendritic projections that grow radially to the marginal synaptic layer of the anterior calyx (Figs. 3D, E). They appear as radial strands emerging from and along the central core of the KC I fibre bundle, crossing the more mature KCII fibre bundles and directed versus the marginal zone of complex synaptic glomeruli. These synaptic structures are strongly f-actin positive. The f-actin-phalloidin fluorescence is accumulated in the dendritic tips of mature type KC II neurones. The neuropil surrounding the MBs displays also high phalloidin staining at synapses, but almost lacking in tracts (Fig. 3D). Glomeruli in the posterior calyx are also endowed with high amounts of f-actin (Fig. 3E).

When entering the anterior calyx the KCI fibre bundle is surrounded by a non stained area (Figs. 2E, F). This space appears to be devoid of cellular material in vibratome sections with fluorescent staining in cells, but filled with electron dense material in tissue prepared for electron microscopy (Figs. 22A, 23A). This extracellular space is large at the border of the calyx cortex to the neuropil and its

extension is diminished to small finger-like protrusions at deeper distal levels of the calyx fibre column (compare electron microscopic findings, section 3.6.2).

3.2.4. Stalk

The descending fibres from the proliferating KCI cluster extend through the calyx to the stalk, to form the central part of the MB stalk column (Fig. 3F-I). The central core occupying about a tenth of the stalk volume contains about 800 fibres (Fig. 3G), counted in electron microscopy images of stalk cross sections.

The distribution of KC fibre bundles is maintained along the stalk, so that arrays of KC axons of the different types can be easily detected. The strongly stained central core cylinder of KC I fibres is surrounded by a neuropil of lower spotted f-actin-phalloidin staining, found along the stalk (Figs. 4A-C). It corresponds to the distribution of KC II fibres of different ages. F-actin-phalloidin spots appear partially aligned along the stalk (Fig. 3I). Interestingly, the neuropil adjacent to the proliferating KC I central core is only weakly stained (Figs. 4A-C). This portion is occupied by KC fibres of small diameters (compare section 3.6.4). The marginal KC III fibres show no f-actin staining, with the exception of the stalk base, where the KC fibres bifurcate into the α - and β -lobe. The differential pattern of f-actin distribution corresponds to the staining revealed in osmicated semithin sections (Figs. 3F, G).

3.2.5. Lobes

At the distal stalk divide the KC axons project into the α - and β -lobes. The KC axons maintain their overall arrangement into gross fibre bundles along the lobes. Centrally located stained type KC I fibres hold a central position in the α -lobe and are shifted to a lateral position in the β -lobe (Figs. 4D, E; 5B-D). In cross sections the KC I fibre bundle occupies an area of about 6 μm with irregular outlines, apparently more voluminous than in the stalk (Figs. 4H, I). The overall phalloidin-staining intensity of KC II fibres appears higher in comparison to corresponding stalk portions. High resolution confocal imaging reveals a network-like f-actin staining. The staining could not be allocated to extrinsic neurones or intrinsic KC elements. The staining is

interpreted to mark synaptic sites (see section 3.4.1.2). The distribution of f-actin staining corresponds to the staining differences observed in toluidine blue stained, osmicated sections (Figs. 4F, G; 5A).

3.3. Tubulin in the MBs

Microtubules are constituting elements in neuronal somata and their axonal fibres. Their formation is closely associated with dynamic events, such as axonal flow, cell motility, occurring in processes of growth and differentiation of neurones. Therefore, the distribution of tubulin molecules in developing and mature KCs was investigated and compared with f-actin distribution, using single or double labelling of vibratome sections (Figs. 6; 7).

During differentiation of the neuron, distinct patterns of microtubules with polarized orientation are established within axons and dendrites (Sharp et al., 1997). Tubulin-like immunoreactivity in the MBs of crickets is found in all parts of the MBs in intrinsic and extrinsic neurones (Figs. 6), but unevenly distributed in the neuropil, showing various degrees of staining intensity (Figs. 7). Tubulin is located codistributed with f-actin in perilemma cells.

3.3.1. Pericaryal layer

Tubulin-like immunoreactivity is found concentrated in KC fibre bundles in the pericaryal layer (Figs. 6C-E). Interestingly, in the pericaryal layer, the portion of mitotic, newly emerging KC I neurones - showing intense phalloidin labelling - appear to be devoid of tubulin-like immunoreactivity. Tubulin occurs, however, in marginal fibre strands of the KC I neurones entouring a tubulin free area (Fig. 6F).

3.3.2. Calyx

In the calyces, tubule-like immunoreactivity is mainly detected in KC fibres (Fig. 7A), and within intruding extrinsic neuronal fibres. The f-actin rich central core fibres of KC I neurones are mainly lacking in tubulin marking. Synaptic complexes of

the anterior calyx margin (microglomerular layer) holding numerous dendritic KC endings do not show considerable amounts of tubulin, but accumulated f-actin (Fig. 7B).

3.3.3. Stalk

The most intense tubulin-like immunoreactivity in the stalk is found in type KC III fibres, whereas type KC I and II fibre bundles display low tubulin marking (Figs. 7C, D). The tubulin-like immunoreactivity of type KC I fibres is concentrated at the boundary of the central core. The distribution of tubulin, forming microtubules and of f-actin in KCs fibres is considered by electron microscopy also (see section 3.6.4). Large fibres surrounding the stalk and the lobes appear strongly tubulin positive (Figs. 7D-F).

3.3.4. Lobes

In the alpha and beta lobe, tubulin labelling is found scattered in between areas with f-actin staining (Figs. 7E, F). The bundle of sprouting KC I fibres shows only weakly stained spots of tubulin marking, but is surrounded by a shell of fibres with distinct tubulin labelling, detected in cross sections. Tubulin staining can also be attributed to invading extrinsic fibres (Figs. 7E, F). A scattered labelling is seen in the KC II fibre areas, often in close association with f-actin containing spots (Fig. 7E), which might indicate synaptic coupling (compare section 3.4.1.2).

3.4. Synaptic areas related to MB compartments and neurones

Integration of mature and developing KCs into the MB neuronal networks, formed by intrinsic and extrinsic neurones, is reflected by the occurrence and distribution and form of synaptic contacts. Synaptic contacts of KCs and extrinsic neurones are investigated, the latter serving for information input and output of MBs and MB compartments. Immuno-light microscopy of the protein synapsin I allows the rough description of presynaptic sites, and by double labelling experiments the

determination of synaptic foci within neurones characterized by transmitter immunocytochemistry can be achieved.

The present light microscopical findings provide a qualitative survey of putative synaptic sites in MB compartments marked by synapsin-like immunoreactivity. Special interest was directed to the sprouting KC I fibre bundles.

To gain some insight into the distribution and synaptic connectivity of extrinsic neurones, GABAergic and serotonergic fibres, known to occur in the MB neuropil (Schürmann, 1987; Strambi et al., 1998; Frambach et al., 2004) were investigated by transmitter immunocytochemistry. GABA and GABAergic neurones belong to the most abundant transmitters and nerve cells in the insect brain, as prominent as cholinergic elements. Cholinergic projection neurones (PNs) in the cricket MBs are restricted to the calyx microglomeruli, not found in other MB compartments (Frambach and Schürmann, 2004). The clear-cut evidence of a structural chemical synapse can only be demonstrated by electron microscopy. The allocation of synapses to MB compartments and especially to KC I neuropil is given in section 3.6.4 (Figs. 32).

3.4.1. Synapsin distribution

3.4.1.1. Calyces

Prominent synapsin-like immunoreactivity is clearly identified in the anterior and posterior calyx (Fig. 8A), partially at levels found in MB surrounding neuropil. In the anterior calyx, the marginal microglomerular area with antennal lobe connecting PNs is intensely labelled (Fig. 8A). PN boutons in the centre of the microglomeruli are presynaptic (Frambach et al., 2004). At the inner rim of the PN input area, synapsin labelled spots are not as densely distributed as in more centrifugal parts (Figs. 8B, C). In the inner fibre column of KC I and II fibres tiny spots of synapsin are scattered, often appearing aligned to radial f-actin-phalloidin stained fibre strands, interpreted to represent dendritic KC fibres, stemming from the central core bundle (Figs. 8B, C). These tiny spots, often at the limit of light microscopical resolution, do not show a ring-like surrounding of f-actin staining, typically seen in the calycal periphery (Fig. 8D). The tiny synapsin spots appear at the distal border of the central

core of KC I fibres. This area with high f-actin contents appears to be free of synapsin and therefore no synapses are expected in this zone. The occurrence of synapsin correlated with synaptic vesicles was investigated by electron microscopy (Figs. 9; 10A-C; 22E, F, see section 3.6.2). The confocal microscopy does not allow us to decide on a presynaptic nature of extrinsic or intrinsic neurones.

3.4.1.2. Stalk and lobes

Stalks and lobes are clearly depicted by their synapsin contents (Fig. 11) and can be discerned from neuropil surrounding the MBs. High resolution confocal imaging shows synapsin spots of sizes found in the inner anterior calyces. They are confined to the portions of KC II fibre bundles along the stalk. Double labelling to demonstrate synapsin and f-actin (Figs. 11D, E) gives hints for the association of these molecules. The central core of KC I elements is devoid of synapsin (Fig. 11D). The peripheral KC III fibre bundles do not exhibit synapsin (Fig. 11D), apart from the base of the stalk.

The columnar lobes with their divisions of parallel KC fibre bundles are filled with synapsin, showing different intensity of labelling from proximal to distal portions of the lobes (Figs. 11F, G). No patterning of synapsin filled elements could so far be resolved in detail by this approach or be related to previous investigations on synaptic distribution. The stalk and lobes appear packed with synaptic vesicles (Figs. 10D-F see below and Schürmann, 1987).

3.4.2. Extrinsic MB GABA-fibres

GABA fibres labelled by immunocytochemistry were investigated in order to compare their distribution in the MB compartments with KC fibre bundles. The relation of GABA fibres to f-actin-phalloidin stained structures was of special interest. All compartments of the MB neuropil are supplied with GABA fibres displaying fine arborizations and forming networks of different densities (Figs. 12), to be stated for other neuropils outside of the MBs too.

3.4.2.1. Calyces

Both the anterior and posterior calyx contain a dense meshwork of tiny GABA fibres, detected as elements contributing the microglomeruli. In horizontal sections of the anterior calyx, radial fibres traversing the KC II fibre bundles extend into the peripheral synaptic layer of microglomeruli. Central core KC I parts appear free of GABA-like immunoreactivity. Evidently, no synaptic contacts of GABA fibres occur in the central core of sprouting KC fibres. This observation is consistent with the findings on synapsin distribution. Tiny GABA fibres exhibit small blebs, which could indicate locations of “en passant synapses” (Figs. 12A-C, compare section 3.4.1.1).

3.4.2.2. Stalk and lobes

Along the stalk, comprising KC I-III fibre bundles, orderly arranged in parallel and in concentric layering, the GABA network is confined to the KC II fibre parts. Again the central core of KC I and the peripheral KC III fibre bundles are not invaded by GABA fibres. A KC II fibre portion shell adjacent to the central core holds only few GABA fibre terminations, not entering the central core (Figs. 12D, E), so that at its rim only scarce GABAergic synapses can be assumed.

The lobe compartments have not been analysed in detail. The GABA network is highly complex, also showing various extents of GABA labelling. Some subdivisions appear free of or only scarcely supplied by GABA fibres, whereas other regions show thick arborizing immunoreactive fibres. A unifying feature of KC I fibre masses is the lack of GABAergic supply (Figs. 12F, G) and synapsin staining.

3.4.3. Extrinsic 5-HT neurones

Serotonergic (5-HT) neurones represent a minority of cells among cholinergic and GABAergic nerve cells of the insect brain. In the cricket *Gryllus bimaculatus*, a total of 60-80 5-HT neurones exist in the brain (Hörner, 1999). These neurones belong to the class of so-called wide field neurones supplying all brain neuropils including the MBs. Their functional roles in the MBs are unknown, but it is commonly agreed that they profoundly affect the exertion of behaviours.

3.4.3.1. Calyces

The microglomerular parts of the anterior and posterior calyces are supplied by a network of 5-HT fibres (Fig. 13A), not as dense as the GABA-network. In the anterior calyx, 5-HT fibres with small bouton-like specialisations are concentrated in the outer regions of the glomerular layer (Fig. 13B). They occupy marginal parts of a microglomerus, in the vicinity of the strong f-actin-phalloidin stained portions (Figs. 13C, D) which contain KC II dendrites around a central PN-bouton (Frambach et al., 2004). These 5-HT boutons are expected to be synaptically coupled to the marginal microglomeruli. The column-like fibre bundles of KC II and KC I fibres in the inner parts of the calyx lack 5-HT fibre networks, different from the GABA fibre distribution.

3.4.3.2. Stalk and lobes

A 5-HT network not as dense as the GABA network is found in the outer parts of the stalk invading the KC II fibres (Fig. 13E) along the stalk column. Large areas of KC I and II fibres are devoid of 5-HT immunoreactivity, also lacking in the marginal KC III fibre subcompartments (Figs. 13E, F).

As stated for the stalk large parts of the lobes do not contain 5-HT fibres (Figs. 14A-D). Especially the compact KC I fibre bundle and adjacent KC II fibres lack supply with 5-HT immunostained elements and are therefore not synaptically coupled to these extrinsic aminergic fibres. The tiny 5-HT fibres are of the varicose fibre type, displaying slight swellings lined up along a fibre (Fig. 14E). 5-HT fibres do not show intimate contact to f-actin-phalloidin spots (Figs. 14B, D, F).

From the distribution of 5-HT fibres in the MBs it is suggested that these serotonergic fibres are concentrated in neuropil portions holding mature KCII fibres, older than more centrally positioned KC fibres, including sprouting fibres.

3.5. Glial cells in the MBs

To investigate glial distribution and its potential contribution to the newly growing cells within the MBs of the adult cricket, double labelling with propidium

iodide and fluorescent phalloidin was used. Propidium iodide labels nucleic acids in neurones and glial cells (Hähnlein and Bicker, 1997; Rössler et al. 1999b; Devaud et al., 2003). Propidium iodide marks perilemma cells and the pericaryal cortex of the MBs (Fig. 15A). However in this MB compartment, glial cells could not be discriminated safely from KC somata. They were identified in the neuropil, lacking neuronal somata. Glial cells with elongated or ovoid somata form flattened cytoplasmic sheaths surrounding and partially separating neuropil compartments, as found for the calyx, stalk and lobes (Figs. 15B-E, 16). The cytoplasmic sheaths are visualized by confocal microscopy, forming tiny strands of propidium iodide fluorescence found to be discontinuous in stacks of optical sections. There is no indication of massive glial patterns inside the MB neuropil, consisting of numerous tiny naked neuronal fibres. No specific colocalization of f-actin-phalloidin staining and glial elements in the MB neuropil was detected. Some glial cells with protrusions exist in the KC I and other fibre bundles do occur (Figs. 15D; 16B). No network-like glial pattern, subserving as guide lines for sprouting neurones can be deduced from the light microscopical studies. The findings correspond to the observations obtained from electron microscopy (Figs. 17, compare section 3.6).

3.6. Ultrastructure of MBs

Ultrastructural studies were performed in order to describe proliferating KC neurones and to investigate and to compare their fine structure with surrounding older KCII elements and with glial cells. Special attention has been devoted to the expression and distribution of some cell organelles (ribosomes, tubules, and mitochondria), membrane specializations and extracellular space. In brief, light microscopical findings could thus be complemented and comparatively evaluated.

The electron microscopical studies are based on conventional TEM. Immunoelectron microscopy and other approaches to visualize molecules at the ultrastructural level were not employed here. In a previous study (Frambach et al., 2004), attempts to demonstrate f-actin bundles in KC dendritic tips failed. Immunoelectron microscopy of synapsin I that boutons with synaptic vesicles and presynaptic active zones are completely filled with electron dense precipitate marking the distribution of this presynaptic protein (Frambach et al., 2004). Therefore, the light

microscopy of synapsin immunoreactivity can be safely taken to show local sites of presynaptic character. Immuno-electron microscopy of the transmitters in GABA and 5-HT fibres was also not performed.

Fortunately, the parallel KC fibres are gathered into compact bundles, so that their areas could be traced throughout the MBs, from the pericaryal rind to the lobe endings. Moreover, sprouting KC I elements are marked by enhanced electron density after osmication. Therefore, KC fibres can be viewed in serial brain sections by light and electron microscopy. For electron microscopy samples were selected from a complete series of semithin sections at different levels of the MBs. Large montages of electron microscopy images made it possible to collect comprehensive information on KC fibres and their contents.

3.6.1. Pericaryal cortex

The mitotic and sprouting KC I cluster exhibits high electron density, to be clearly separated from surrounding older KC somata (Figs. 18). The cellular equipment does not differ qualitatively from more mature pericarya. Shape differences are obvious. The electron dense KCs are mainly not separated by glial cytoplasm, which typically encapsulates older KC somata (Figs. 19) and KC fibre bundles. Glial finger-like protrusions are encountered in the KC I area, but no pattern of glial elements within this somata cluster and fibre bundle is present. In the pericaryal rind and its fibre bundles no large extracellular spaces occur, but in a compact area of irregularly shaped fibres, forming interdigitating extensions of sprouting KC I elements, entoured by the electron dense KC I somata, small areas of glial protrusions are found. These KC I fibres form growth cone-like structures with tiny filopodia (Figs. 20A, B). These KC I extensions contain ribosomes, microtubules and mitochondria. Actin fibres could not be detected. In the KC I cone-like area, the cell membranes of directly neighbouring somata and fibres display in parts enhanced electron density at their outer, extracellular side (Figs. 20C, D). These specialized membranes with electron dense covering are of variable length (up to 5 μm) form a sort of spacing junction (about 25 nm), with a small translucent extracellular midline. Such junctions have not been found between more mature KC somata and fibre bundles. Fibres bundles of older KCs appear free of ribosomes (Fig. 19B). Synaptic

vesicles were not found in KC I divisions. Very rarely, synaptic-like membrane specializations were detected in the somatic layer of KCs II between fibres not identified (Figs. 20C, D), indicating putative functional coupling.

In deeper layers of the MB pericaryal rind dark KC I somata are no longer present, but a central column of KC I fibres is traced on its way to the calyx. The central area contains irregularly shaped fibre profiles, representing growth cone-like structures (Fig. 21A). These fibres are encircled by tiny less electron dense fibre profiles of older KCs. This column is surrounded by a dark discontinuous glial sheath, separating it from KC II somata (Fig. 21A). Small glial interdigitations, only resolved by electron microscopy, extend from the glial shell into the KC I bundle. These glial elements are partially associated with widened extracellular space, filled with electron dense material of unknown origin and composition. These electron dense areas are in direct contact to small KC I fibre protrusions (Figs. 21B, C), without adjacent glia. These extracellular spaces are seen as belonging to a vast extracellular system at the cortex-calyx rim, prominent in the proximal central anterior calyx (Fig. 21B). The extracellular system is not found in the posterior calyx and in the cortex of KC III neurones.

3.6.2. Calyx

The electron dense fibre bundle (Figs. 22A, B) of central core KC I axons holds profiles with finger-like extensions as found in the somatic cortex, still containing ribosomes partly attached to endoplasmic reticulum (Figs. 22C, D). The sprouting KC I fibres find direct contact to extracellular spaces (Figs. 23; 24). The forming of dendritic fibre bundles of radially sprouting KC I axons indicated by light microscopical findings could not be determined in sufficient detail. They seem to join small bundles of mature KC II dendrites. A transient nature of the KC I fibres could not be established.

The prominent extracellular space is centrally traversed by the central f-actin rich and electron dense KC I fibre bundles (Figs. 24A; 25A, B). This extracellular space is becomes smaller at distal parts of KC fibres which descend into the stalk. The extracellular spaces are partially in contact to glial cytoplasmic invasions (Figs.

25C-E). No signs of cytophagic activities were usually detected (compare section 3.7 on degeneration). No synapses were detected in the KC I and central core region.

3.6.3. Stalk and lobes

The electron dense core region of KC fibres is traced along the stalk, surrounded by a set of tiny fibre profiles, distally concentrically positioned KC II fibre bundles (Figs. 26A-C). The central core of KC fibres contains the large growth cone-like fibre profiles found in the calyces and the KC cortex. These KC fibre elements no longer contain ribosomes. No synaptic vesicles or synaptic contacts were detected. Profiles of extracellular space surrounded by KC fibres best seen in cross sections of the stalk (Figs. 26C, D). The tiny fibres around the electron dense area of KC profiles are scarcely equipped with mitochondria. Synaptic contacts and extrinsic fibres are occasionally found. They are both regularly found in surrounding KC II fibre masses, but missing in the outer layers of KC III fibre bundles (Figs. 26E, F). These ultrastructural findings correspond to the results obtained from synapsin – immunolight microscopy (see section 3.4.1.2). Also four electron microscopic serial sections were used to study the sequential generation of the central core fibres of the stalk (Figs. 27).

The KC I and II fibre bundle positions in the stalk are maintained in the α -lobe. The KC central core is free of synapses and neuronal ribosomes, but still holds growth cone-like enlarged fibre profiles (Figs. 28; 29A). KC II fibres form blebs with synaptic contacts and appear to be packed with vesicles along the axons. KC II fibres often synaptically converge to intruding extrinsic fibres (Fig. 29B). Axonal membrane coupling by spacing junctions found in the pericaryal layer and in the calyx were not observed in the stalk and lobes.

In the β -Lobe, fibre bundles of KC I-III axons remain in their subdivisions, but their positions are transformed (Fig. 29C-E). The ultrastructural equipment is very similar to the α -lobe situation.

In the stalk and lobes, no patterning of glial elements was detected. The KC I fibre bundle is not supplied with extensive glial material (compare section 3.5).

3.6.4. KC fibre classes: profiles associated with organelles and synaptic sites

As demonstrated by light microscopy (sections 3.2, 3.6) and by systematic qualitative inspection of the ultrastructure, insight was gained into sites of dynamic processes of growing KC neurones and their relation to established network parts within the MB compartments. The results were mainly obtained from samples of thin sections taken at intervals of 3.5 μm in between a complete series of horizontal semithin sections. Using this procedure, complete MB areas ranging from central parts to the MB borders could be viewed in large thin sections on slot grids. This section plane delivers cross sections of the compact columnar KC fibre bundles arranged in parallel and of similarly orientated extrinsic fibres. Therefore, intrinsic and extrinsic elements could not be discriminated from each other when they exhibit the same diameters and internal equipment. However, extrinsic fibres in the calyx, stalk and lobes are mainly not organized in columns in parallel to KC fibres, but invade the columns at different levels by transverse arborizations, to synaptically contact KC fibres (Schürmann, 1974; Frambach et al., 2004).

A main initial finding was that the innermost central core parts of the KC fibre bundle fortunately could be identified by their enhanced electron density and be discriminated from surrounding older, more mature KC fibres, representing different stages of age signalled by structural characters. However, the outlines of the central core do not form a proper circular ring, but appear fuzzy and not identical at different levels of the stalk and lobe columns. Moreover, the electron density is not equal in all central core parts, but often gradually decreasing towards centrifugal portions. By the method used it was also not possible to recognize or trace the small portion of growing dendrites of newly added KC neurones intermingled with abundant KC II dendrites in the anterior MB calyx.

Attempts to determine structural differences between KC fibres of different age in mature brains by measuring transversely cut fibre profiles and by counting of organelles had to be restricted to some samples of thin sections taken at different MB levels. Only parts of a cross section through an MB column covering areas along a line from the central core to the column rim were analysed (Figs. 30A-D; 31A-D).

Shapes and dimensions of fibre profiles were only determined for the stalk and α -lobe showing a similar organization of KC I and II fibres at all levels of their columns (Figs. 30E; 31E). The central cores of the stalk and α -lobe show a small portion of irregularly shaped large profiles, sometimes forming tiny protrusions. These elements are interpreted as growth cone-like structures, forming filopodia. The central core area of the stalk contains the KC fibre profiles with smallest areas (about $0.019 \mu\text{m}^2$, corresponding to small diameter fibres, dimension about $0.01 \mu\text{m}$). In the centrifugal direction the fibre profile areas become gradually larger, up to a dimension of $0.052 \mu\text{m}^2$. These fibre profiles are mainly from KCII neurones (Fig. 30B). The set of KC III fibre profiles is clearly set apart by their large dimensions ($0.2 \mu\text{m}^2$) from the peripheral adjacent KC II fibres. Counting of cross sectioned tubules per fibre profile in the same squares used for fibre dimension measurements revealed that the number of tubules is correlated to the size of fibre profiles (Fig. 30F). Interestingly, the central core region shows a relatively high amount of tubules per fibre profile.

In the α -lobe (Fig. 31B) the innermost profiles of the central core are seen with similar shapes and dimensions as stated for the stalk, intermingled and surrounded by a homogenous population of tiny fibres (dimension $0.1 \mu\text{m}^2$, diameters around $0.042 \mu\text{m}$). Some small fibres show tiny filopodia-like fingers. The outer portions of the α -lobe contain KC II fibres with enlarged dimensions, because here the KC fibres form abundant presynaptic blebs filled with synaptic vesicles along the lobes. Synapsing blebs were not found in the central core area. This enlargement of KC fibres and the abundance of extrinsic invading elements make α - and β -lobes more voluminous in comparison to the stalk. KC III fibre profiles were not analysed.

Numbers of mitochondria and synapses were determined for the MB calyx, stalk and lobes from adjacent squares aligned from the central core to the MB margin. The association of mitochondria and synapses to intrinsic KC or extrinsic elements was not discriminated. Synaptic sites were detected from their electron dense membrane appositions. Synapses were not detected in central core regions as interpreted from immuno-light microscopy of synasin, but not allowing a precise statement because the tiny single synaptic foci are beyond the limit of confocal imaging.

In the calyx the central core region is free of synapses. Synapse numbers increase towards centrifugal neuropil parts, and a peak is found in the region of the peripheral microglomerular layer (Fig. 32A). In the stalk, the number of synapses increases at first with distance from the central core, in the areas occupied by KC II fibres (Fig. 32C). In the lobes, the most peripheral areas show less synapses (Figs. 32E, F). This phenomenon is due to a high contribution of large invading extrinsic fibres without synapses to the squares selected for counting. The extrinsic fibres arborize to tiny higher order fibres, often perpendicularly orientated between KC fibres which they synaptically contact. The KC III fibre bundles in the stalk do not contain synapses, with the exception of the distal stalk base.

The amount of mitochondria roughly parallels the situation observed for synapse numbers: together with an increase of synaptic specialisations, more mitochondria in the squares were encountered (Figs. 32A, B, D, F). A more detailed extended description is not presented because of the large amount of data and other limitations. A stereological analysis was beyond the aim of this study.

In general the ultrastructural findings confirm, complement and extend results obtained and interpreted from light microscopical investigations. The process of maturing and aging of KC neurones added in imaginal life takes place in a centrifugal manner, starting in the central core region and progressing towards the peripheral neuropil areas of the MB columnar neuropils. Dynamic changes involve the shaping of fibres, the increase of their diameters and an enrichment with organelles (tubules, mitochondria) and synaptic contacts. The progress of growth and maturing seems to be a continuous process. No indication of stepwise changes could be derived from the ultrastructural studies. The central core region with electron dense fibre profiles of different shape and with small diameter fibres of variable electron densities, not displaying synaptic connectivity, are interpreted as neuronal elements not directly integrated into fully operating functional networks of KCs and extrinsic neurones. The central core region seen by electron microscopy corresponds to the f-actin rich area of extending KC fibres detected by fluorescence microscopy.

3.7. Degeneration in the MBs

Continuous addition of newly formed KCs in larval and imaginal brains requires space in all compartments of the MBs, especially in the calyces where sprouting axons give rise to radially extending dendrites. This study provides some evidence for degeneration and loss of KCs in the pericaryal layer and in the MB neuropil. First qualitative observations have been gained from osmicated tissue of mature brains (one week old) prepared for electron microscopy. In osmicated tissue, pycnotic somata and fibres in the neuropil can be clearly discerned from intact cells by their enhanced electron density (Schürmann, 1987). The cursory findings presented from two of seven brains revealed degenerating KCs in between or clustered among intact somata. The degenerating cells in different transient states of degeneration occur intermingled or in rows in the population of KC II somata, often in peripheral parts occupied by the oldest KCs (Figs. 33A-C). The population of newly emerging KC somata display a similar electron density stated for the dying KCs, but are structurally intact (i.e. equipment and distribution of organelles). Degenerating KCs exhibit signs of autolysis, leading to a loss of membranes of organelles, finally ending with cell degradation. Degenerating somata were not found in the sprouting KC somata cluster. Events of degeneration were observed in the stalk KC I central core and small surrounding regions (Figs. 33D-G). Holes and decaying organelles point to a loss of neuronal fibres.

Further systematic studies of brains of different ages are needed to determine the role of degenerative processes in the MBs, which may accompany the addition of new cells to deliver space by replacement of old neurones.

4. Discussion

This study investigated structural characters of sprouting neurones in an adult functional brain of the insect *Gryllus bimaculatus*, in order to compare the newly added local neurones with older neurones of the same class of nerve cells. The continuously emerging cells are precursors of MB KC neurones, subjected to structural changes in the course of maturing. Dynamic processes in a large variety of neuron types generally take place in immature larval stages of insects.

In crickets, belonging to the group of hemimetabolous insects, environment, habits of life and behavioural performances of larvae obviously require functional nervous networks similar to those employed in adult forms. This holds true in particular for olfactory and mechanosensory networks in the brain, comprising the prominent primary neuropil of the antennal lobes and the secondary neuropil of the massive MBs. These two brain compartments are crucially involved in information processing of antennal sensory input and belong to the most intensely studied brain areas (Cayre et al., 2002). In fact, the small larval brains of hemimetabolous insects in principal show the structural design of the antennal lobes and MBs found in the adult insects (Farris and Strausfeld, 2001; Malaterre et al., 2002).

Mitotic events in brains of cricket larvae and also in adult brains increasing the amount of neurones have been documented for different insect groups (Cayre et al., 1996). In a number of insect species, MB neuroblast proliferation is observed during postembryonic development (Panov, 1957; Nordlander and Edwards, 1970) but in most insect species it does not continue after preimaginal development (Ito and Hotta, 1992; Fahrbach et al., 1995; Malun, 1998; Farris et al., 1999; Ganeshina et al., 2000). Persistent neurogenesis in MBs of adult insects has been described in Orthoptera and Coleoptera (Cayre et al., 1994; 1996; Gu et al., 1999), but can be missing in related forms.

An important difference between larvae and imagines with persistent formation of neurones is seen in the fact that diverse neuron types are produced in larvae,

whereas the addition of neuron types is reduced in adult brains. Therefore, the analysis of neuron development in larvae appears to be highly complex. In adult crickets, the addition of newly formed neurones stemming from persistent neuroblasts is restricted to one class of small neurones of simple design, the KCs of the MBs. The fixed position of only one cluster of these KCs within the MB space has facilitated investigation of structural features of the growing KCs. However, several limitations for a comprehensive investigation were encountered in the course of the study. Though the cricket MBs belong to the best investigated brain neuropils, their sophisticated design is far from understood. This is true for the MBs of all insect forms.

Some structural characters expressed in newly emerging and growing KCs have been given previously (Cayre et al., 1996; Malaterre et al., 2002), but a detailed study based on a number of marker molecules has not yet been provided for MBs in brains of adult crickets or other insect forms. Namely electron microscopic studies of developing KCs in the neuropil have not been undertaken. Electron microscopy is the only reliable tool for directly visualising details of the formation and sizes of neurones, and of the distribution of organelles and synapses within the tiny meshwork of fibres in the insect central nervous system (see review Watson and Schürmann, 2002).

The comparative discussion is therefore focussed firstly on some new findings on synaptic connectivity in the MBs and, secondly, more intensely on results concerning the newly added growing KCs in the central parts of the columnar MB neuropil.

4.1. Synaptic connectivity in the MBs

The present study relies on previous investigations on the layout and synaptic complexes of the MBs of the cricket and comparative studies, available for some representatives of other insect groups (Schürmann, 1987; Strausfeld et al., 1998), providing some unifying features such as compartmental design, extrinsic and intrinsic neuron types and synaptic input and output of MBs.

In particular, extrinsic MB neurones of different types and synaptically connected inside and outside the MBs have been only fragmentally investigated. Direct synaptic connectivity of two neuron types should be identified in the strict sense when both neurones have been labelled, and investigated by electron microscopy and electrophysiology. This is so far best shown only for the cholinergic iACT-PNs with KCs in the calyces in the cricket MBs (Frambach et al., 2004). A massive contribution of GABAergic extrinsic fibres considered as inhibitory elements has been found for all insect species investigated (Homberg, 1994; Leitch and Laurent, 1996; Strambi et al., 1998). The present study also shows that GABAergic fibres are unevenly distributed in the MBs of *Gryllus*, similar to the findings on the closely related species *Acheta domesticus* (Strambi et al., 1998), suggesting different weighting of GABA in MB subcompartments. The study of *Acheta* also provides information about the distribution of a GABA receptor. Interestingly, a gradient of GABA receptor density from central to peripheral portions is present in stalk column cross sections, matching the density differences of GABAergic fibres. From the studies on *Acheta* and *Gryllus* it can be deduced that the central core KC neuropil does not exhibit synaptic activity of GABA-elements or receptors indicative of postsynaptic fibres. For methodological reasons however, The study of *Acheta* does not make it possible to determine fine morphological details of GABA fibres pointing to their synaptic sites. Our study using confocal microscopy reveals small boutons in the calyces as parts of the complex glomeruli, as found in *Drosophila* (Yasuyama et al., 2002) and in bees (Schürmann and Elekes, 1997; Ganeshina and Menzel, 2001). The calycal glomeruli in the cricket and other insect species of distinct groups points to a design conserved in evolution. MB complex glomeruli of insects appear to be organised similarly to the vertebrate cerebellar glomeruli (Yasuyama et al., 2002).

Furthermore, GABAergic blebs appear to be aligned along the proximal KC dendrites, and electron microscopy shows reciprocal synapses of extrinsic fibres with KC fibres. If GABAergic blebs take part in these reciprocal synaptic complexes, the wiring of KC dendrites is more complex than previously interpreted (postsynaptic inhibition of KC dendrites). There is no sound reason from both morphological and electrophysiological investigations (Leitch and Laurent, 1996) to consider GABAergic

elements in the calyces as pure or dominant feed back neurones originally proposed for bee MBs (Bicker et al., 1985) and uncritically accepted by other investigators.

The distribution of 5-HT fibres in *Gryllus bimaculatus* corresponds to *Acheta domesticus* (Strambi et al., 1989). The study of *Acheta*, however, does not allow us to interpret for synaptic sites. The present study shows large 5-HT boutons in the peripheral calycal glomeruli, corresponding to the distribution sites of old KC II fibres. These 5-HT boutons might be central parts of complex glomeruli as stated for the cholinergic elements in *Drosophila* (Yasuyama et al., 2003) and *Gryllus* (Frambach et al., 2004). Electron microscopy shows two types of calycal boutons: a preponderant one filled with translucent synaptic vesicles and another with synaptic vesicles and dense core vesicles. The latter with two populations of vesicles may represent 5-HT boutons as found by immuno-electron microscopy (Watson and Schürmann, 2002).

The abundant classical transmitters acetylcholine, GABA and amines have not been detected in KCs (Homberg, 1994) and the nature of transmitters of KCs has not been convincingly proved up till now. Some KC classes of the cricket show a high amount of glutamate immunoreactivity, so that this compound might be a transmitter candidate in KCs (Schürmann et al., 2000). Interestingly, the central core areas of the cricket MBs and surrounding small fibres are mainly devoid of glutamate (the so called KC I fibre areas showing no or a small amount of synapses). It remains to be shown whether glutamate-like immunoreactivity is indicative of metabolic activity and/or a transmitter in the insect central nervous system.

The present study adds some findings on synaptic connectivity in some MB areas. The meaning of the complex connectivity is mainly not understood in functional terms. The functional segregation of the non isomorphous KCs and MB areas remains to be investigated by delicate electrophysiological approaches (Laurent, 2002).

4.2. The addition of newly formed KCs into the MBs of mature brains: morphological characters

The main purpose of this study on MBs of imaginal brains was to find out the newly added KCs and their growing fibres, and to describe some characters throwing light on the continuous processes leading to integration of KCs into functional synaptic networks. These networks - as discussed above - are highly complex. However, previous studies have delivered a useful basis for understanding the meaning of some synaptic pathways. The use of molecular markers signalling growth events and conventional electron microscopy has made it possible to allocate structural changes in the MBs, namely in the neuropil. In particular, no electron microscopical study has been devoted to growing immature KCs in any adult brains of any insect species. The information gained from *Gryllus bimaculatus* MBs of course only reflects some events leading to mature, fully integrated KCs.

4.2.1. The sprouting KC cluster

Our study using a technique to mark mitotic cells indicates that a conic cluster of proliferative cells exists at the anterior cortex of the MBs in imagos of *Gryllus bimaculatus*. This cluster produces new cells at all ages tested during life as first indicated by Cayre et al. (1994; 1996) in *Acheta domesticus*. No alterations of the site of mitotic activities have been stated for *Acheta* and *Gryllus*. The BRDU technique employed in the studies on KCs in *Acheta* made it possible to follow the shifting and migration of the KCs in the course of aging (Cayre et al., 1996). The cricket KCs of the cell cluster grow from the inside out at any developmental stage: the centre of the anterior MB cortex contains the youngest KCs (Cayre et al., 2000).

In a 50-day-old adult cricket, about 20% of KCs are produced during adult life, requiring a permanent remodelling of the MB cortex (Malaterre et al., 2002). It is so far not clear whether this important augmentation of KCs underlies specific cues inducing mitotic graded steps and modifying mitotic rates. If external environmental cues are considered important for mitotic activities of KC precursors, then variations

of total KC numbers and MB volumes can be expected, with the caveat that newly added KCs do not compensate for degeneration and cellular loss by aging, and volume changes are not due to shrinkage of neurones in the course of life. In fact, loss of neurones during aging is commonly observed in vertebrate and invertebrate nervous systems (Blaschke et al., 1998; Diaz et al., 1999).

Volume changes in insect brains with special regard to MBs have been investigated for larval and adult forms (Bieber and Fuldner, 1979). They are seen in the pericaryal rind and in the neuropil. Plasticity of MB volumes correlated with changes of habits of life and with environment have been reported for bees and ants (Bernstein and Bernstein, 1969; Gronenberg et al., 1996) and other insect groups (for a review see Schürmann, 1987; Meinertzhagen, 2001). In *Drosophila* differences in fibre numbers in the MB stalk are related to the modes of rearing (Technau, 1984), and increase in fibre numbers is seen in adult fruit flies, not showing mitotic activities. These volume changes in fruit flies, bees and ants concern fibre mass changes, and not MB somata. Volume changes by degeneration and shrinkage have not been systematically investigated for insect brains. MBs with a simple neuropil design found in crickets represent a suitable system for such studies.

4.2.2. Actin in developing KCs

Actin is a prominent cytoskeletal protein in the central nervous system, found unevenly distributed in somata, dendrites, axons and at synapses (Matus et al., 1982; Dailey and Smith, 1996; Felts and Smith, 1996; Kaech et al., 1997; Fischer et al., 1998; Micheva et al., 1998, Frambach et al. 2004). Actin forms filaments (polymerized F-actin) or exists in unpolymerized globular subunits (G-actin) (Capani et al., 2001). Both forms appear in neurones mixed together or separately.

In the hippocampus of vertebrate brains, an area displaying high structural and functional plasticity, an intense staining is observed for f-actin in mossy fibres. Mossy fibres continue to grow and sprout in adult brains, unlike other neuronal fibres (Amaral and Dent, 1981). During development, the actin cytoskeleton is important for such dynamic processes associated with growth cone motility and collapse, as well

as neurite modelling (Tanaka and Kirschner, 1991; Fan et al., 1993) and neuronal migration (Rakic and Komuro, 1995).

Strong accumulation of f-actin within glomerular synaptic neuropils indicates that actin plays an important role in morphological changes during neurogenesis and in established functional synaptic contacts of adult neurones (Matus, 1999; Morales et al., 2000; De Camilli et al., 2001).

To localize f-actin, binding of fluorescent phalloidin has been used in a variety of studies (Wulf et al., 1979; Rössler et al., 2002). Phalloidin labelling has provided valuable information on structures rich in f-actin, such as spines in cultured neurones and in slice preparations studied by light microscopy (Allison et al., 1998; Halpain et al., 1998). Phalloidin labelling has been found a powerful tool for spatial mapping of olfactory glomeruli in vertebrate and insect primary neuropils (Rössler et al., 2002). A recent study has demonstrated f-actin accumulation in KC dendritic tips of cricket MBs (Frambach et al., 2004). In *Drosophila* larval MBs, phalloidin heavily stained the core areas with growing KCs (Kurusu et al., 2002).

By employing this light microscopical technique, we successfully discriminated old KCs from a portion of young growing and sprouting KC elements. These neurones and their fibre bundles could be traced in detail throughout the MB neuropil of the last instar and in imaginal MBs by position and staining intensity.

The compact fibre bundle emerging from the pericaryal cluster of dividing MB cells confirms the view of a parallel arrangement of KC axons ending at the tops of α - and β -lobes derived from Golgi impregnations (Schürmann, 1973) and experimental dextran staining (Frambach and Schürmann, 2004) in crickets and in other insect species (Mobbs, 1982), and from electron microscopy (Schürmann, 1974). However, the present study could not solve the question of whether the f-actin stained central core bundles comprise all young sprouting KC fibres together with fully established axons termed KC I neurones from Golgi studies, or whether KCI fibres occur besides or intermingled with KC elements with shorter fibres and growth

cones. This is probably the case as deduced from double labelling experiments showing f-actin and tubulin (see below). A study of Malaterre et al. (2002) shows a marking of sprouting KC neurones by immunocytochemical labelling with an antibody against lachesin, an external membrane protein. This tubulin study gives the impression that more KCs are labelled than by f-actin, but does not provide information on the process of continuous growth of central core KCs. Studies to label fibres in the central core by dextran filling were mainly negative, whereas small fibres adjacent to the central core, representing older KC elements with only faint f-actin labelling could be successfully demonstrated (Frambach, personal communication). These fibres do not appear to be fully integrated synaptic KC parts.

Newly formed dendrites of young sprouting KCs could not be traced to form synapses in the calyx glomeruli. Their radial spreading of tiny f-actin positive fibre bundles from the central core suggests that they join established old KC II dendrites, serving as guide lines for the outgrowing dendrites. It is also not clear whether dendrites are formed before the new KC axons have been developed fully. An association of f-actin with extrinsic neuronal fibres, the synaptic partners of KC neurones could not be determined from limits given by their size and by confocal imaging, though this is expected. The synaptic integration of KCs and invading extrinsic fibres requires structural plasticity of both neuron classes. F-actin accumulation is not only present in dendritic but also in axonal endings of some insect neuron types (Rössler et al., 2002).

4.2.3. Tubulin expression

Microtubules are essential cytoskeletal elements providing support for the development, growth and maintenance of neuronal fibres. These organelles also represent a substantial substrate along which other organelles and molecules are transported in both directions within axons (Ahmad and Baas, 1995; Dent et al., 1999). Recent studies have indicated interactions between the actin and microtubule cytoskeletal systems, suggesting a cooperation of microtubules in many actin-requiring cellular processes, including motility and shaping of cells (Goslin et al.,

1989; Vega and Solomon, 1997; Waterman-Storer and Salmon, 1997). Interaction between microtubules and the actin cytoskeleton is needed for axonal branching (Dent and Kalil, 2001). Furthermore, a selective propagation of microtubules in growth cone steering, in response to extracellular cues, has been proposed (Lin and Forscher, 1993; Bentley and TP, 1994; Tanaka and Kirschner, 1995).

In growing MBs of *Drosophila* late larvae, tubulin is uniformly distributed in the axonal stalk and in the dorsal and medial lobe fibres of different KC classes (Watts et al., 2003). In the present study on the MBs of the cricket, immunocytochemistry showing tubulin distribution made it possible to detect staining differences for KC types, so far not investigated in MBs of adult insect brains.

In the MB anterior pericaryal layer, holding so called KC I and II somata, tubulin-like immunoreactivity occurs in marginal fibre bundles surrounding the f-actin stained central bundle which appears free of tubulin immunoreactivity or only faintly stained. This does not point to a prominent accumulation of tubules, although detected by electron microscopy. The intensity of tubulin staining is also low in dendritic fibres and in general in synaptic areas of the neuropil. Tubulin positive KC fibre bundles were traced through the columnar neuropil of the calyces, stalks and lobes outside the f-actin rich central core. The most intensely stained fibres are KC III elements of the posterior MB pericaryal rind, not showing mitotic activity in imaginal brains. In contrast, central core neuropil displays only faint expression of tubulin. This is interpreted in view of not fully developed KC fibres, not extending through the whole MB neuropil. The KC I fibres originally discerned from KCII neurones by Golgi impregnation (Schürmann, 1973) might represent gradually maturing KCs centrifugally shifted and becoming the form of the more centrifugally positioned KC II neurones. A discrimination of two types would thus no longer be valid, if KC I neuron class only represents transitional forms (see below, section electron microscopy 4.5).

4.3. Synaptic complexes in MB compartments related to KC neurones of different age

4.3.1. Synapsin distribution

Immunocytochemistry of synapsin I and electron microscopy were successfully employed in an attempt to correlate the establishment and distribution of synapses in the MBs. Synapsin labelling made it possible to safely detect presynaptic sites in the MB system, because this synaptic protein fills the whole cytoplasmic space, surrounding synaptic vesicles and mitochondria (Fabian-Fine et al., 1999), shown by immuno electron microscopy (Frambach et al., 2004). Synaptic vesicles and presynaptic active zones often occupy only minor parts of presynaptic profiles of insect synapses, below the limits of light microscopical resolution (Yasuyama et al., 2003), so that specific immunocytochemical labelling of precise sites of synaptic coupling can mainly not be used for the insect central nervous system, but at large neuro-muscular junctions (Prokop, 1999; Sigrist et al., 2000).

Light microscopy of synapsin distribution did not reveal synaptic sites in the MB pericaryal cortex. This was expected because somatic layers in insect and invertebrate nervous systems are only exceptionally endorsed with synapses, e.g. in dopaminergic fibres at KC somata of bee MBs (Blenau et al., 1999). Synaptic-like contacts were, however, occasionally detected in the MB cortex of the cricket (this study) by electron microscopy, but could not be allocated to neurones or glial cells. Glial cells may receive synaptic input (Watson and Schürmann, 2002; this study).

The central core parts of the columnar neuropil, characterized by its high levels of f-actin apparently lack synapsin staining. This area occupied by the youngest sprouting KCs and devoid of invading extrinsic fibres is interpreted not to be synaptically integrated. However, the tiny fibres directly surrounding the central core scarcely show small spots of synapsin, being in a more advanced state of development. More peripheral areas with so-called KC I fibres show higher levels of synapsin, indicating a higher density of synapses in more mature KCs. This

complements results gained from electron microscopy (Schürmann, 1974; 1987; this study). All together, the findings on synapsin and by electron microscopy (see below) are interpreted to support the view of an age-related continuous development of young KCs to become KC fibres of the KC II Golgi impregnation type, with fully expressed gestalt and synaptic coupling into operating networks. The time course leading to fully developed KCs remains to be determined. A continuous growth of newly added KCs in mature cricket brains was first proposed for *Acheta* (Cayre et al., 1996; Malaterre et al., 2002) from cortex studies, but the changes in the neuropil were not considered in these studies. Studies on larvae of the cockroach (Salecker and Boeckh, 1995) have given valuable details on sequential steps in the structural development of sensory and interneurons in the antennal lobe neuropil, but cannot explain the time course of maturing KCs.

4.3.2. Extrinsic fibres in relation to growing KCs

Identified extrinsic neurones in the MBs have mostly remained uninvestigated with respect to their synaptic layout and connectivity, with the exception of cholinergic fibres (Yasuyama et al., 2002; 2003; Frambach et al., 2004) and GABA neurones (Schürmann and Elekes, 1987; Leitch and Laurent, 1996; Ganeshina and Menzel, 2001). A putative synaptic coupling of transmitter defined extrinsic neurones with developing KCs is investigated for the first time by the present study.

No invasion of extrinsic GABA fibres is found in the central core region. A few GABA fibres terminate at the rim of the central core, in between the ring of small KCs which do not show a full development of their shape. This supports the view that the central core fibres and adjacent KC fibre bundles are not or are only marginally involved in functional networks, indispensable for olfactory information processing and for behavioural programs (Hildebrand and Shepherd, 1997; Menzel, 2001; Fiala et al., 2002; Laurent, 2002).

Interestingly no evidence was found that 5-HT fibres directly interact with young sprouting KCs. 5-HT has been repeatedly reported to be involved in the regulation of neuronal growth processes in insects and other invertebrates (Bicker, 1999; Cayre et al., 2002).

4.4. Growing KCs and ultrastructural characters

Details of ultrastructural changes during neurogenesis in larval and adult nervous systems are apparently rarely available for invertebrates (Meinertzhagen, 1996), in comparison to studies on vertebrates. An exception is the most detailed and comprehensive study of Salecker and Boeckh (1995). This study investigated growing neurones of different types in the brain antennal lobes of larval stages of the hemimetabolous cockroach, considering extracellular space, glia-neuron relationship, growth cone-like structures, membrane specializations and emerging synapses. Growing cells display a prominent overall diffuse cytoplasmic electron density in comparison to developed neurones. This is also typical for the growing KCs in the pericaryal rind and neuropilar central core of the cricket MBs. The growth cones and filopodia in larval cockroach and adult cricket brains are similarly designed. Membrane junctions of the desmosome type and synapses, present in the developing cockroach neuropil, were not detected in areas with newly added KCs in the cricket MBs. For the cockroach larval neuropil, no spacing junctions of membranes, found in the cricket MBs, have been reported. The large extracellular space in larval neuropil of *Periplaneta* appears free of electron dense material, but is indicated for the central core neuropil and between mitotic KC precursors in the cricket brain.

A striking difference between growing neurones in the cockroach and the cricket is the abundance of ribosomes in the sprouting KC fibres in the central core, far away from their somata, even detected in the distal calyx region. This is a speciality, as ribosomes are generally not found in neuronal fibres in the neuropil (Schürmann, 1987), earlier demonstrated by autoradiographic studies.

Attempts to quantify dynamic changes at the cellular and subcellular level from electron microscopic investigations in insect nervous systems have been mainly focussed on brain neuropils such as the optic lobes (Meinertzhagen, 1996), to antennal lobes (Mercer et al., 1999; Devaud et al., 2001) and MBs of *Drosophila* (Technau, 1984). These studies, not confined to newly emerging neurones, deal with distribution and dimensions of synapses, with fibre growth in relation to

developmental stages, and remodelling of networks following environmental and behavioural changes.

In imaginal *Drosophila* MBs, showing a design remarkably similar to cricket MBs, the amount of stalk fibres initially increases, to finally decrease in 3- to 4-week-old brains. Moreover, olfactory and mechanosensory deprivation led to a reduction of stalk fibres (Technau and Heisenberg, 1982; Technau, 1984). Our countings of organelles and synapses in samples of cross sections from adult cricket brains provide good evidence of growth processes in the neuropil, starting in the central core KC elements, leading to fibre outgrowth and subsequent equipment with structures reflecting functional integration into a synaptic network. The mature structure of KCs is seen in the so-called KC II neurones with their axonal fibres distant from the central core region of sprouting cells. The progressive maturation of KCs in adult brains has been proposed for *Acheta* KCs based on BRDU marking of somata (Cayre et al., 1996; Malaterre et al., 2002), showing a centrifugal shifting of somata. However, these studies did not give information on structural dynamics in the neuropil, relevant for bioelectric events and functional operation of MBs.

The present electron microscopic study though based on a small number of samples, is the first to provide information of KC fibre volume changes, tubule and synapse equipment in KC fibre bundles of different age. The ultrastructural findings complement well and extend the results gained at the light microscopical level, which have shown age correlated expression of molecule distribution. The distinction of persistent KC I and II neuron types (Schürmann, 1973) should be revised also on electron microscopic observations, when we see KC I neurones as a transient form finally becoming mature KCs of the KC II status.

4.5. Glial cells, growth and degeneration processes

Glial cells in both vertebrate and invertebrate nervous systems are highly dynamic cells, indispensable for the development and maintenance of neuronal networks. These cells are therefore in intimate relationship to neurones, and also subjected to structural dynamics (Tucker et al., 2004). An important glial role during

embryogenesis is the forming of guidance structures for migrating neurones or outgrowing axons (Rakic, 1971; 1972; Boyan et al., 1995).

In developing vertebrate brains, the class of radial glial cells guide migrating neurones by directing the outgrowth of axons (Kandel, 2000). In vertebrate and invertebrate olfactory systems, neuron-glia interactions regulate the sorting and targeting of olfactory receptor axons and the development of glomeruli (Rössler et al., 1999a; Tucker et al., 2004). (Rössler et al., 1999a) have demonstrated for antennal sensory neurones in an insect brain, that the ingrowth of axons into the antennal lobe neuropil requires glial cells in order to properly select glomeruli and to establish a somatotopic map of sensory input. Glia may affect the cell fate (Xiong and Montell, 1995) when it participates in the selective removal of degenerated cells.

In insects, the glial cells fall into different classes of cell types (Strausfeld, 1976). Unfortunately, these glial cell classes cannot be selectively demonstrated by labelling with specific molecular markers at present (Hartenstein et al., 1998). For light microscopy, propidium iodide was successfully employed to visualize neuropil glia in *Drosophila* (Devaud et al., 2003) and in the butterfly *Manduca* (Rössler et al., 1999a). The staining, however, only marks nucleic acids in the nuclei and in the cytoplasm. Glial cytoplasm can only partially be demonstrated by light microscopy, because large cytoplasmic portions do not contain ribosomes and may form small sheaths, only detected by electron microscopy. Despite these methodological limitations, some statements on glial distribution in the cricket MBs could be given. No massive contribution of glial cells to the areas of sprouting KCs was found, notably the actin rich central core fibre bundles and in the cluster of developing neurones of the pericaryal rind, nor in the neuropil occupied by older KCs. No patterns of glial cells were detected by light or electron microscopy. These findings did not make it possible to associate glial distribution with stages of KC development or with guidance functions. The observations on glia in adult MBs of the cricket *Gryllus* correspond to studies on other species (Cayre et al., 1996; Devaud et al., 2003), but cannot be generalized, because studies on the olfactory neuropil point to

glial involvement in sorting of neurones within neuropils (Salecker and Boeckh, 1995; Rössler et al., 1999a).

The question arises of which cues for the directed accurate parallel outgrowth of KC axonal fibres and for dendrites in imaginal brains could be employed if a glial role cannot be deduced from morphology. If the y-form of KC neurones has been established in early larval stages of hemimetabolous insects, these KCs with fully established fibre scaffold, neighbouring the f-actin rich central core bundle could deliver guidance information by molecules expressed at the fibre membranes to sprouting KCs (Bate, 1976; Goodman, 1996). The light microscopical findings on glial distribution are in accordance with results obtained from electron microscopy of MBs of the fruit fly and of other insect species (Schürmann, 1987; Yasuyama et al., 2002).

A direct relationship of glial and extracellular systems has been observed for the cricket MBs. Continuous disposition of extracellular space to newly added, growing KCs is needed. It remains to be shown by further investigations, how the glia is involved in extracellular space delivering processes, e.g. degeneration of neurones and growth cone modelling (Tucker et al., 2004). The decline and removal of insect neurones is performed by glial activity (Schürmann, 1980).

Genetically regulated programmed cell death (PCD) is an important process, taking place during the development and remodelling of many tissues and organs in both vertebrates and invertebrates (Saunders, 1966; Robinow et al., 1993; Blaschke et al., 1998; Diaz et al., 1999). PCD occurs via apoptosis, following a well-characterized genetic program (Kerr et al., 1972). The balance between cell death and cell division is essential to maintain cell number within a tissue. PCD could participate in regulating cell number within the neuroectoderm (Evan et al., 1995; Sanders and Wride, 1995; Conlon and Raff, 1999). Neurogenesis and neuronal cell death can occur simultaneously (Harzsch et al., 1999). This has also been suggested for lesion-induced plasticity in the olfactory system of crayfish (Sandeman et al., 1998).

In holometabolous insects, MBs in pupae undergo massive degeneration and reorganization to prepare the complex brain structure in imagos (Nordlander and Edwards, 1969; Booker and Truman, 1987; Monsma and Booker, 1996; Armstrong et al., 1998; Crittenden et al., 1998).

A massive degeneration in the MBs of adult crickets was not found, but a quantitative study on MBs of different ages is needed to understand the relationship between glia, developing neurones and extracellular space.

5. Summary

The structure and aspects of structural changes caused by the incorporation of newly generated neurones in the mushroom bodies (MBs) in the brain of the adult insect *Gryllus bimaculatus* have been investigated using light and electron microscopic methods.

The paired MBs represent a prominent columnar neuropil in the central insect brain, serving for multimodal sensory integration, most important for the organization of olfactory behaviour, and for memory and learning. The MBs always contain a class of local interneurones, the Kenyon cells (KCs) and classes of extrinsic relay neurones, connecting this neuropil with other brain areas. In adult cricket brains - in contrast to most other insect species - solely a group of KCs is continuously formed from persisting neuroblasts throughout adult life. These growing and differentiating neurones become integrated into structurally established, functional synaptic networks of complex design, which are indispensable for organizing olfactory behaviours. The processes of maturation of these newly added KCs are reflected by structural changes. The MB system of the cricket is therefore a model system allowing to describe cellular and subcellular characters in a defined cluster of emerging and sprouting local interneurones of simple design. The study employs diverse light microscopical marking techniques revealing the distribution of molecules (f-actin, tubulin, synapsin, GABA, 5-HT) and organelles essential for growth processes and indicating synaptic integration in differentially aged neurones and neuropil areas. Light microscopical studies are complemented by electron microscopy.

The study is the first approach systematically investigating the sprouting neurones in the whole MB system at the cellular and subcellular level. The main findings are listed below.

- 1) The reinvestigation of synaptic circuits in the calyx points to reciprocal synapses at KC dendrites with GABA-fibres.

- 2) The differential supply of GABA and 5-HT extrinsic fibres in the MB compartments is shown.
- 3) Sprouting new KCs localised in a small somatic cluster are the only newly added cells in adult brains, found throughout the animal's life. The cluster is already present in the brain of the last instar.
- 4) The sprouting KC somata form a compact fibre bundle extending through the whole MBs, marked by intense f-actin staining in a central core region.
- 5) Dendritic KC fibre bundles in the calyx radially project from the central core towards the peripheral layer of synaptic glomeruli. The stained fibre bundles seem to accompany unstained developed dendritic fibres.
- 6) Actin-tubulin double labelling is mainly found at the marginal parts of the central core, mainly remaining free of tubulin staining.
- 7) Light microscopy of the central core fibre bundle does not show the protein synapsin indicating lack of synapses.
- 8) The central core is not invaded by extrinsic GABA- and 5-HT-fibres. This also indicates that this region of developing KCs is not synaptically integrated.
- 9) The mitotic KC somata and the f-actin rich central core fibre bundle analysed by light microscopy corresponds to areas with cells of enhanced electron density, visualized by electron microscopy. The region of sprouting elements could be therefore easily discriminated from surrounding fibre bundles of more mature KCs.
- 10) The cluster of sprouting somata forms a fibre bundle with growth cone like structures and filopodia, also detected in the neuropil central core parts as detected by electron microscopy.
- 11) The KC fibre bundle of the central core contains ribosomes down to the level of the calyx, different from more mature fibres.
- 12) In electron micrographs no synapses and synaptic vesicles are found in the sprouting central core area.
- 13) Sprouting fibres seek extracellular space regions, filled with electron dense material of unknown origin. Extracellular space is also in direct contact to glial cytoplasm.

- 14) The central core and surrounding neuropil is mainly devoid of glial cells, forming small extensions between neuronal fibres. No pattern of glia is detected.
- 15) Determination of fibre sizes, fibre numbers, counts of tubules, mitochondria and of synapses point to a continuous growth of newly added KCs. These new KCs shift surrounding more mature KCs towards the periphery of the MBs. These results indicate that KC I and KC II neurones previously classified from Golgi impregnations should not be taken for different types, but represent KCs of different state of development.
- 16) Degeneration of KCs was only occasionally detected in one week old imaginal brains. An augmentation of KCs during adult life could occur.

The findings on the structure and structural dynamics, caused by the continuous production of KCs in adult brains are compared to results on sprouting neurones in vertebrate and insect nervous systems.

6. References

- Ahmad FJ, Baas PW. 1995.** Microtubules released from the neuronal centrosome are transported into the axon. *J Cell Science* 108: 2761-2769.
- Ajiro K, Yoda K, Utsumi K, Nishikawa Y. 1996.** Alteration of cell cycle-dependent histone phosphorylations by okadaic acid. Induction of mitosis-specific H3 phosphorylation and chromatin condensation in mammalian interphase cells. *J Biol Chem* 271: 13197-13201.
- Allison DW, Gelfand VI, Spector I, Craig AM. 1998.** Role of actin in anchoring postsynaptic receptors in cultured hippocampal neurons: Differential attachment of NMDA versus AMPA receptors. *J Neurosci* 18: 2423-2436.
- Altman J. 1962.** Are neurons formed in the brains of adult mammals? *Science* 135: 1127-1128.
- Altman J, Das GD, 1965.** Autoradiographic and histological evidence of postnatal hippocampal neurogenesis in rats. *J Comp Neurol* 124: 319-335.
- Amaral DG, Dent JA. 1981.** Development of the mossy fibers of the dentate gyrus: I. A light and electron microscopic study of the mossy fibers and their expansions. *J Comp Neurol* 195: 51-86.
- Armstrong JD, de Belle JS, Wang Z, Kaiser K. 1998.** Metamorphosis of the mushroom bodies; large-scale rearrangements of the neural substrates for associative learning and memory in *Drosophila*. *Learning Mem* 5: 102-114.
- Bate CM. 1976.** Embryogenesis of an insect nervous system. Part I: A map of the thoracic and abdominal neuroblasts in *Locusta migratoria*. *J Embryol Exp Morphol* 35: 107-123.
- Bentley D, TP OC. 1994.** Cytoskeletal events in growth cone steering. *Curr Opin Neurobiol* 4: 43-48.

- Bernstein S, Bernstein RA. 1969.** Relationships between foraging efficiency and the size of the head and component brain and sensory structures in the red wood ant. *Brain Res* 16:85–104
- Bicker G. 1999.** Histochemistry of classical neurotransmitters in antennal lobes and mushroom bodies of the honeybee. *Microsc Res and Tech* 45: 174-183
- Bicker G, Schäfer S, Kingan TG. 1985.** Mushroom body feedback interneurons in the honeybee show GABA-like immunoreactivity. *Brain Res* 360: 394-397.
- Bieber M, Fuldner D. 1979.** Brain growth during adult stage of a holometabolous insect. *Naturwissenschaften* 66: 426.
- Blaschke AJ, Weiner JA, Chun J. 1998.** Programmed cell death is a universal feature of embryonic and postnatal neuroproliferative regions throughout the central nervous system. *J Comp Neurol* 396: 39-50.
- Blenau W, Schmidt M, Schürmann F-W. 1999.** Neurons with dopamine-like immunoreactivity target mushroom body Kenyon cell somata in the brain of some hymenopteran insects. *Int J Insect Morphol Embryol* 28: 203-210.
- Booker R, Truman JW. 1987.** Postembryonic neurogenesis in the CNS of the tobacco hornworm, *Manduca sexta*. II. Hormonal control of imaginal nest cell degeneration and differentiation during metamorphosis. *J Neurosci* 7: 4107-4114.
- Boyan GS, Williams JLD, Reichert H. 1995.** Organization of a midline proliferative cluster in the embryonic brain of the grasshopper. *Roux's Arch Dev Biol* 205: 45-53.
- Capani F, Ellisman MH, Martone ME. 2001.** Filamentous actin is concentrated in specific subpopulations of neuronal and glial structures in rat central nervous system. *Brain Res* 923: 1-11.
- Cayre M, Malaterre J, Charpin P, Strambi C, Strambi A. 2000.** Fate of neuroblast progeny during postembryonic development of mushroom bodies in the house cricket, *Acheta domesticus*. *J Insect Physiol* 46: 313-319.

- Cayre M, Malaterre J, Scotto Lomassese S, Strambi C, Strambi A. 2002.** The common properties of neurogenesis in the adult brain: From invertebrates to vertebrates. *Comp Biochem Physiol B* 132: 1-15.
- Cayre M, Strambi C, Charpin P, Augier R, Meyer MR, Edwards JS, Strambi A. 1996.** Neurogenesis in adult insect mushroom bodies. *J Comp Neurol* 371: 300-310.
- Cayre M, Strambi C, Strambi A. 1994.** Neurogenesis in adult insect brain and its hormonal control. *Nature* 368: 57-59.
- Chadee DN, Taylor WR, Hurta RA, Allis CD, Wright JA, Davie JR. 1995.** Increased phosphorylation of histone H1 in mouse fibroblasts transformed with oncogenes or constitutively active mitogen-activated protein kinase kinase. *J Biol Chem* 270: 20098-20105.
- Chetverukhin VK, Polenov AL. 1993.** Ultrastructural radioautographic analysis of neurogenesis in the hypothalamus of the adult frog, *Rana temporaria*, with special reference to physiological regeneration of the preoptic nucleus. I. Ventricular zone cell proliferation. *Cell Tissue Res* 271: 341-350.
- Colicos MA, Collins BE, Sailor MJ, Goda Y. 2001.** Remodeling of synaptic actin induced by photoconductive stimulation. *Cell* 107: 605-616.
- Conlon I, Raff M. 1999.** Size control in animal development. *Cell* 96: 235-244.
- Crittenden JR, Skoulakis EMC, Han KA, Kalderon D, Davis RL. 1998.** Tripartite mushroom body architecture revealed by antigenic markers. *Learning Mem* 5: 38-51
- Dailey ME, Smith SJ. 1996.** The dynamics of dendritic structure in developing hippocampal slices. *J Neurosci* 16: 2983-2994.
- De Camilli P, Benfenati F, Valtorta F, Greengrad P. 1990.** The synapsins. *Annu Rev Cell Biol* 6: 433-460.

- De Camilli P, Haucke V, Takei K, Mugnaini E. 2001.** The Structure of synapses. Cowan MW, Südhof TC, Stevens CF, Davis K, Editors. Synapses. Baltimore: The John Hopkins University Press. P. 89-133.
- De Camilli P, Thomas A, Cofield R, Folli F, Lichte B, Piccolo G, Meinck HM, Austoni M, Fassetta G, Bottazzo GF, Bates D, Cartlidge N, Solimena M, Kilimann MW. 1993.** The synaptic vesicle-associated protein amphiphysin is the 128-kD autoantigen of Stiff-Man syndrome with breast cancer. *J Exp Med* 178: 2219-2223.
- Dent EW, Callaway JL, Szebenyi G, Baas PW, Kalil K. 1999.** Reorganization and movement of microtubules in axonal growth cones and developing interstitial branches. *J Neurosci* 19: 8894-8908.
- Dent EW, Kalil K. 2001.** Axon branching requires interactions between dynamic microtubules and actin filaments. *J Neurosci* 21: 9757-9769.
- Devaud JM, Acebes A, Ferrus A. 2001.** Odor exposure causes central adaptation and morphological changes in selected olfactory glomeruli in *Drosophila*. *J Neurosci* 221: 6274-6282.
- Devaud JM, Keane J, Ferrus A. 2003.** Blocking sensory inputs to identified antennal glomeruli selectively modifies odorant perception in *Drosophila*. *J Neurobiol* 56(1): 1-12.
- Diaz B, Pimemtel B, De Pablo F, De La Rosa EJ. 1999.** Apoptotic cell death of proliferating neuroepithelial cells in the embryonic retina is prevented by insulin. *Eur J Neurosci* 11: 1624-1632.
- Dujardin F. 1850.** Memoire sur le systeme nerveux des insectes. *Ann Sci Nat Zool* 14: 547-560.
- Erber J, Homberg U, Gronenberg W. 1987.** Functional roles of the mushroom bodies in insects. In *arthropod brain: Its evolution, development, structure, and functions* (ed. P. Gupta), P. 485-511. John Wiley & Sons, New York, NY.

- Eriksson PS, Perfilieva E, Bjork-Eriksson T, Alborn AM, Nordborg C, Peterson, DA, Gage FH. 1998.** Neurogenesis in the adult human hippocampus. *Nat Med* 4: 1313-1317.
- Evan GI, Brown L, Whyte M, Harrington E. 1995.** Apoptosis and the cell cycle. *Curr Opin Cell Biol* 7: 825-834.
- Fabian-Fine R, Volkhardt W, Seyfarth EA. 1999.** Peripheral synapses at identifiable mechanosensory neurons in the spider *Cupiennius salei*: Synapsin-like immunoreactivity. *Cell Tissue Res* 295: 13-19.
- Fahrbach SE, Strande JL, Robinson GE. 1995.** Neurogenesis is absent in the brains of adult honeybees and does not explain behavioural neuroplasticity. *Neurosci Lett* 197: 145-148.
- Fan J, Mansfield SG, Redmond T, Gordon-Weeks PR, Raper JA. 1993.** The organization of f-actin and microtubules in growth cones exposed to a brain-derived collapsing factor. *J Cell Biol* 121: 867-878.
- Farris SM, Robinson GE, Davis RL, Fahrbach SE. 1999.** Larval and pupal development of the mushroom bodies in the honeybee, *Apis mellifera*. *J Comp Neurol* 414: 97-113.
- Farris SM, Sinakevitch I. 2003.** Development and evolution of the insect mushroom bodies: Towards the understanding of conserved developmental mechanisms in a higher brain center. *Arthropod Structure & Development* 32: 79-101.
- Farris SM, Strausfeld NJ. 2001.** Development of laminar organization on the mushroom bodies of the cockroach: Kenyon cell proliferation, outgrowth, and maturation. *J Comp Neurol* 439: 331-351.
- Felts PA, Smith KJ. 1996.** Blood-brain barrier permeability in astrocyte-free regions of the central nervous system remyelinated by Schwann cells. *Neuroscience* 75: 643-655.
- Fiala A, Spall T, Diegelmann S, Eisermann B, Sachse S, Devaud JM, Buchner E, Galizia CG. 2002.** Genetically expressed cameleon in *Drosophila*

- melanogaster* is used to visualize olfactory information in projection neurons. Curr Biol 12: 1877-1884.
- Fischer M, Kaech S, Knutti D, Matus A. 1998.** Rapid actin-based plasticity in dendritic spines. Neuron 20: 847-854.
- Frambach I, Rössler W, Winkler M, Schürmann F-W. 2004.** F-actin at identified synapses in the mushroom bodies of the insect brain. J Comp Neurol 475: 303-314.
- Frambach I, Schürmann F-W. 2004.** Separate distribution of deutocerebral projection neurones in the mushroom bodies of the cricket brain. Acta Biol Hung 55(1-4): 21-29.
- Ganeshina O, Menzel R. 2001.** GABA-immunoreactive neurons in the mushroom bodies of the honeybee: An electron microscopic study. J Comp Neurol 437: 335-349.
- Ganeshina O, Schäfer S, Malun D. 2000.** Proliferation and programmed cell death of neuronal precursors in the mushroom bodies of the honeybee. J Comp Neurol 417: 349-365.
- Goodman CS. 1996.** Mechanisms and molecules that control growth cone guidance. Annu Rev Neurosci 19: 341-377.
- Goslin K, Birgbauer E, Banker G, Solomon F. 1989.** The role of cytoskeleton in organizing growth cones: a microfilament-associated growth cone component depends upon microtubules for its localization. J Cell Biol 109: 1621-1631.
- Gould E, Beylin A, Tanapat P, Reeves A, Shors TJ. 1999.** Learning enhances adult neurogenesis in the hippocampal formation. Nat Neurosci 2(3): 260-265.
- Greengrad P, Valtora F, Czernik AJ, Benfenatti F. 1993.** Synaptic vesicle phosphoproteins and regulation of synaptic function. Science 259: 780-785.

- Gronenberg W, Heeren S, Hölldobler B. 1996.** Age-dependent and task-related morphological changes in the brain and the mushroom bodies of the ant, *Camponotus floridanus*. J Exp Biol 119: 2011-2019.
- Gu SH, Tsia WH, Chiang AS, Chow YS. 1999.** Mitogenic effects of 20-hydroxyecdysone on neurogenesis in adult mushroom bodies of the cockroach *Diploptera punctata*. J Neurobiol 39: 264-274.
- Hähnlein I, Bicker G. 1997.** Glial patterning during postembryonic development of central neuropiles in the brain of the honeybee. Dev Genes Evol 207: 29-41.
- Halpain S, Hipolito A, Saffer L. 1998.** Regulation of f-actin stability in dendritic spines by glutamate receptors and calcineurin. J Neurosci 18: 9835-4984.
- Harris KM. 1999.** Structure, development, and plasticity of dendritic spines. Curr Opin Neurobiol 9: 343-348.
- Hartenstein V, Nassif C, Lekven A. 1998.** Embryonic development of the *Drosophila* brain II. The glia cells of the brain. J Comp Neurol 402: 32-48.
- Harzsch S, Miller J, Benton J, Beltz B. 1999.** From embryo to adult: Persistent neurogenesis and apoptotic cell death shape the Lobster deutocerebrum. J Neurosci 19(9): 3472-3485.
- Heisenberg M. 1998.** What do the mushroom bodies do for the insect brain? An introduction. Learning Mem 5: 1-10.
- Heisenberg M, Heusipp M, Wanke C. 1995.** Structural plasticity in the *Drosophila* brain. J Neurosci 15: 1951-1960.
- Hildebrand JG, Shepherd GM. 1997.** Mechanisms of olfactory discrimination: Converging evidence for a common principle across Phyla. Annu Rev Neurosci 20: 595-631.
- Hörner M. 1999.** Cytoarchitecture of histamine-, dopamine-, serotonin- and octopamine-containing neurons in the cricket ventral nerve cord. Microscopy Research and Technique 44: 137-165.

- Homberg U. 1994.** Distribution of neurotransmitters in the insect brain. Rathmeyer W. (ed.) Progress in Zoology. Fischer Verlag, Stuttgart, P. 1-88.
- Honegger H-W, Schürmann F-W. 1975.** Cobalt sulfide staining of optic fibres in the brain of the cricket, *Gryllus bimaculatus*. Cell Tissue Res 159: 213-225.
- Huber F. 1960.** Untersuchungen über die Funktion des Zentralnervensystems und insbesondere des Gehirns bei der Fortbewegung und der Lauterzeugung der Grillen Z Vergl Physiol 44: 60-132.
- Huntley GW, Benson DL, Colman DR. 2002.** Structural remodeling of the synapse in response to physiological activity. Cell 11: 1-4.
- Huttner WB, Schiebler W, Greengrad P, De Camilli P. 1983.** Synapsin I (protein I) a nerve terminal-specific phosphoprotein. III. Its association with specific vesicles studied in a highly purified synaptic vesicle preparation. J Cell Biol 96: 1374-1388.
- Ito K, Hotta Y. 1992.** Proliferation pattern of postembryonic neuroblasts in the brain of *Drosophila melanogaster*. Dev Biol 149: 134-148.
- Johansson AS. 1957.** The nervous system of the milkweed bug *Oncopeltus fasciatus* (Heteroptera, Lygaeidae). Trans Amer Entomol Soc 83: 119-183.
- Johns PR, Easter SS. 1977.** Growth of the adult goldfish eye II. Increase in retinal cell number. J Comp Neurol 176: 331-342.
- Kaech S, Fischer M, Doll T, Matus A. 1997.** Isoform specificity in the relationship of actin to dendritic spines. J Neurosci 17: 9565-9572.
- Kandel ER. 2000.** Nerve cells and behavior. In "Principles of Neural Science" Ed. Kandel ER et al., 4 Edition. McGraw-Hill, P. 19-35.
- Kaplan MS, Hinds JW. 1977.** Neurogenesis in the adult rat: Electron microscopic analysis of light autoradiographs. Science 197: 1092-1095.

- Kempermann G, Gage FH. 1999.** Experience-dependent regulation of adult hippocampal neurogenesis: Effects of long-term stimulation and stimulus withdrawal. *Hippocampus* 9: 321-332.
- Kenyon CF. 1896.** The meaning and structure of so-called " mushroom bodies" of the hexapod brain. *Am Naturalist* 30: 643-650.
- Kerr JF, Wyllie AH, Currie AR. 1972.** Apoptosis: a basic biological phenomenon with wide-ranging implications in tissue kinetics. *Br J Cancer* 26: 239-257.
- Klagges BRE, Heimbeck G, Godenschwege TA, Hofbauer A, Pflugfelder GO, Reifegerste R, Reisch D, Schaupp M, Buchner S, Buchner E. 1996.** Invertebrate synapsins: A single gene codes for several isoforms in *Drosophila*. *J Neurosci* 16: 3154-3165.
- Knobel KM, Jorgensen EM, Bastiani MJ. 1999.** Growth cones stall and collapse during axon outgrowth in *Caenorhabditis elegans*. *Development* 126(20): 4489-4498.
- Kurusu M, Awasaki T, Masuda-Nakagawa LM, Kawauchi H, Ito K, Furukubo-Tokunaga K. 2002.** Embryonic and larval development of the *Drosophila* mushroom bodies: Concentric layer subdivisions and the role of fasciclin II. *Development* 129: 409-419.
- Laurent G. 2002.** Olfactory network dynamics and the coding of multidimensional signals. *Nat Rev Neurosci* 11: 884-95
- LeDizet M, Piperno G. 1991.** Detection of acetylated alpha-tubulin by specific antibodies. *Methods Enzymol* 196: 264-274.
- Leitch B, Laurent G. 1996.** GABAergic synapses in the antennal lobe and mushroom body of the locust olfactory system. *J Comp Neurol* 372: 487-514.
- Liddell E, Weeks I. 1996.** Antikörper-Techniken: Spektrum Akademischer Verlag GmbH Heidelberg, Berlin, Oxford.

-
- Lin CH, Forscher P. 1993.** Cytoskeletal remodeling during growth cone-target interactions. *J Cell Biol* 121: 1369-1383.
- Mahadevan LC, Willis AC, Barratt MJ. 1991.** Rapid histone H3 phosphorylation in response to growth-factors, phorbol esters, okadaic acid, and protein-synthesis inhibitors. *Cell* 65: 775–783
- Malaterre J, Strambi C, Aouane A, Strambi A, Cayre M. 2002.** Development of cricket mushroom bodies. *J Comp Neurol* 452: 215-227.
- Malun D. 1998.** Early development of mushroom bodies in the brain of the honeybee *Apis mellifera* as revealed by BrdU incorporation and ablation experiments. *Learning Mem* 5: 90-101.
- Mashaly A, Schürmann F-W, Frambach I. 2003.** A substrate for plasticity: Sprouting neurons in an olfactory neuropile of the mature cricket brain. In: Mommsen TP, Walsh PJ. (eds.) *Comparative biochemistry and physiology. Abstracts of the annual main meeting of the society for experimental biology*, Elsevier 134A(3): 67.
- Matus A. 1999.** Postsynaptic actin and neuronal plasticity. *Curr Opin Neurobiol.* 9: 561-565.
- Matus A. 2000.** Actin-based plasticity in dendritic spines. *Science* 290: 754-758.
- Matus A, Ackermann M, Pehling G, Byers HR, Fujiwara K. 1982.** High actin concentrations in brain dendritic spines and postsynaptic densities. *Proc Natl Acad Sci USA* 79: 7590-7594.
- Meinertzhagen IA. 1996.** Ultrastructure and quantification of synapses in the insect nervous system. *J Neurosci Methods* 69: 59-73.
- Meinertzhagen IA. 2001.** Plasticity in the insect nervous system. *Adv Insect Physiol* 28: 84-167
- Menzel R. 2001.** Searching for the Memory Trace in a Mini-Brain, the Honeybee. *Lern & Mem* 8: 53-62.

- Mercer AR, Brown S, Dunston C, Kirchhof B, Kokay I, Perk C, Sigg D, Winnington A. 1999.** Behaviour-related plasticity in the antennal lobes of the honey bee, *Apis mellifera* L., Göttingen Neurobiology Report, Volume I, N. Elsner and U. Eysel (Eds), Thieme Verlag, (1999) 129
- Micheva KD, Vallée A, Beaulieu C, Herman IM, Leclerc N. 1998.** β -actin is confined to structures having high capacity of remodelling in developing and adult rat cerebellum. *Eur J Neurosci* 10: 3785-3798.
- Mobbs PG. 1982.** The brain of the honeybee *Apis mellifera*. I. Connections and spatial organization of the mushroom bodies. *Philos Trans R Soc Lond (Biol)* 298: 309-354.
- Monsma SA, Booker R. 1996.** Genesis of the adult retina and outer optic lobes of the moth, *Manduca sexta*. I. Patterns of proliferation and cell death. *J Comp Neurol* 367: 10-20.
- Morales M, Colicos MA, Goda Y. 2000.** Actin-dependent regulation of neurotransmitter release at central synapses. *Neuron* 27: 539-550.
- Neder R. 1959.** Allometrisches Wachstum von Hirnteilen bei drei verschieden großen Schabenarten. *Zool Jb Anat* 77: 411-464.
- Nordlander RH, Edwards JS. 1969.** Postembryonic brain development in the monarch butterfly, *Danaus plexippus plexippus* L. I. Cellular events during brain morphogenesis. *Wilhelm Roux Archiv für Entwicklungsmechanik der Organismen (Berlin)* 162:197-217
- Nordlander RH, Edwards JS. 1970.** Postembryonic brain development in the monarch butterfly, *Danaus plexippus* L. *Wilhelm Roux Arch* 164: 247-260.
- Panov AA. 1957.** The structure of the brain in insects in successive stages of postembryonic development. *Entomol Rev USSR* 36: 269-284.
- Panov AA. 1960.** The structure of insect brain during successive stages of postembryonic development. III Optic lobes. *Rev Entomol URSS* 39: 55-68.

- Pipa RL. 1973.** Proliferation, movement, and regression of neurons during the postembryonic development of insects. In: Developmental neurobiology of arthropods (ed. Young D.) P. 105-129, New York, Cambridge University Press.
- Prokop A. 1999.** Integrating bits and pieces: Synapse structure and formation in *Drosophila* embryos. *Cell Tissue Res* 29: 169-186.
- Rakic P. 1971.** Neuron-glia relationship during granule cell migration in developing cerebellar cortex. A Golgi and electron microscopic study in *Macacus rhesus*. *J Comp Neurol* 141: 283-312.
- Rakic P. 1972.** Mode of cell migration to the superficial layers of fetal monkey neocortex. *J Comp Neurol* 145: 61-84.
- Rakic P, Komuro H. 1995.** The role of receptor / channel activity in neuronal cell migration. *J Neurobiol* 26: 299-315.
- Raymond PA, Easter SS. 1983.** Postembryonic growth of the optic tectum in goldfish. I. Location of germinal cells and numbers of neurons produced. *J Neurosci* 3: 1077-1091.
- Reynolds ES. 1963.** The use of lead citrate at high pH as an opaque stain in electron microscopy. *J Cell Biol* 17: 208-212.
- Rössler W, Kuduz J, Schürmann F-W, Schild D. 2002.** Aggregation of f-actin in olfactory glomeruli: A common feature of glomeruli across phyla. *Chem Senses* 27: 803-810.
- Rössler W, Oland LA, Higgins MR, Hildebrand JG, Tolbert LP. 1999a.** Development of a glia-rich axon-sorting zone in the olfactory pathway of the moth *Manduca sexta*. *J Neurosci* 19: 9865-9877
- Rössler W, Randolph PW, Tolbert LP, Hildebrand JG. 1999b.** Axons of olfactory receptor cells of transsexually grafted antennae induce development of sexually dimorphic glomeruli in *Manduca sexta*. *J Neurobiol* 38: 521-541.

- Robinow S, Talbot WS, Hogness DS, Truman JW. 1993.** Programmed cell death in the *Drosophila* nervous system is ecdysone-regulated and coupled with specific ecdysone receptor isoform. *Development* 119: 1251-1259.
- Robinson DG, Ehlers U, Herken R, Herrmann B, Mayer F, Schürmann F-W. 1985.** Präparationsmethodik in der Elektronenmikroskopie –Eine Einführung für Biologen und Mediziner-. Springer-Verlag Berlin Heidelberg New York Tokyo.
- Rosbach W. 1962.** Histologische Untersuchungen über die Hirne naheverwandter Rüsselkäfer (Curculionidae) mit unterschiedlichem Brutfürsorgeverhalten. *Z Morphol Ökol Tiere* 50: 616-650.
- Salecker I, Boeckh J. 1995.** Embryonic development of the antennal lobes of a hemimetabolous insect, the cockroach *Periplaneta americana*: Light and electron microscopic observations. *J Comp Neurol* 352: 33–54
- Sandeman RE, Clarke D, Sandeman D, Manly M. 1998.** Growth-related and antennular amputation-induced changes in the olfactory centers of crayfish brain. *J Neurosci* 18: 6195-6209.
- Sandeman RE, Sandeman DC. 2000.** "Impoverished" and "Enriched" living conditions influence the proliferation and survival of neurons in crayfish brain. *J Neurobiol* 45: 215-226.
- Sanders EJ, Wride MA. 1995.** Programmed cell death in development. *Int Rev Cyto* 163: 105-173.
- Sasaki DT, Dumas SE, Engleman EG. 1987.** Discrimination of viable and non-viable cells using propidium iodide in two color immunofluorescence. *Cytometry* 8: 413-420.
- Saunders JW. 1966.** Death in embryonic systems. *Science* 154: 604-612.
- Schildberger K. 1981.** Some physiological features of mushroom body linked fibers in the house cricket brain. *Naturwissenschaften* 67: 623

- Schildberger K. 1983.** Local interneurons associated with the mushroom bodies and the central body in the brain of *Acheta domesticus*. Cell Tissue Res 230: 573-586.
- Schildberger K. 1984.** Multimodal interneurons in the cricket brain: Properties of identified extrinsic mushroom body cells. J Comp Physiol A 154: 71-79.
- Schmidt, M. 2001.** Neuronal differentiation and long-term survival of newly generated cells in the olfactory mid-brain of the adult spiny lobster, *Panulirus argus*. J. Neurobiol. 48: 181-203.
- Schürmann F-W. 1971.** Synaptic contacts of association fibres in the brain of the bee. Brain Res 26: 169-176.
- Schürmann F-W. 1972.** Über die Struktur der Pilzkörper des Insektenhirns II. Synaptische Schaltungen im Alpha-Lobus des Heimchens *Acheta domesticus* L. Z Zellforsch 127: 240-257
- Schürmann F-W. 1973.** Über die Struktur der Pilzkörper des Insektenhirns. III. Die Anatomie der Nervenfasern in den Corpora pedunculata bei *Acheta domesticus* L.: (Orthoptera): Eine Golgi-Studie. Z Zellforsch 145: 247-285.
- Schürmann F-W. 1974.** Bemerkungen zur Funktion der Corpora pedunculata im Gehirn der Insekten aus morphologischer Sicht. Exp Brain Res 19: 406-432.
- Schürmann F-W. 1980.** Experimental anterograde degeneration of nerve fibers: A tool for combined light- and electron-microscopic studies of the insect nervous system. In: Strausfeld NJ, Miller TA, (Ed.) Neuroanatomical techniques, insect nervous system. Springer, New York Heidelberg Berlin. P. 263-281.
- Schürmann F-W. 1987.** The architecture of the mushroom bodies and related neuropiles in the insect brain. In Gupta AP, Ed. Arthropod brain: Its evolution, development, structure and functions. Wiley and Sons, New York P. 231-264.
- Schürmann F-W, Elekes K. 1997.** Synaptic connectivity in the mushroom bodies of the honey bee brain: Electron microscopy and immunocytochemistry of

- neuroactive compounds. In: Menzel R, Mercer A, (Ed.) Neurobiology and behaviour in honeybees. Springer, Berlin P. 225-234.
- Schürmann F-W, Ottersen OP, Honegger HW. 2000.** Glutamate-like immunoreactivity marks compartments of the mushroom bodies in the brain of the cricket. *J Comp Neurol* 418: 227-239.
- Scotto Lomassese S, Strambi C, Strambi A, Aouane A, Augier R, Rougon G, Cayre M. 2003.** Suppression of adult neurogenesis impairs olfactory learning and memory in an adult insect. *J Neurosci* 23: 9289-9296.
- Scotto Lomassese S, Strambi C, Strambi A, Cayre M. 2002.** Sensory inputs stimulate progenitor cell proliferation in an adult insect brain. *Current Biology* 12: 1001-1005.
- Scotto Lomassese S, Strambi C, Strambi A, Charpin P, Augier R, Aouane A, cayre M. 2000.** Influence of environmental stimulation on neurogenesis in the adult insect brain. *J Neurobiol* 45: 162-171.
- Sharp DJ, Yu W, Ferhat L, Kuriyama R, Rueger DC, Baas PW. 1997.** Identification of a microtubule-associated motor protein essential for dendritic differentiation. *J Cell Biol* 138(4): 833-843.
- Sigrist SJ, Thiel PR, Reiff DF, Lachance PE, Lasko P, Schuster CM. 2000.** Postsynaptic translation affects the efficacy and morphology of neuromuscular junctions. *Nature* 405: 1062-1065.
- Sinakevitch I, Farris SM, Strausfeld NJ. 2001.** Taurine-, aspartate-, and glutamate-like immunoreactivity identifies chemically distinct subdivisions of Kenyon cells in the cockroach mushroom body. *J Comp Neurol* 439: 352-367.
- Stopfer M, Jayaraman V, Laurent G. 2003.** Intensity versus identity coding in an olfactory system. *Neuron* 39: 991-1004.
- Strambi C, Bennis N, Renucci M, Charpin P, Augier R, Strambi A, Cymborowski B, Puizillout J-J. 1989.** Serotonin-immunoreactive neurons in the cerebral complex of *Acheta domesticus*. Experimental study in normal and drug treated

- insects. Zoologischer Jahrbucher Abteilung fur Allgemeine Zoologie und Physiologie der Tiere. 93: 353-374.
- Strambi C, Cayre M, Satelle DB, Augier R, Charpin P, Strambi A. 1998.** Immunocytochemical mapping of an RDL-Like GABA-receptor subunit and of GABA in brain structures related to learning and memory in the cricket *Acheta domestica*. Learning Mem 5: 78-88.
- Strausfeld NJ. 1976.** Atlas of an insect brain. Springer, Berlin, Germany.
- Strausfeld NJ, Hansen L, Li Y, Gomez RS, Ito K. 1998.** Evolution, discovery, and interpretations of arthropod mushroom bodies. Learning Mem 5: 11-37.
- Strausfeld NJ, Li Y. 1999.** Organization of olfactory and multimodal afferent neurons supplying the calyx and pedunculus of the cockroach mushroom bodies. J Comp Neurol 409: 603-625.
- Tanaka EM, Kirschner MW. 1991.** Microtubule behavior in the growth cones of living neurons during axon elongation. J Cell Biol 115: 345-363.
- Tanaka E, Kirschner MW. 1995.** The role of microtubules in growth cone turning at substrate boundaries. J Cell Biol 128: 127-137.
- Technau G. 1984.** Fiber number in the mushroom bodies of adult *Drosophila melanogaster* depends on age, sex, and experience. J Neurogenet 1: 113-126.
- Technau G, Heisenberg M. 1982.** Neural reorganization during metamorphosis of the corpora pedunculata in *Drosophila melanogaster*. Nature 295: 405-407.
- Tucker ES, Oland LA, Tolbert LP. 2004.** In vitro analyses of interactions between olfactory receptor growth cones and glial cells that mediate axon sorting and glomerulus formation. J Comp Neurol 472: 478-495.
- Van Praag H, Christie BR, Sejnowski TJ, Gage FH. 1999.** Running enhances neurogenesis, learning and long-term potentiation in mice. Proc Natl Acad Sci USA. 13427-13431.

- Vega LR, Solomon F. 1997.** Microtubule function in morphological differentiation: Growth zones and growth cones. *Cell* 89: 825-828.
- Vowles DM. 1964.** Olfactory learning and brain lesions in the wood ant (*Formica rufa*). *J Comp Physiol Psychol* 58: 105-111.
- Waterman-Storer CM, Salmon ED. 1997.** Actomyosin-based retrograde flow of microtubules in the lamella of migrating epithelial cells influences microtubule dynamic instability and turnover and is associated with microtubule breakage and treadmilling. *J Cell Biol* 139: 417-434.
- Watson AHD, Schürmann F-W. 2002.** Synaptic structure distribution and circuitry in the central nervous system of the locust and related insects. *Microsc Res Tech* 56: 210-226.
- Watts RJ, Hoopfer ED, Luo L. 2003.** Axon pruning during *Drosophila* metamorphosis: Evidence for local degeneration and requirement of the ubiquitin-proteasome system. *Neuron* 38: 871-885.
- Weiss MJ. 1981.** Structural patterns in the corpora pedunculata of Orthoptera: A reduced silver analysis. *J Comp Neurol* 203: 515-525.
- Witthöft W. 1967.** Absolute Anzahl und Verteilung der Zellen im Hirn der Honigbiene. *Zeitschrift für Morphologie der Tiere* 61: 160-164.
- Wulf E, Deboen A, Bautz A, Faulstich H, Wieland TH. 1979.** Fluorescent phalloidin, a tool for the visualization of cellular actin. *Proc Natl Acad Sci USA* 76: 4498-4502.
- Xiong W -C, Montell C. 1995.** Defective glia induce neuronal apoptosis in the *repo* visual system of *Drosophila*. *Neuron* 14: 581-590.
- Yang MY, Armstrong JD, Vilinsky I, Strausfeld NJ, Kaiser K. 1995.** Subdivision of the *Drosophila* mushroom bodies by enhancer-trap expression patterns. *Neuron* 15: 45-54.

Yasujama K, Meinertzhagen IA, Schürmann F-W. 2002. Synaptic organization of the mushroom body calyx in *Drosophila melanogaster*. *J Comp Neurol* 445: 211-226.

Yasujama K, Meinertzhagen IA, Schürmann F-W. 2003. Synaptic connections of cholinergic antennal lobe relay neurons innervating the lateral horn neuropile in the brain of *Drosophila melanogaster*. *J Comp Neurol* 466: 299-315.

Zars T, Fischer M, Schulz R, Heisenberg M. 2000. Localization of short-term memory in *Drosophila*. *Science* 288: 672-675.

7. Appendix of figures

The appendix contains plates of light micrographs (Figures 2-8, 11-16) and electron micrographs (Figures 9, 10, 17-31, 33). All confocal and epifluorescence images are from vibratome sections. All toluidine blue stained micrographs are from semithin sections of brains fixed for conventional electron microscopy. All abbreviations used in figures and figure legends can also be found in the list of abbreviations.

Figure 2: Mushroom body sprouting Kenyon cells. Toluidine blue staining of semithin sections (A;B); f-actin-phalloidin staining (green) and anti-phospho histone mitosis marking of somata (red); confocal images (C-F).

A: Cluster of proliferating KCs (arrowhead) at the margin of the pericaryal layer (PL); dark extracellular space (triangle) in the central anterior calyx (CA); posterior calyx (CP); glomerular layer in the marginal CA (asterisks); frontal section.

B: Cluster of sprouting Kenyon cells (SKC) in the pericaryal layer (PL); note the shell of surrounding weakly stained KCs; horizontal section.

C: Sprouting KCs form a distinct intensely stained fibre bundle (arrow), descending from the pericaryal layer into the central anterior calyx and projecting through the alpha- (AL) and beta- (BL) lobes (arrows). The marginal glomerular calyx zone (asterisk) and other synaptic neuropils are also stained; sagittal section.

D: The cluster of mitotic cells (arrowheads, anti-phospho histone immunocytochemistry) in the centre of the pericaryal layer is intensely stained, frontal section.

Inset: Higher magnification from (D) showing the mitotic cell cluster (arrowhead), surrounded by a shell of unstained KCs.

E, F: Double staining of the MB mitotic cells (arrowheads, red) in the central pericaryal layer; note the fluorescent bundle (green, arrows) descending to the anterior calyx (CA) with radial branches (small arrow), directed towards the marginal glomerular calyx neuropil (asterisks). The glomeruli are intensely marked, forming a pattern of fluorescent spots; the central sprouting fibre bundle projects through the calyx to the stalk (P); note unstained extracellular space (triangle); images from a stack of optical sections: Posterior calyx (CP), frontal sections.

Scale bars: A: 30 μm ; B: 20 μm ; C, D: 50 μm ; Inset D, E, F: 20 μm .

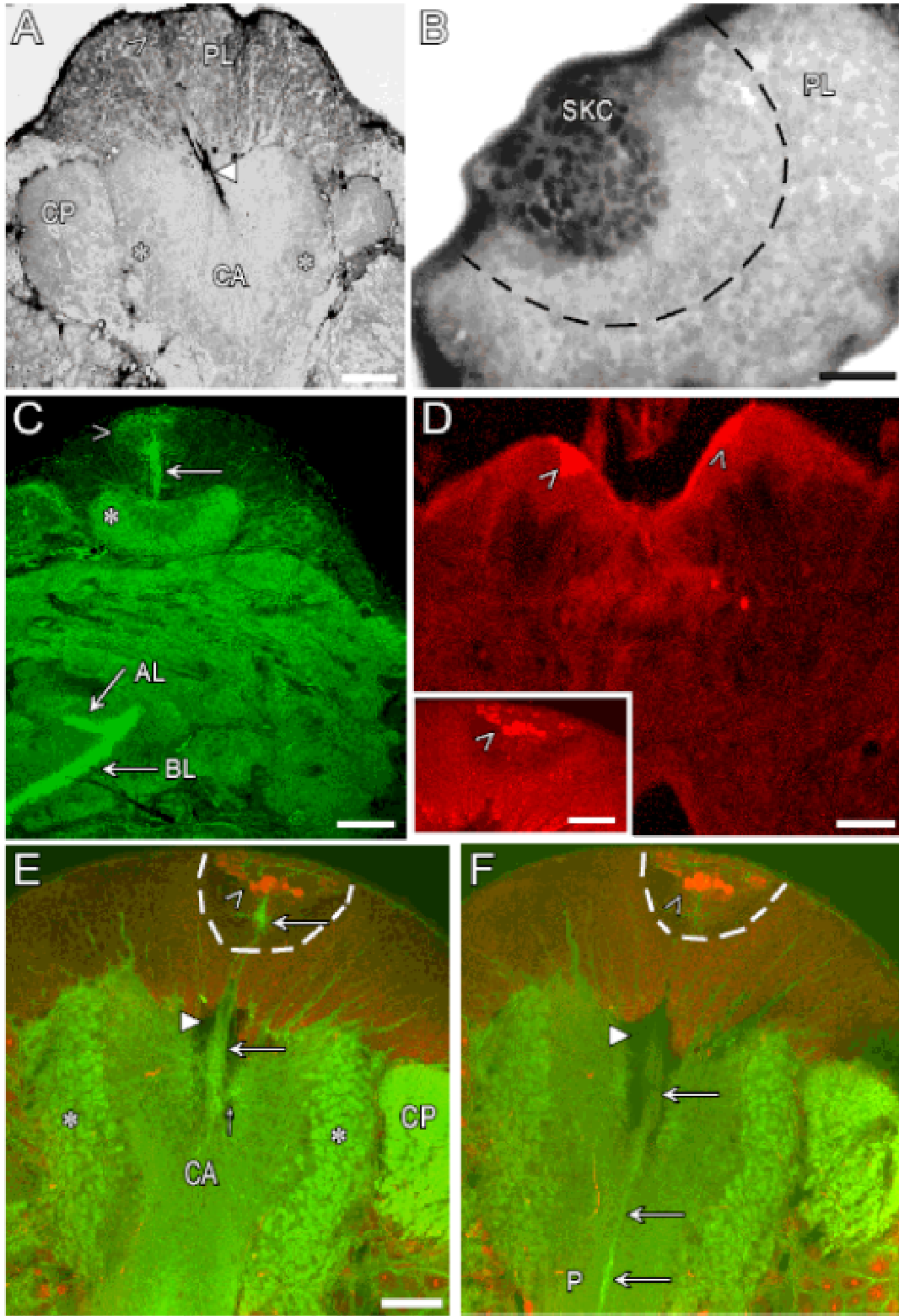


Figure 3: Confocal images of MBs stained with phalloidin (A-E, H, I) or toluidine blue (F, G). The scheme at the top left indicates the arrangement of KC fibre columns and the levels of sections serving for images.

A: F-actin-phalloidin staining indicates the descending sprouting fibre bundle emerging from the KC pericaryal layer (arrows) and descending to the central anterior calyx. Note the marginal glomerular calyx zone (asterisk) also marked by green fluorescence; frontal section.

B, C: The f-actin positive central core zone (arrow) is detected in the MBs of the last instar (C) well as in two months old imagines (D), cross sections through the MB stalks.

D: Sprouting, dendritic like projections (small arrows) in the anterior calyx (CA), extending from the central core fibre bundle (arrow) to the glomerular layer (asterisk) of micro- glomeruli; horizontal section.

E: The sprouting fibre bundle (arrows) in the pericaryal layer (PL) and in the anterior calyx (CA) with tiny, radial dendritic like projections (small arrows). Note the intense staining of glomeruli in the anterior and posterior calyx (CP) and the unstained descending axon bundles (circles) of KC III neurones, descending from the CP; frontal section.

F, G: The central region of the stalk containing the f-actin central core fibre bundle (arrows) surrounded by mature type II and III KC fibres; toluidine blue staining, sagittal (F) and horizontal section (G) .

H: Intense staining of f-actin in the central stalk (central core KC fibre bundle, arrow).

I: The f-actin positive central core column (arrow) in the stalk (longitudinal section) with adjacent sprouting elements lined up along the stalk (small arrows). Scattered green spots are interpreted as synaptic sites in more centrifugal stalk parts (asterisk).

Scale bars: A: 50; B, C, G: 10 μm ; D, E: 20 μm ; F, H: 40 μm ; I: 5 μm .

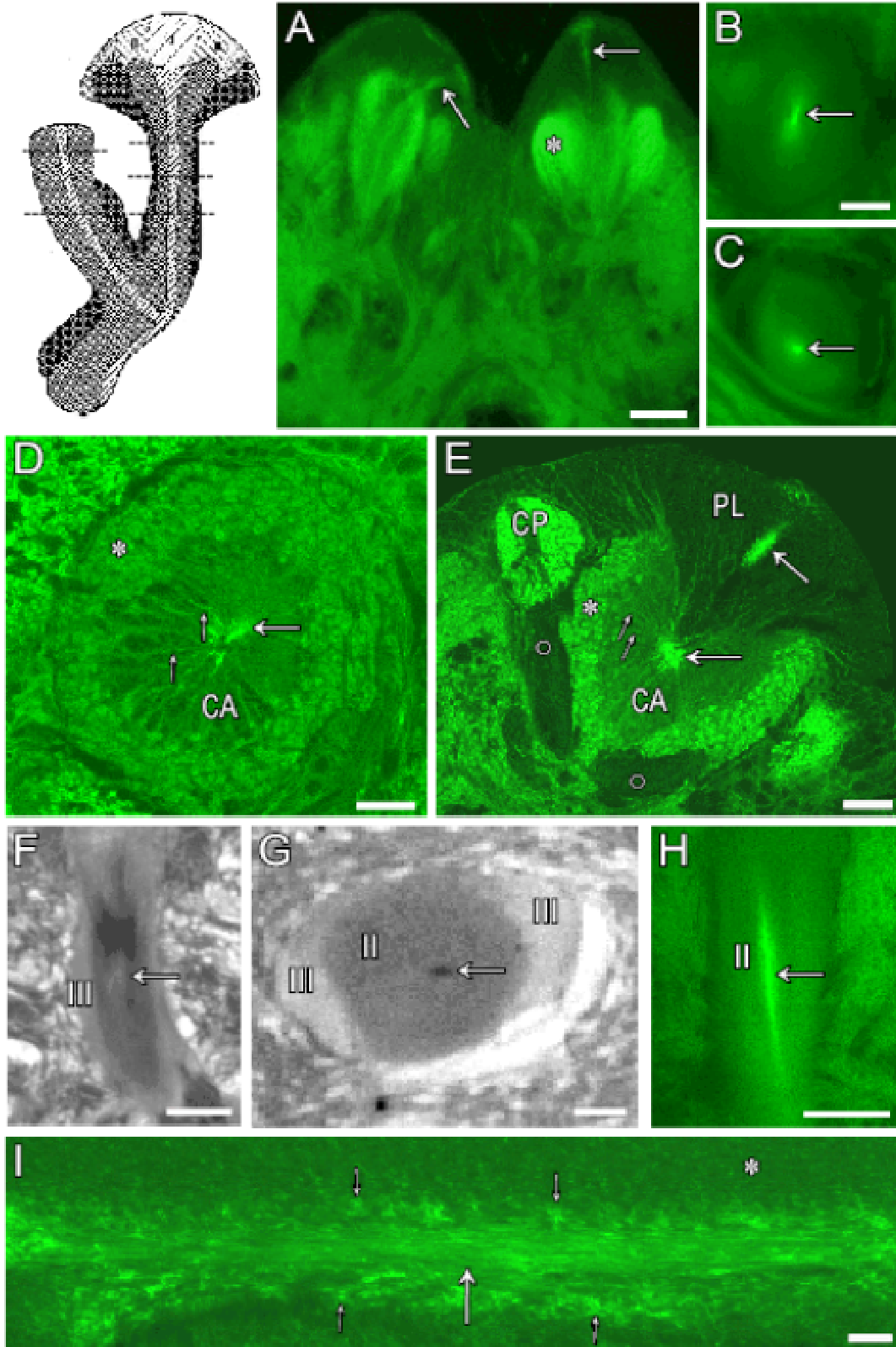


Figure 4: The f-actin positive central core in the stalk and alpha lobe, confocal images (A-E, I, H) and toluidine blue stained semithin sections (F, G).

A-C: Central f-actin positive fibre bundle (arrows) at the top, medial and basal parts of the stalk respectively; horizontal sections.

D: The f-actin positive central core (arrows) in the alpha- (AL) and beta- (BL) lobes; frontal section.

E: Strong staining of f-actin of central core fibres in the alpha lobe (arrow). Note also the differential staining in areas occupied by KC II fibres, and perpendicular sprouting elements (small arrow); frontal section.

F, G: The central region of the alpha lobe with the f-actin central core (arrows). Note the dark spot surrounded by a ring of faintly stained fibres.

H, I: Central f-actin stained fibre bundle (arrows) at the top and basic parts of the alpha lobe, horizontal sections. Note the radially sprouting fibres (small arrows) emerging from the central core (arrows) and the green spots in the synaptic neuropil (arrowheads).

Scale bars: A-C, G-I: 10 μ m; D-F: 20 μ m.

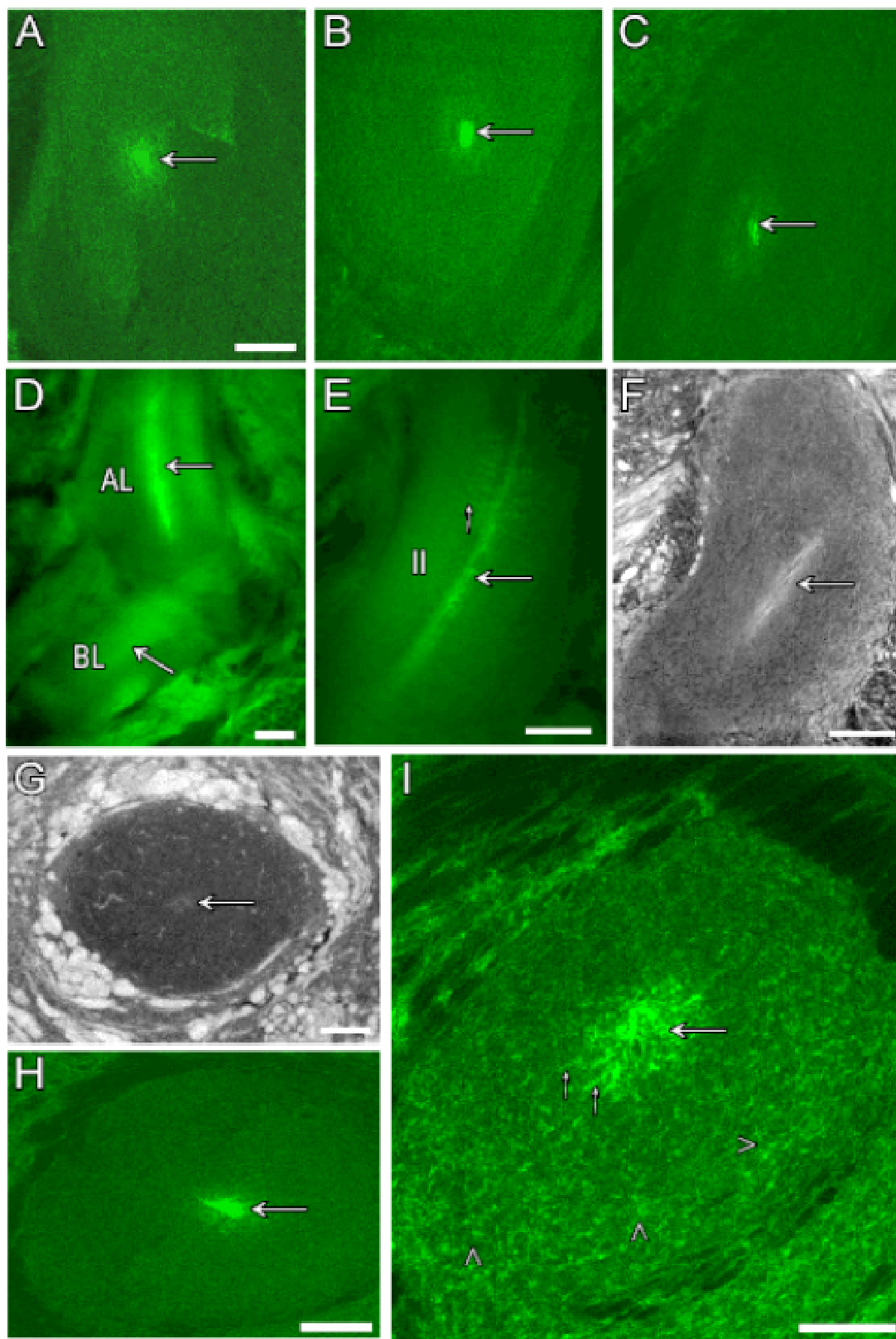


Figure 5: The central core in the beta lobe, toluidine blue staining (A), phalloidin staining, confocal images (B-D).

A: The f-actin central core fibres (arrow) occupy a lateral position in the beta lobe; mature KCs (II); frontal section.

B: Intense staining of the growing KCs (arrows), surrounded by neuropil with mature KCs (II).

C, D: Note a marginal position of the stained central core KC fibre bundle (arrows); horizontal sections.

Scale bar: A - D: 10 μ m.

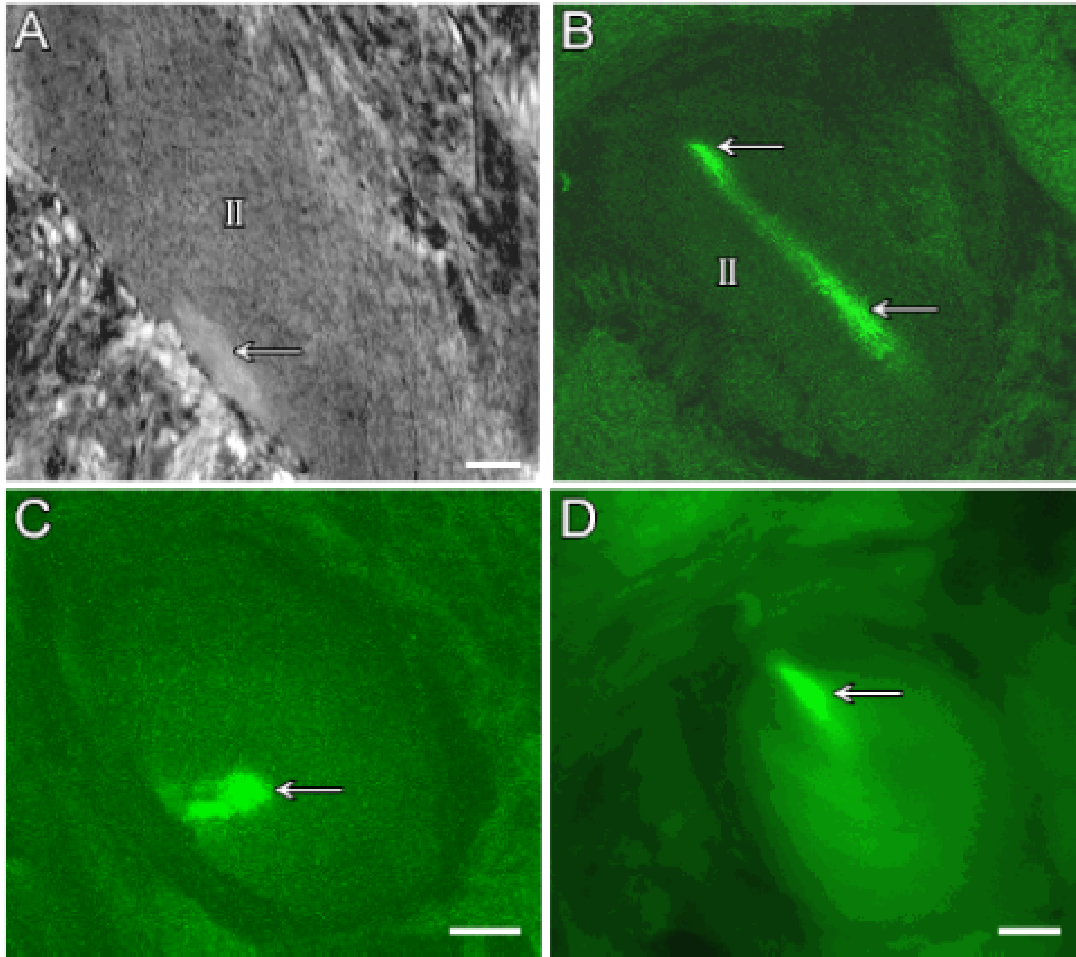


Figure 6: Tubulin in the MBs, immunostaining (red), phalloidin-f-actin staining (green); confocal images, frontal sections.

A-C: Same section to show differential distribution of f-actin and tubulin. Stainings of tubulin (A, C) and phalloidin (B, C) indicate the distribution of tubules in the pericaryal layer (PL) and in the MB neuropil. The posterior calyx (CP) and the stalk (P) show bundles of KC III fibres (arrowheads). The central core fibres (arrow) show an intense phalloidin staining and appear to be devoid of tubulin. Fibre tracts outside the MBs mainly lack f-actin. Extracellular space in the anterior calyx (triangle). KC fibre bundle (small arrows).

D: Double staining in the pericaryal layer showing the tubulin immunostaining of KC fibre bundles (small arrows) in the pericaryal layer descending into the anterior calyx (CA), there forming a central fibre column which holds radial KC dendrites. This calyx portion also contains considerable amounts of actin (yellow parts); The glomerular zone appears mainly green. Note compact bundle of KC III fibres (arrowheads) descending from the CP.

E: Pericaryal layer at higher magnification shows small fibre bundles merging to form compact bundles of descending KCII axons (small arrows).

F1-F3: Pericaryal layer (PL) with tubulin staining (F1, F3) and phalloidin staining (F2, F3). The tubulin immunostaining (F3, arrowhead) is concentrated at the boundary of the central core fibres (F1; arrow). Double labelling shows that the massive f-actin positive central core fibre bundle (F2) is composed of a marginal portion showing intense tubulin-phalloidin contents (F3; yellow) and an inner portion devoid of tubulin. Note that the SKC cluster appears to be free of tubulin. The perilemma glia (white arrow) forming the brain sheath contains tubulin and f-actin.

Scale bars: A, B: 100 μm ; C: 50 μm ; D: 25 μm ; E, F1-F3: 15 μm .

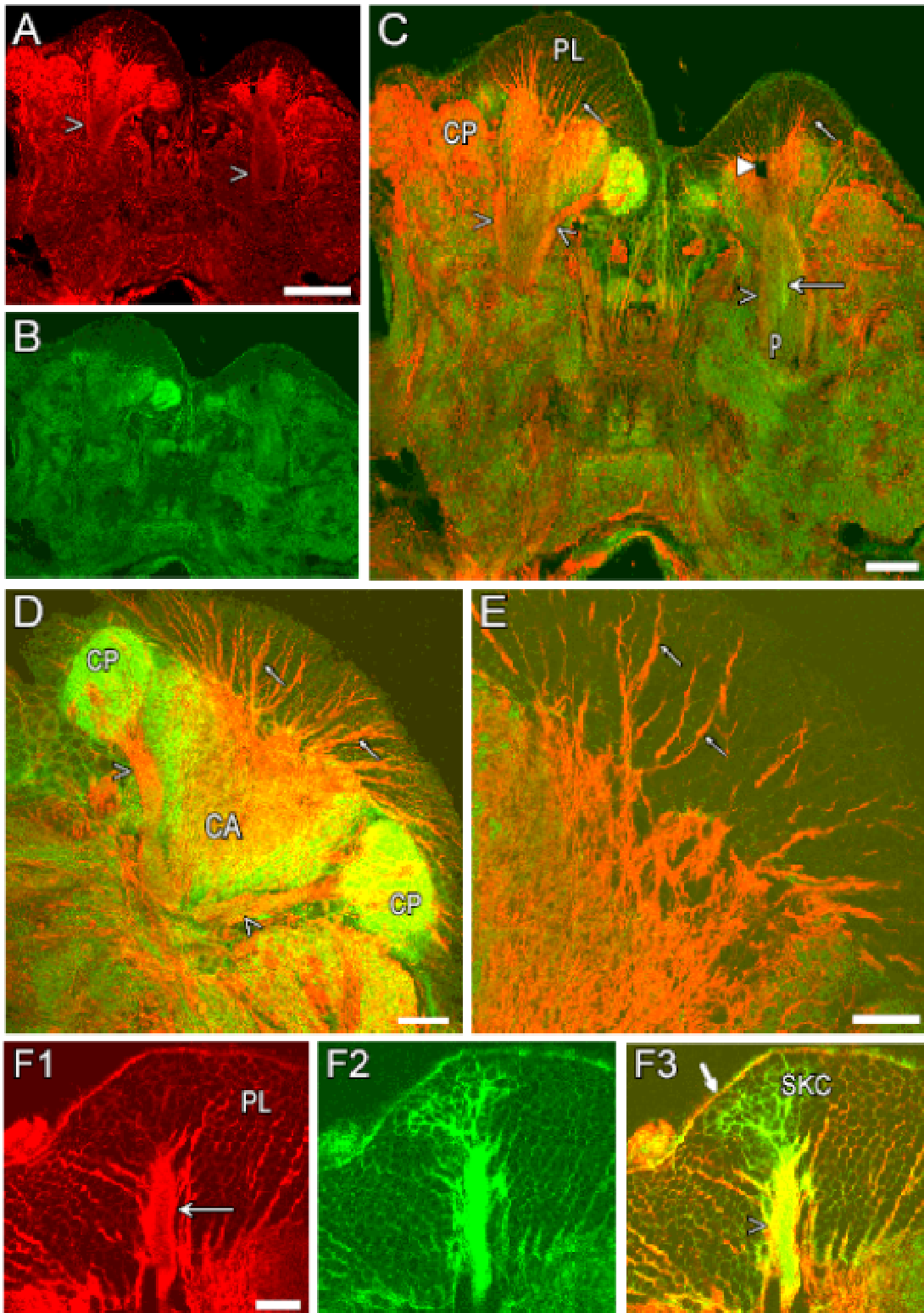
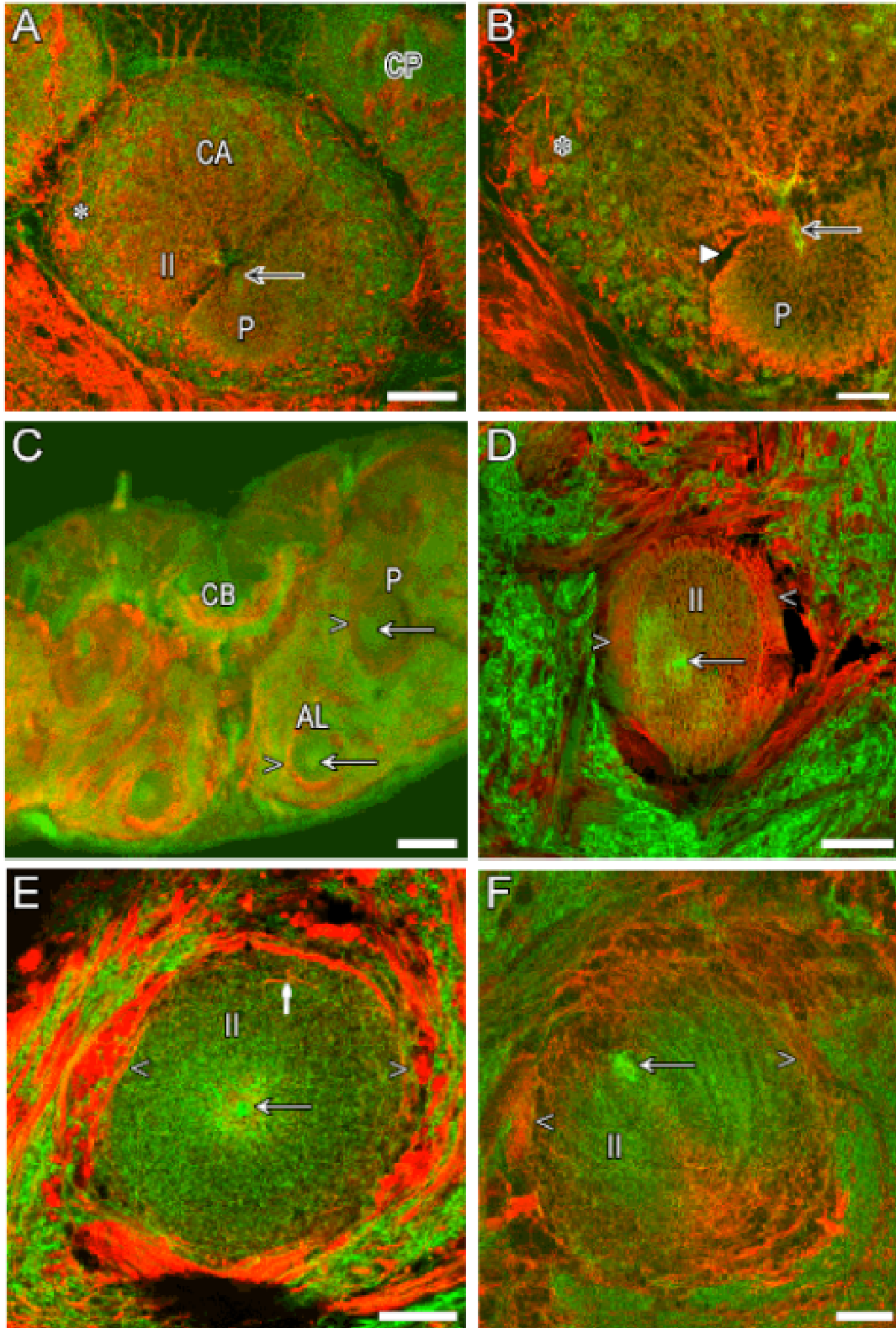


Figure 7: Tubulin-f-actin double labelling in MB compartments, confocal images; tubulin (red); phalloidin (green); horizontal sections.

- A:** The central core fibre bundle (arrow) of the anterior calyx (CA) is lacking tubulin immunostaining. The red immunostaining appears in the area of KC II fibres, whereas in the glomerular area (asterisk) tubulin marking is less intense (compare B). Note the tubulin staining of KC III fibre bundles in the posterior calyx (CP). Stalk (P).
- B:** Tubulin staining in the anterior calyx; high magnification from A. The low tubulin marking of the synaptic area (asterisk) and of the central core (arrow) is visible. Note the extracellular processes (triangle), stalk (P).
- C:** Overview showing tubulin distribution in the stalk (P) and alpha-lobe (AL). The central core fibre bundle (arrows) shows intense f-actin marking and minor amounts of tubulin. Strong tubulin staining is found in KC III fibres (arrowheads) and fibres adjacent to the lobes. Note the immunoreactivity in the central bridge (CB), which is subdivided into a posterior part rich in tubulin and an anterior portion with abundant f-actin.
- D:** Tubulin immunoreactivity of the KC fibre bundles (I-III) in the stalk. Note the strong immunoreactivity in KC III fibres (arrowheads) and lower immunoreactivity of the KC II fibre area, whereas KC I fibre area (arrow) shows intense phalloidin staining.
- E:** Differential immunostaining of the KC fibres (I-II) in the alpha lobe. Note the strong tubulin staining of large fibres surrounding the lobe (arrowheads) and the high immunoreactivity in the ring surrounding the central core (arrow). The tubulin staining in the lobe area with KC II fibres is weak. This area is full of synapses and shows scattered spots of phalloidin. The central core region holds a high amount of f-actin (sprouting KC fibres). A profile of an extrinsic neuron filled with tubulin is marked (white arrow).
- F:** In the beta-lobe tubulin staining is weak in KC II fibre bundle areas and in the central core area (arrow), but concentrated in peripheral β -lobe portions (arrowheads).

Scale bars: A, D: 20 μ m; B, E, F: 10 μ m; C: 50 μ m.



Figures 8: Synapsin-phalloidin staining in the calyx, confocal images, horizontal sections.

A-C: The MB anterior calyx with synapsin immuno-staining (A, C; red) and phalloidin staining (A, B; green, B and C of same section). Intense staining of synaptic glomeruli (asterisks) and small spots of synapsin indicating presynaptic complexes in the inner calyx holding the columnar KC II fibres are found (C). They appear aligned to f-actin fibre bundles (B). The central core (arrow) appears free of synapsin and full of phalloidin-f-actin staining. Extracellular space is positioned at the central core (triangle). Note presynaptic small spots.

D1-D4: Series of four optical images from a stack (taken from same section as in B). The small synaptic spots are aligned to dendritic like, phalloidin stained fibre bundles (small arrows).

Scale bar: A: 20 μm ; B-D: 10 μm .

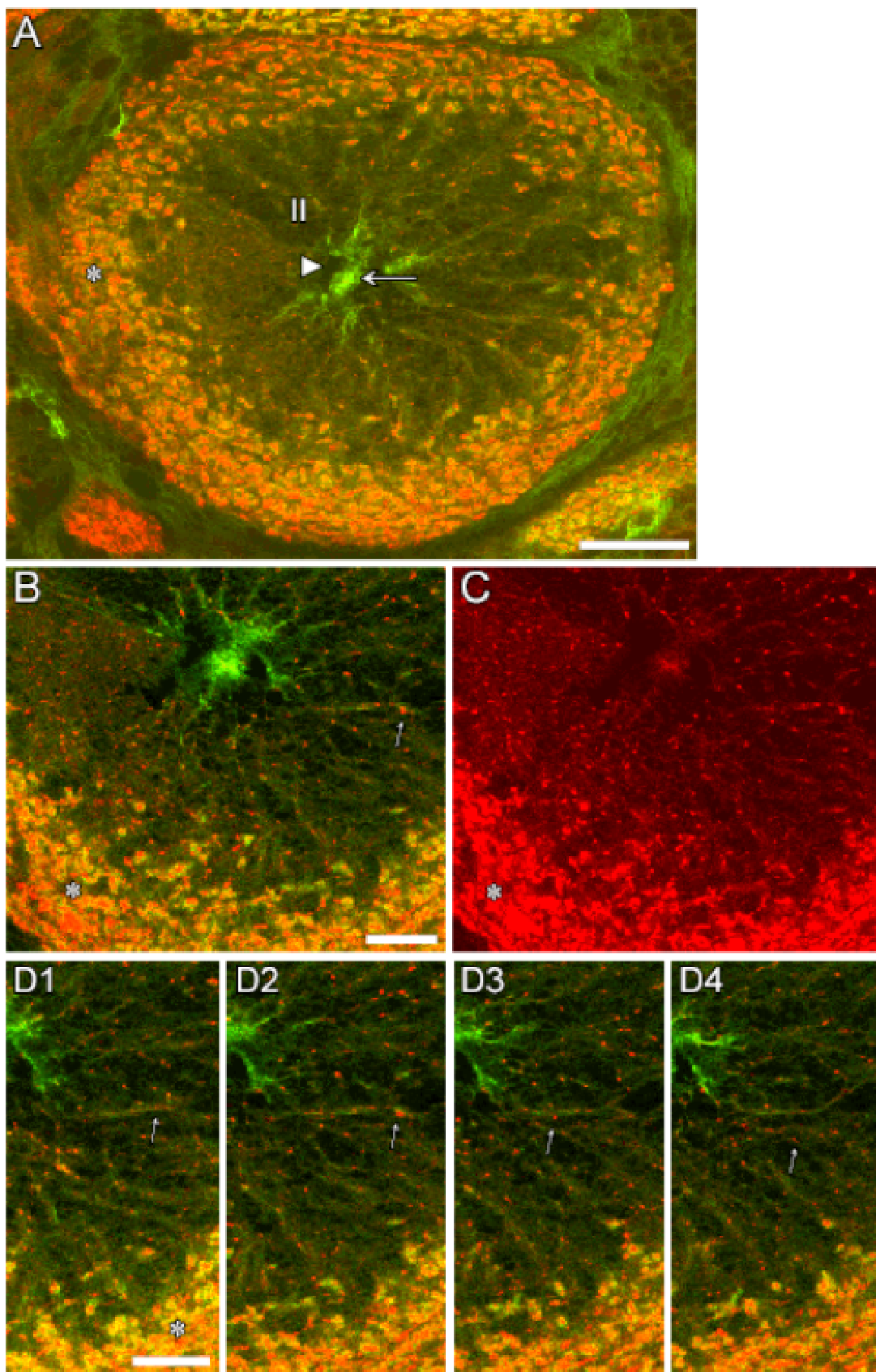


Figure 9: Glomerular neuropil of the anterior calyx; electron micrographs; horizontal (A, B) and sagittal (C, D) sections.

A: Glomeruli with presynaptic boutons (rhombus).

B: Inset from A; a presynaptic bouton filled with synaptic vesicles and with synaptic sites (arrows) surrounded by tiny dendritic profiles.

C: A presynaptic bouton (rhombus) with synaptic sites (arrows), containing small synaptic vesicles and dense core vesicles; inner margin of the glomerular neuropil. Descending KC fibres at the right (asterisk).

D: Inset from C; a fibre profile with pre- and postsynaptic sites (arrows).

Scale bars: A, C: 1 μm ; B, D: 0.5 μm .

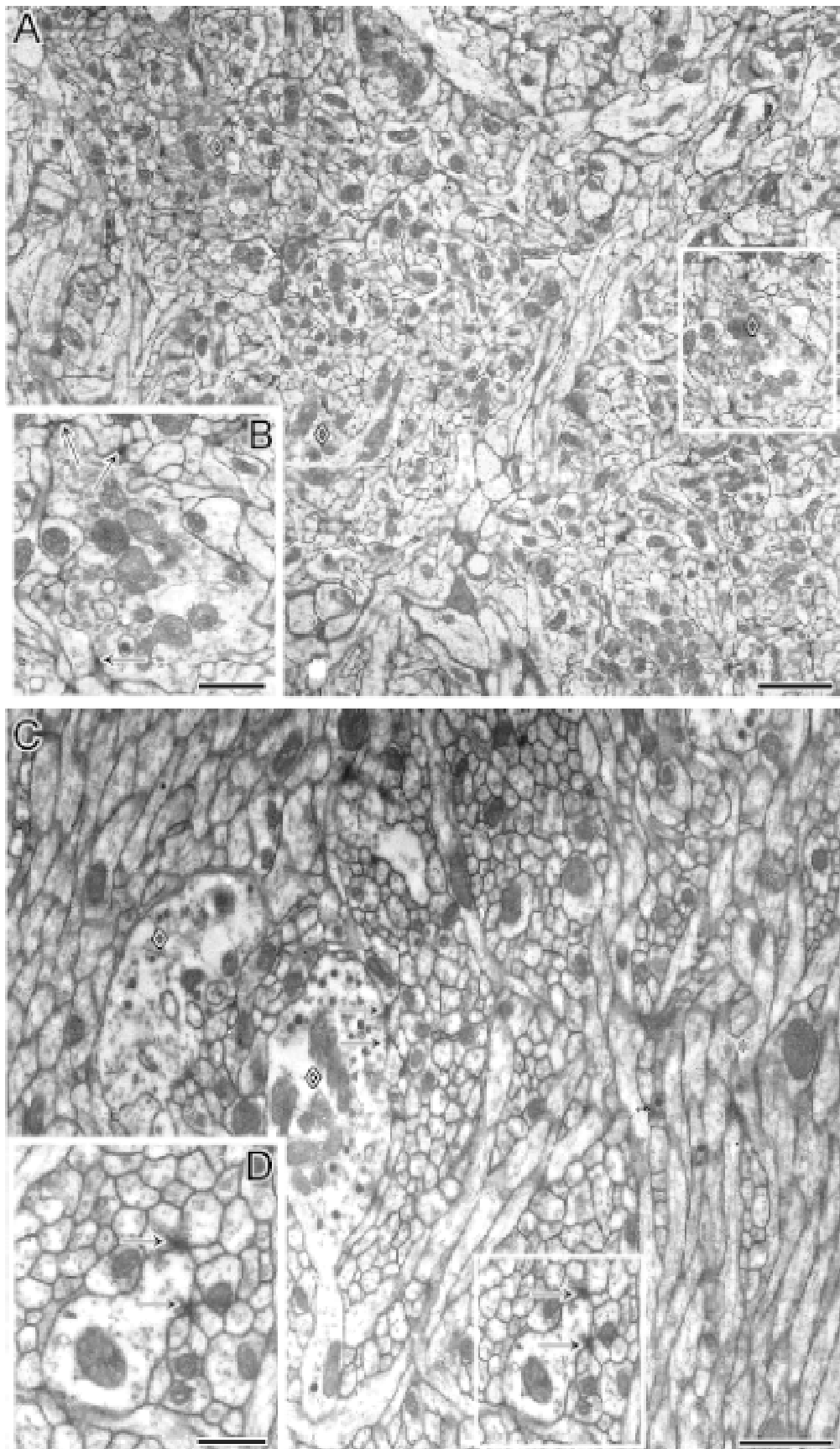


Figure 10: Electron micrographs of synaptic contacts in MB compartments, sagittal (A, B) and horizontal (C - F) sections.

A: Columnar neuropil of the anterior calyx. Small arrows point to presynaptic sites. Note glial cytoplasm (thick arrow).

B: Presynaptic sites (arrows) in translucent fibres, coupled to dark non degenerating fibre profiles in the calyx area of KC II fibres.

C: Presynaptic sites marked by arrows. Extrinsic fibre profiles with synaptic contacts (small arrows) to cross sectioned KC II fibres in the anterior calyx.

D: Presynaptic KC fibres (arrows) in the stalk may in turn be coupled to extrinsic elements (reciprocal synapses), as for example seen at the bottom right in D. Presynaptic bouton (rhombus), synaptic contacts (small arrows).

E: Alpha lobe, postsynaptic extrinsic fibres coupled to small KC fibres (arrows). Note abundant vesicles in the small fibre profiles (arrowheads).

F: Profiles with abundant vesicles (arrowhead) and synaptic sites (arrows); area of KC II fibre bundles in the alpha lobe.

Scale bars: A, B, E, F: 0.4 μm ; C: 0.5 μm ; D: 0.3.

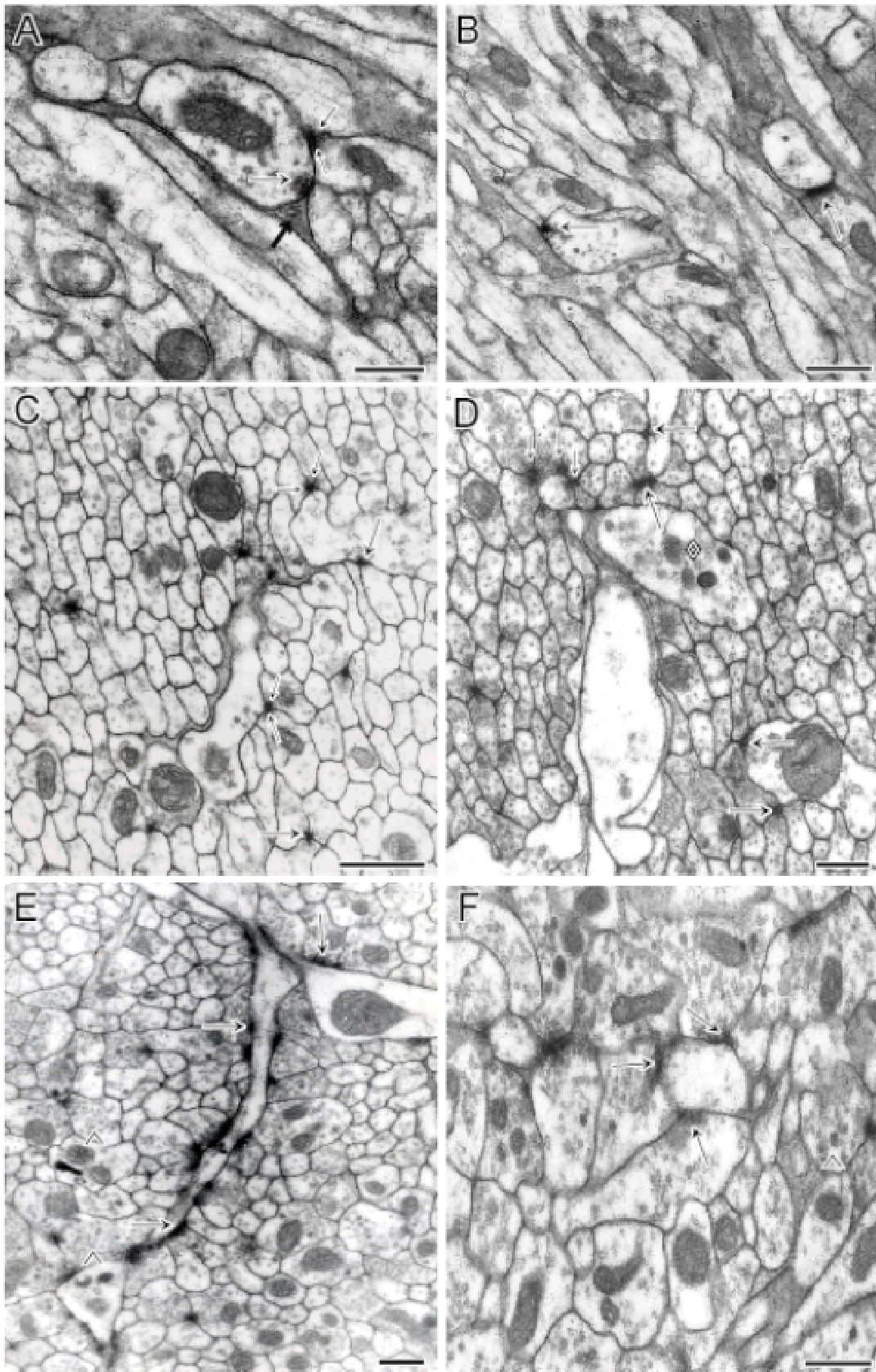


Figure 11: Synapsin-phalloidin staining in the stalk and alpha and beta lobes, confocal images, horizontal sections

A-C: Overview showing synapsin immunoreactivity (A) and phalloidin staining (B); green) in the stalk (P) and alpha lobe (AL); merged image in C. The central core fibre bundle (arrows) appears free of synapsin. The central body (Cb) is strongly double labelled.

D: Synapsin staining in the stalk marks small presynaptic profiles in the area of KC II fibre bundles. Synapsin I immunoreactivity is lacking in the central core region (arrow), showing strong phalloidin staining.

E1-E4: Examples of synapsin staining, showing a gradient from the central core to centrifugal portions. E1, E2 double labelling, E3, E4 single staining with phalloidin.

F: In the alpha lobe, synapsin immunoreactivity appears in type II and III KC fibres. The phalloidin stained central core fibre bundle (arrow) appears devoid of synapsin.

G: Synapsin staining in the beta-lobe appears in KC II and III fibre areas, but is not detected in the central core fibre bundle (arrow), which is strongly phalloidin stained.

Scale bars: A-C: 50 μm ; D-G: 10 μm .

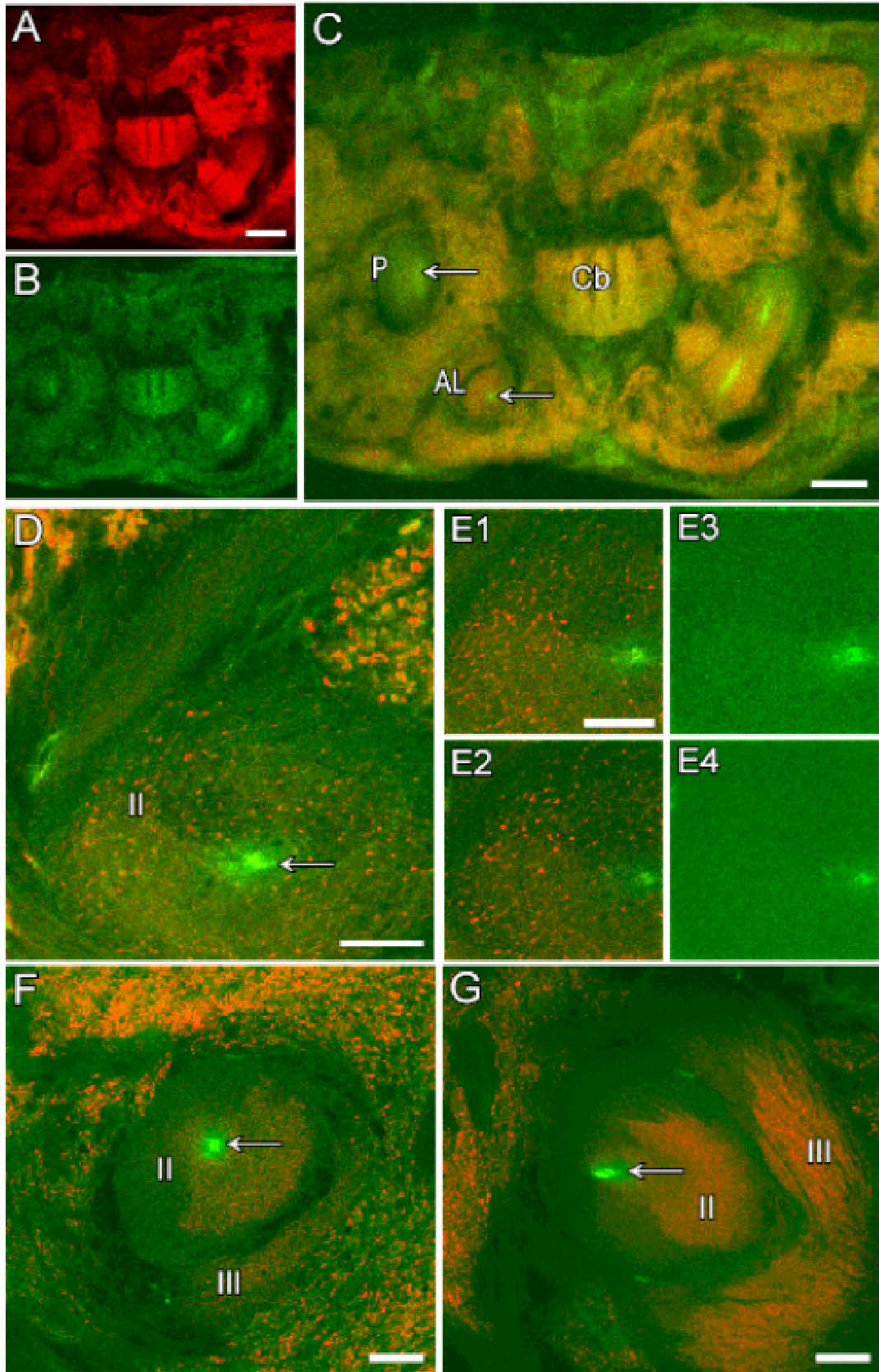


Figure 12: Extrinsic immunostained GABA fibres (red) and phalloidin labelling (green) of neuropil, confocal images (A-C) and epifluorescence micrographs (D- G); horizontal sections.

A: GABA fibres in the anterior calyx are concentrated in the column parts occupied by KC II fibres. The central core fibres (arrow) are lacking GABA and appear phalloidin stained (green). The immunoreactivity is concentrated in type II KC fibres. Note radial spreading of GABA fibres from the central core to the peripheral zone of glomeruli.

B, C: High resolution images of the same section to demonstrate the distribution of GABA stained blebs. The central core fibre area (arrows) appears devoid of GABA.

D, E: In the stalk, the central core fibre area (arrows) and the KC III fibre bundle are free of GABA immunoreactivity. Blebbed GABA fibres are abundant in the area of KC II fibres.

F: In the alpha lobe column, GABA immunoreactivity is partial apparent in regions with KC II and III fibres, whereas central column parts are mainly lacking GABA fibres (compare with D, E).

G: In the columnar beta lobe, the central core region (arrow) is free of GABA (compare with F).

Scale bars: A - C: 20 μm ; D - G: 10 μm .

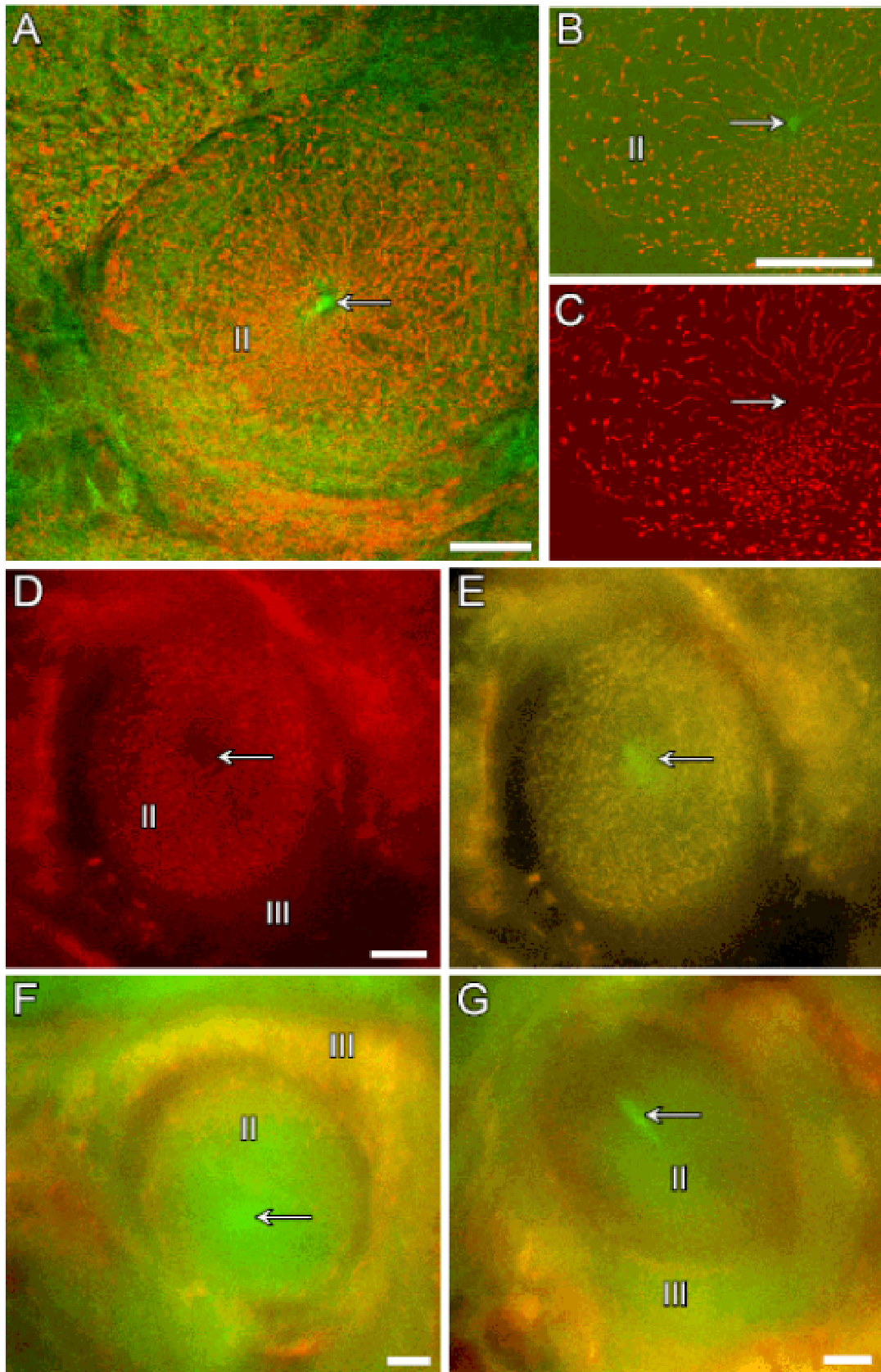


Figure 13: Extrinsic 5-HT neurones in the calyx and stalk. Double labelling: 5-HT immunostaining (red) and phalloidin staining (green). Confocal images, horizontal sections, laser scan micrographs.

A, B: 5-HT fibres (arrowhead) in the anterior (CA) and posterior calyx (CP) are confined to parts of the glomerular areas. The inner columnar area of the anterior calyx with the central core containing sprouting KC fibres (arrows) is lacking 5-HT.

C, D: Enlarged portions of figure B, showing 5-HT immunoreactivity (arrowheads) in parts of the glomeruli.

E, F: 5-HT immunoreactivity in the stalk areas with KC II fibres (arrowheads). Central core fibres (arrows) and KC III fibre bundles are free of 5-HT.

Scale bars: A, B, : 20 μm ; C, D: 10 μm ; E, F: 10 μm .

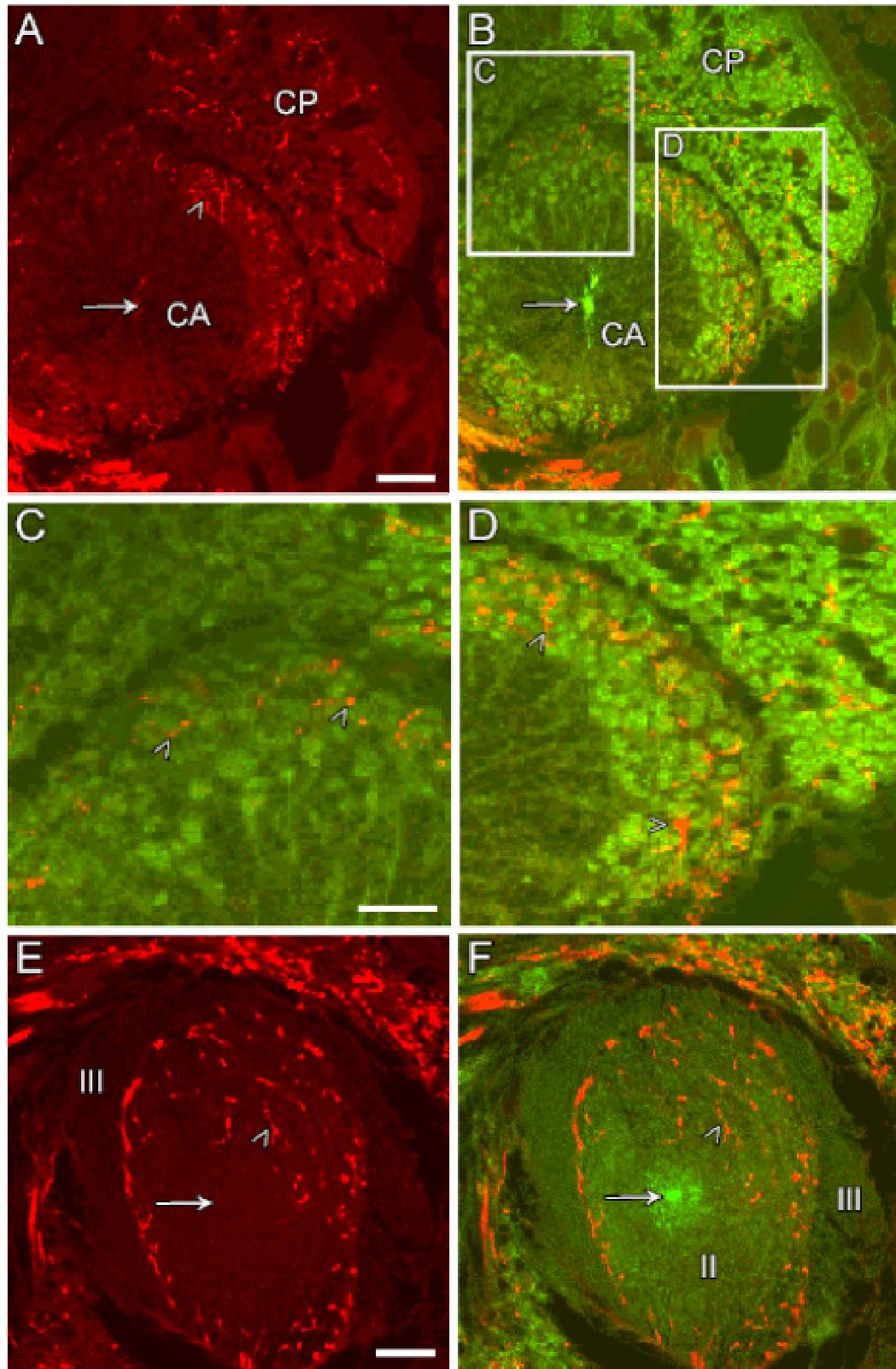


Figure 14: Extrinsic 5-HT neurones in the α - and β - lobes. 5-HT immunostaining (red) and phalloidin labelling (green). Confocal images; horizontal sections.

A, B: Along the alpha lobe column, some 5-HT fibres (arrowheads) are encountered in peripheral areas. Large inner portions of the column are not supplied with 5-HT elements. The sprouting KC fibre bundle (arrows) is always devoid of invading 5-HT fibres.

C, D: 5-HT immunoreactivity in the beta lobe. The central core area (arrows) is devoid of 5-HT. 5-HT elements (arrowheads) are scattered in peripheral regions.

E, F: Enlarged images of C/D.

Scale bars: A - D: 10 μ m; E, F: 5 μ m

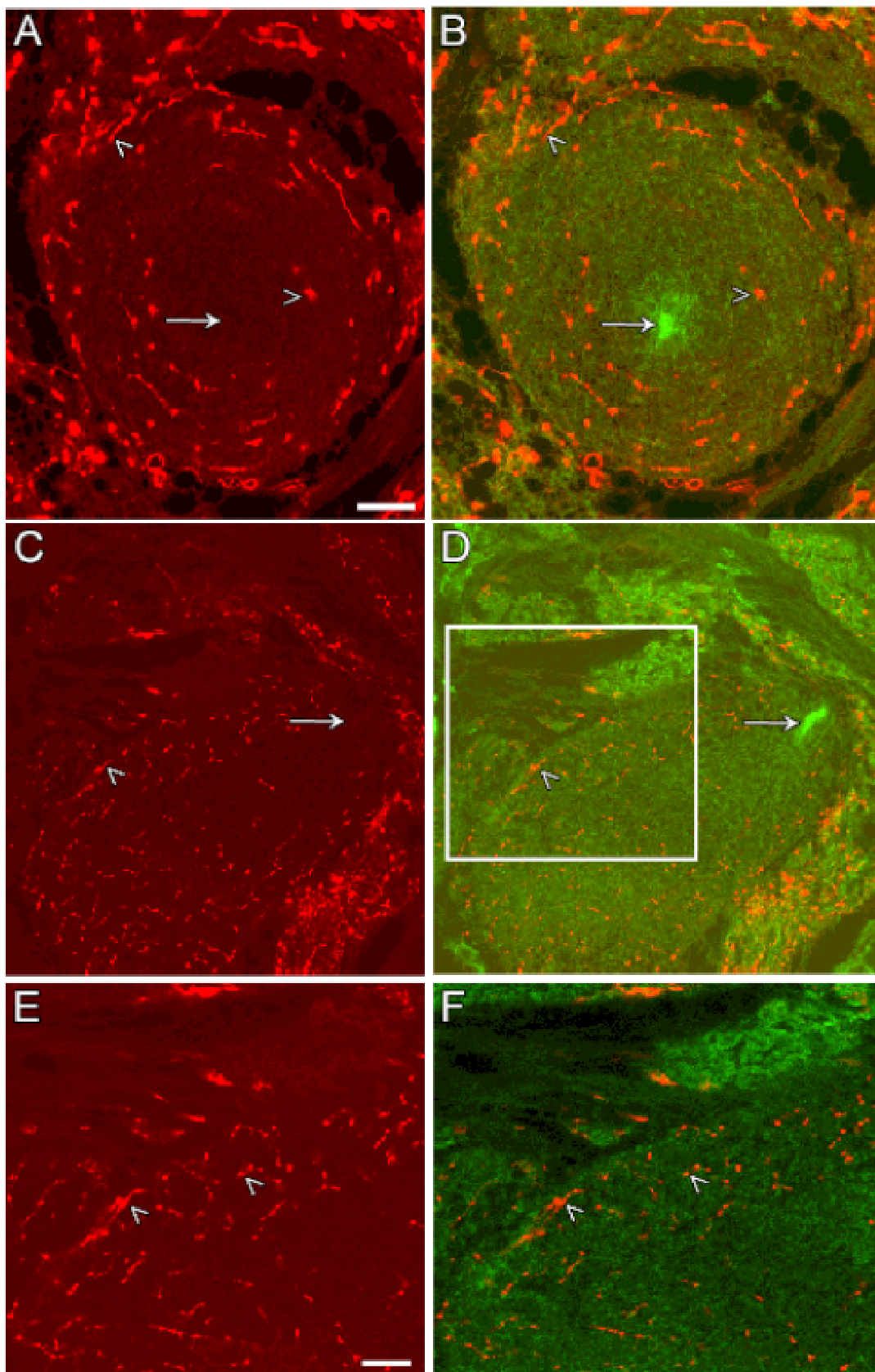


Figure 15: Glial cells in the MB pericaryal layer and calyx, double labelling with propidium iodide (red) and phalloidin (green), confocal images; frontal sections.

A, B: Propidium iodide stains the somatic layer of KCs including the cluster of sprouting cells (SKC) and neuropil glia found at the margin of the MBs and at borders of subcompartments (black arrows). Sprouting fibre bundle (white arrows) in the anterior calyx (CA) adjacent to extracellular space (triangles). Posterior calyx (CP).

C1-C4: Series of optical images showing the glia distribution in the anterior calyx central core area neuropil, at the border of the pericaryal layer.

D: Glia (black arrows) in the anterior calyx. The central core fibre bundle (white arrow) is mainly free of glia; some glia elements (red spots) can be detected in the neuropil.

E1-E4: Series of optical images showing the glia in and around the anterior calyx, propidium iodide staining.

Scale bars: A, C, E: 20 μm ; B, D: 10 μm .

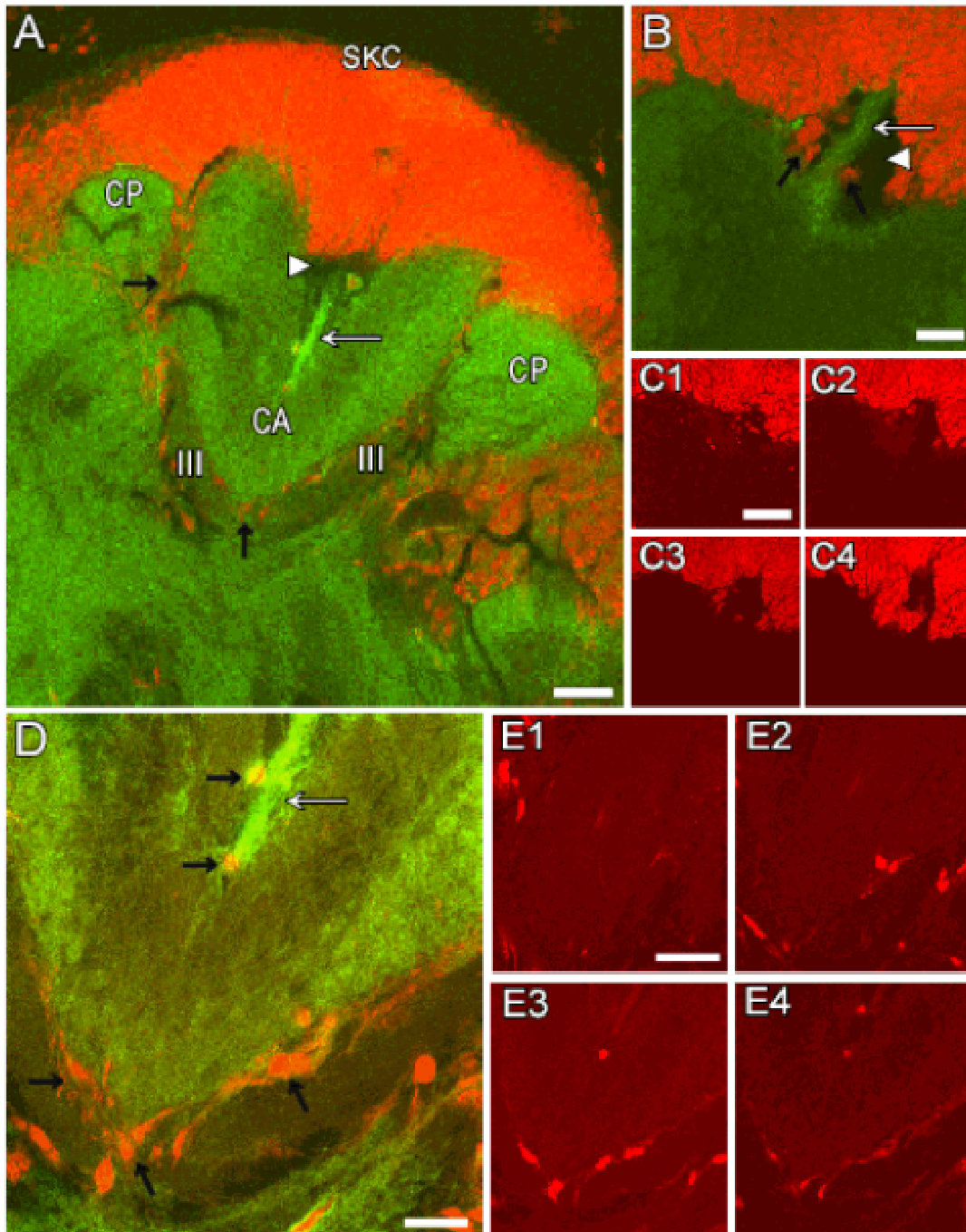


Figure 16: Glial cells in the MB calyx, stalk, alpha and beta lobes. Double labelling with propidium iodide (red) and phalloidin (green), confocal images; horizontal sections.

A: The sprouting KC fibre bundle (white arrow) of the calyx appears devoid of glia. Glia (black arrows) is seen at margins of the calyx.

B, C, D: As stated for the calyx, glia (black arrows) is found at the borders of the stalk (B), and of alpha- (C) and of beta-lobes (D).

Scale bars: A - D: 10 μ m

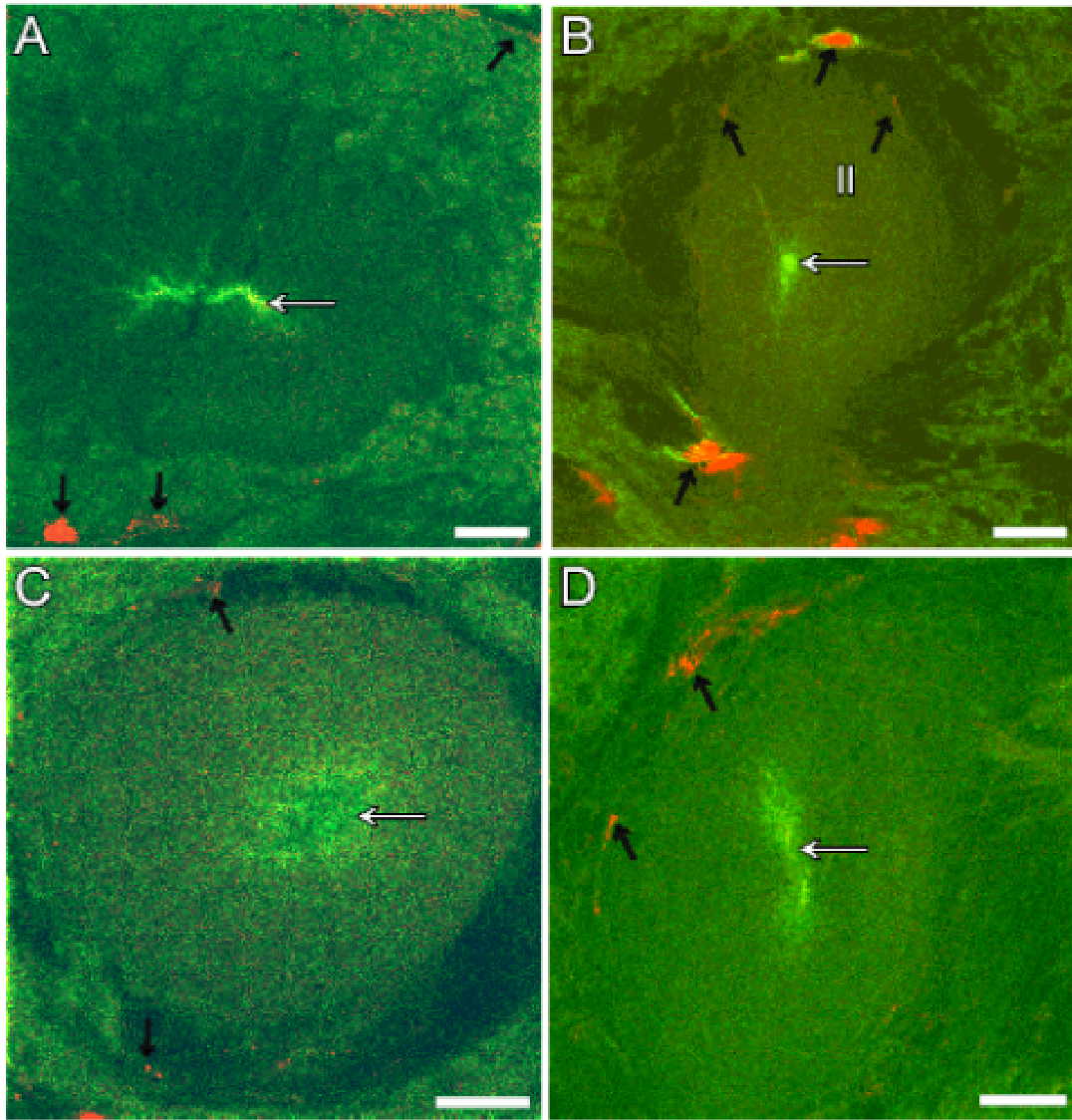


Figure 17: Glia in the MB neuropil; electron micrographs (A, C, D) and light micrograph of toluidine blue stained semithin section (B).

A: Thin glial elements (black arrows); central core region of sprouting fibres (asterisk) in the anterior calyx shows areas of extracellular space (EX) filled with electron dense material. Note irregular shaping of sprouting KC fibres.

B: Toluidine blue staining in the MB calyx showing the position of the central sprouting fibre bundle (asterisk) and adjacent extracellular space (triangle). Note degenerating KC somata (white arrow).

C: Glia elements (black arrows) in the calyx. Note a synapse (small arrow) of a neuronal profile presynaptic to glia.

D: Glial cytoplasm (Gc) in contact with the electron dense extracellular space (triangle) extending between KC profiles in the alpha-lobe. Synaptic sites marked by arrows.

Scale bars: A: 0.7 μm ; B: 30 μm ; C, D: 0.5 μm .

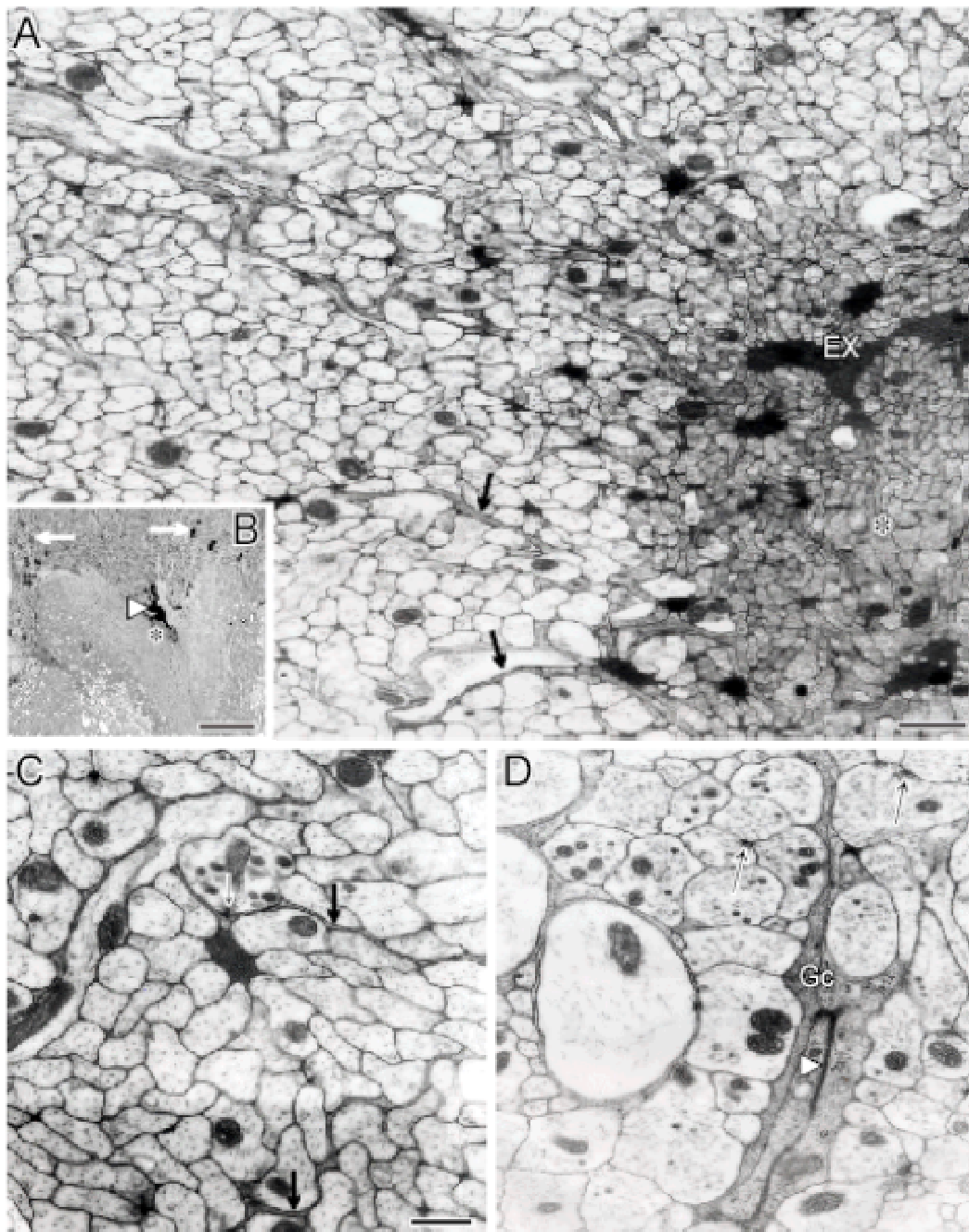


Figure 18: The proliferative cluster in the MB pericaryal layer, electron micrographs and light micrograph of a semithin section (B); horizontal sections (section level given in the scheme).

A: The dark mitotic cells give off sprouting fibres, forming a central core (asterisk), glial perilemma cells (Gc) at the border of the proliferative cluster invade the central core.

B: The proliferative cluster of dark cells with the central core area of sprouting fibres (asterisk) is surrounded by faintly stained KC somata.

C: The central core contains fibres of irregular shape.

D: High magnification from C. The fibres are full of ribosomes (triangles) and show tubules (arrowhead) and endoplasmic reticulum (ER). These fibres are interpreted as growth cone like structures.

Scale bars: A: 2 μm ; B: 5 μm ; C: 0.5 μm ; D: 0.2 μm .

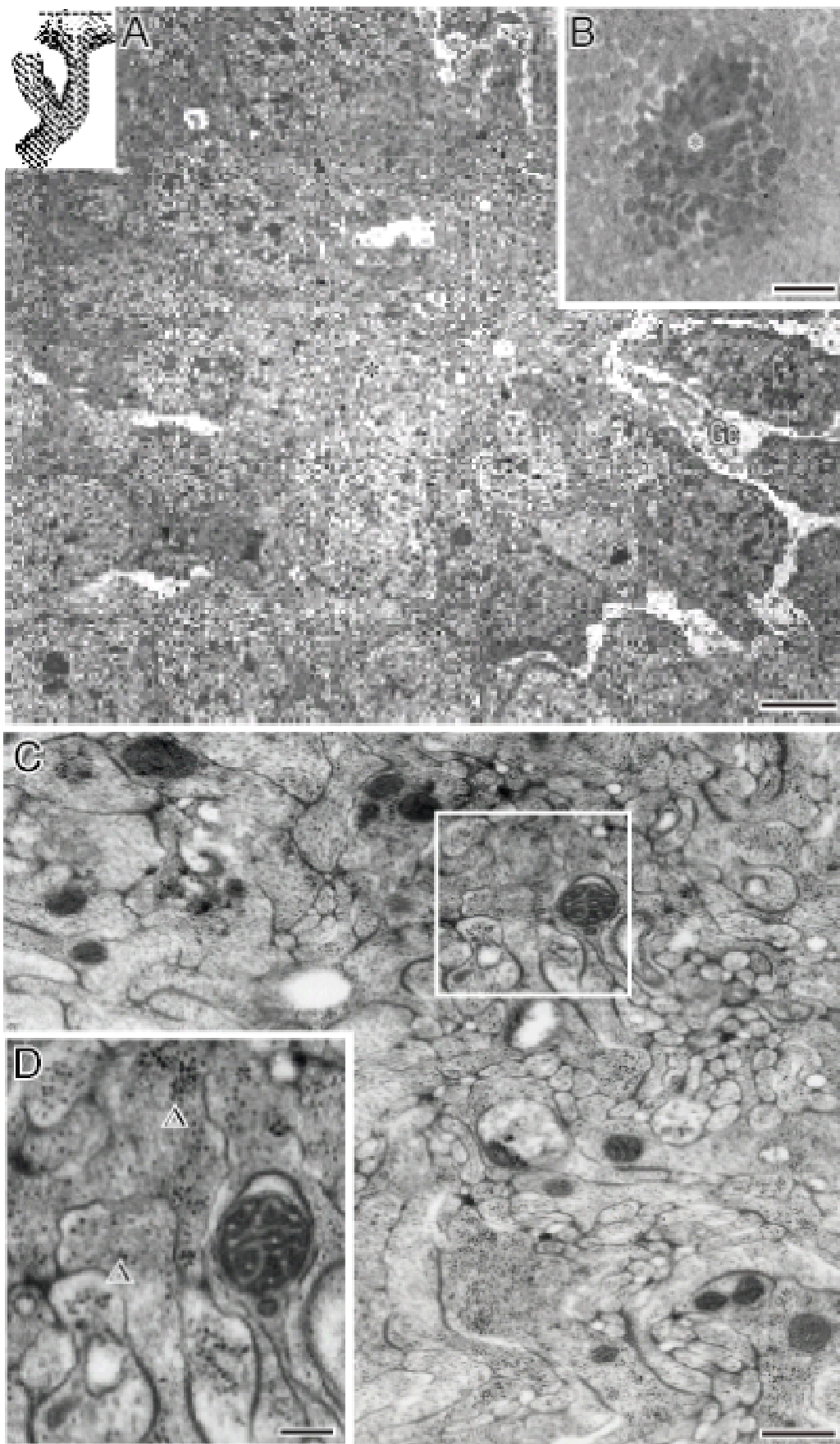


Figure 19: Kenyon cell somata in the pericaryal layer; electron micrographs, horizontal sections.

A: KCs in the pericaryal layer with large nuclei (N). Sprouting KCs (SKC) can be clearly discriminated from postmitotic KCs (rhombus). Fibre bundles of postmitotic KCs are surrounded by glial sheaths, also often separating somata.

B: Glial sheath (small arrows) separates KC somata. Nucleus (N).

C: Glial cytoplasm (Gc) adjacent to a KC soma. Scattered ribosomes (triangles).

Scale bars: A, B: 2 μm ; C: 0.5 μm .

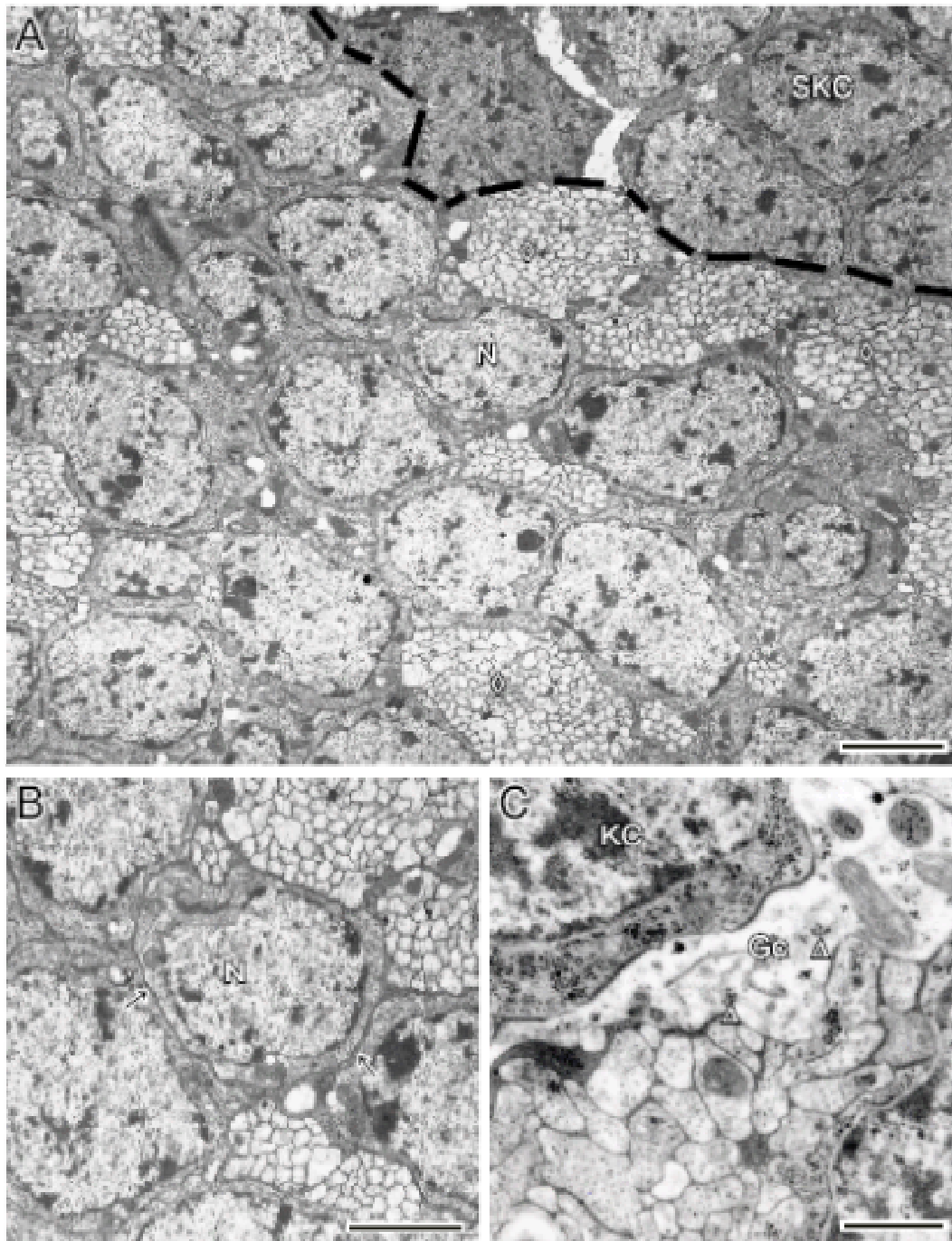


Figure 20: Developing KC somata, electron micrographs.

A: Sprouting KCs fibres forming growth cone-like structures with tiny filopodia (asterisk). Nucleus (N).

B: Area with small filopodia, forming membrane contacts.

C: Somata with direct membrane contacts; note membranes with partial enhancement of electron density.

D: High magnification from C

Scale bars: A: 1 μm ; B: 0.5 μm , C: 0.7 μm ; D: 0.4 μm .

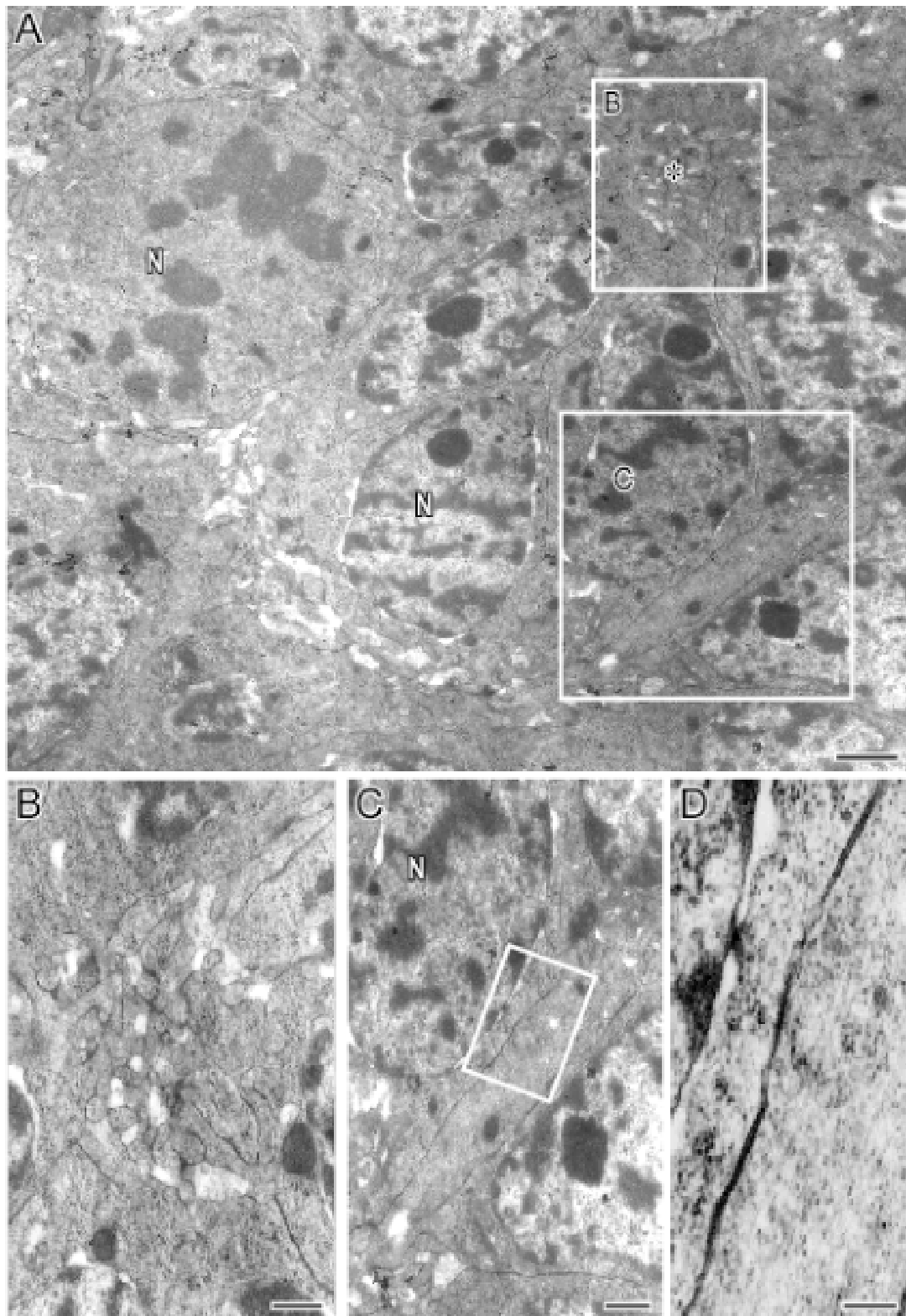


Figure 21: KC pericaryal layer; level of section indicated in the scheme, electron micrographs.

A: The central core KC fibre bundle contains sprouting dark fibres with growth cone like structures (asterisk), surrounded by a ring of small, more translucent fibres (zone of non sprouting KC fibres). The massive fibre bundle is ensheathed by glia, which is accompanied by electron dense extracellular space, intruding the fibre bundle (triangle); glial cell (Gc) with electron opaque cytoplasm contacts the KC fibres and the extracellular space.

B, C: Higher magnifications of the central core region in A. Dark fibre profiles containing ribosomes, endoplasmic reticulum (ER) and tubules (arrowhead). Note electron dense extracellular spaces (triangles), glial cell (Gc).

Scale bars: A: 2 μm ; B: 0.4 μm ; C: 0.3 μm .

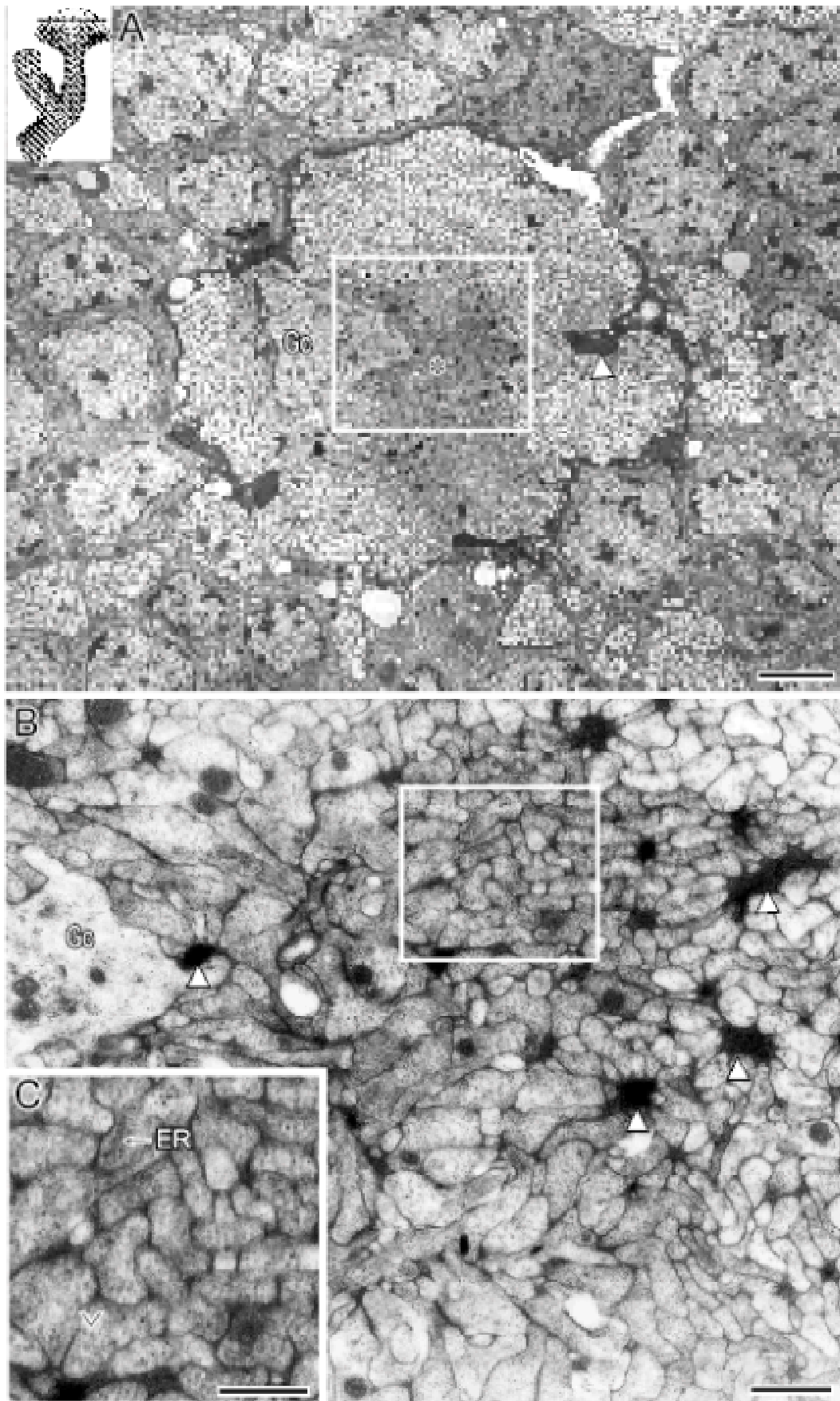


Figure 22: Central calyx area; section level indicated in the scheme; electron micrographs.

A: Central core area (asterisk) with growth cone like structures; surrounded by more mature KC fibres. Note invading extracellular space (EX).

B: Micrograph of toluidine blue stained semithin section showing the central core (asterisk) with extracellular processes (triangle).

C,D: Central core fibres with ribosomes (triangle) and tubules (arrowhead).

E,F: Synapses (arrows) in the KC pericaryal layer. Glial sheath marked by a small arrow

Scale bar: A: 2 μm ; B: 10 μm ; C: 0.2 μm ; D: 0.1 μm ; E: 0.4 μm ; F: 0.3 μm .

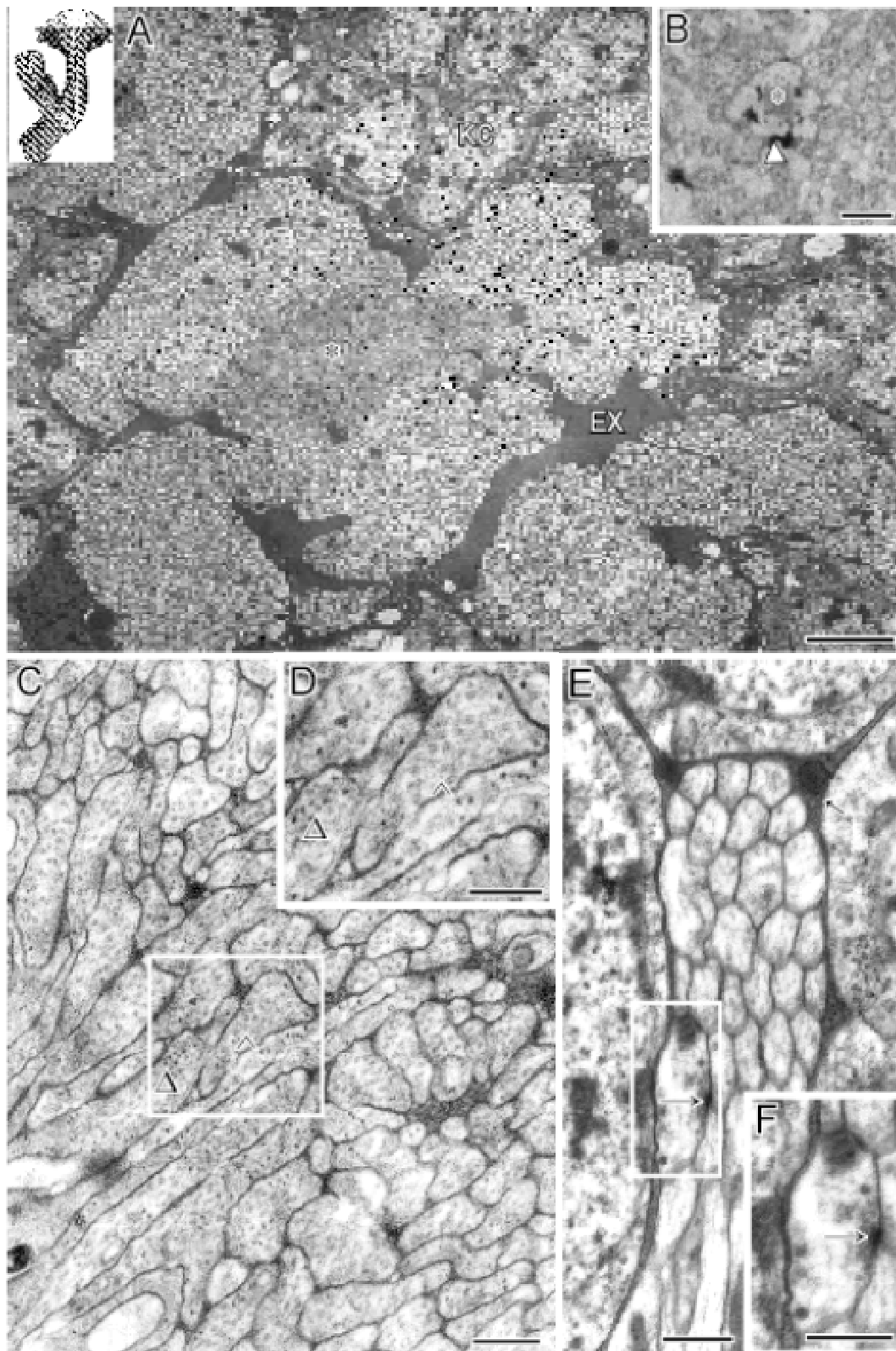


Figure 23: Anterior calyx; electron micrographs (A, C, D); light micrograph of toluidine blue stained semithin section (B); section level indicated in scheme

A: Central core area (asterisk); note large extracellular space (EX).

B: Central core (asterisk) and extracellular space (triangle) in the anterior calyx (CA).

C: Central core area with sprouting KC fibres; extracellular space (EX).

D: Detail from B; sprouting elements with tubules (arrowheads).

Scale bars: A: 2 μm ; B: 30 μm , C: 0.4 μm ; D: 0.1 μm .

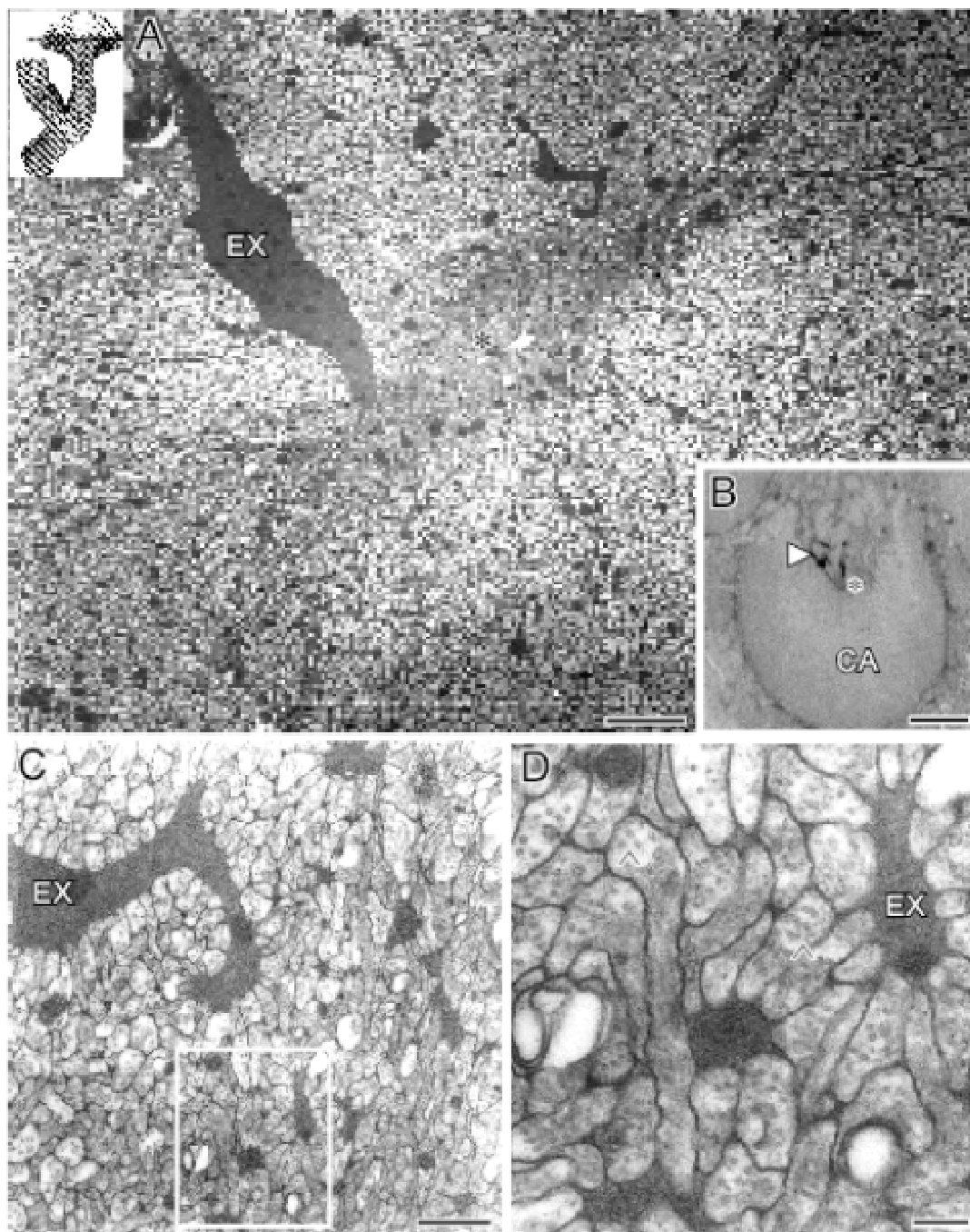


Figure 24: Central core area at the basal part of the anterior calyx, electron micrographs (A, C, D); light micrograph of semithin section (B); section level indicated in scheme.

A: Central core sprouting fibres. Note the many extracellular processes (EX) and a degenerating element (deg).

B: The central core (asterisk) is surrounded by KC fibre bundles, separated from the discrete area of glomerular neuropil (dotted line).

C, D: Details from A, sprouting fibres (rhombus) extend projections to the extracellular spaces. Note tubules (arrowheads) and ribosomes (triangle).

Scale bars: A: 0.4 μm ; B: 40 μm ; C, D: 0.2 μm .

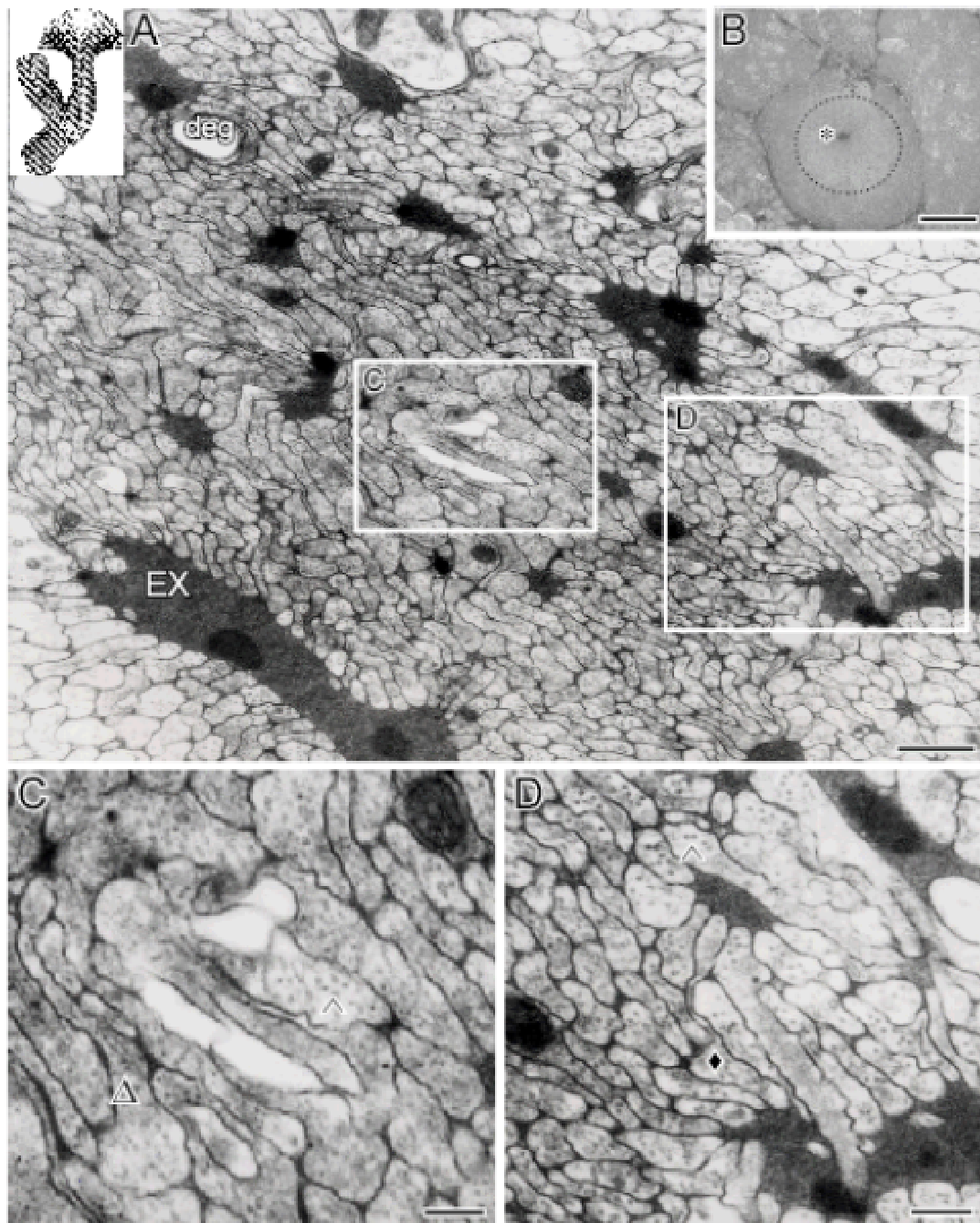


Figure 25: Anterior calyx; electron micrographs.

A: Extracellular space (EX) directly contacted by KC fibres; tubules (arrowheads).

B: Detail from A; KC fibre membrane contacting the EX, not surrounded by a membrane

C-E: Contact of extracellular space (EX) to glial cytoplasm (Gc), forming small extensions (arrows). D; magnification from C: Note single glial membrane (triangle)

Scale bars: A, C, E: 0.2 μm ; B, D: 0.1 μm .

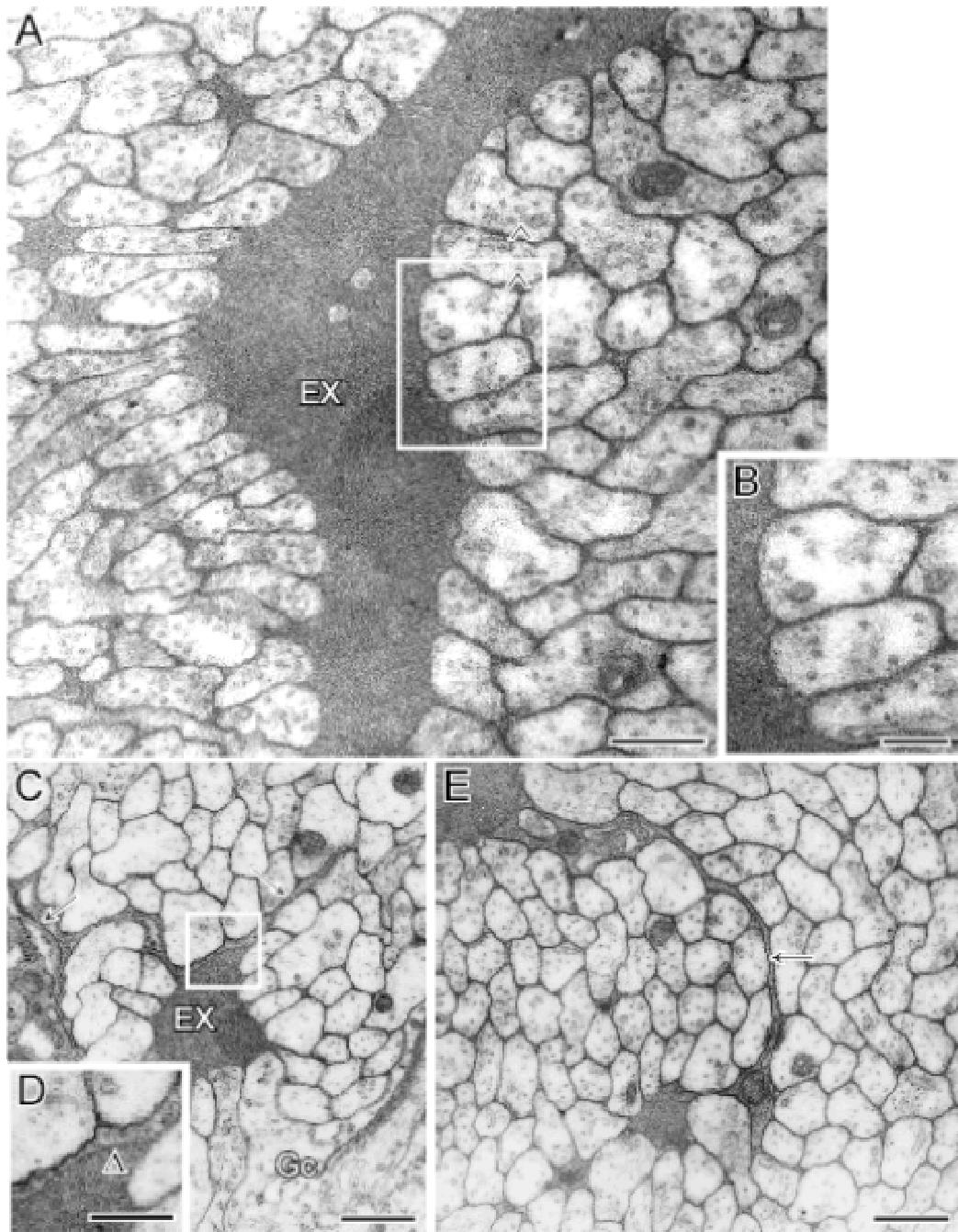


Figure 26: Stalk, KC fibre bundles; light micrographs of semithin sections (A, B), electron micrographs; sagittal section (A); cross sections (B-F).

A: Dark central core part (arrow) and surrounding KC fibres in the stalk, anterior calyx (CA), posterior calyx (CP) holding KC III neurones. Position of brain in the head indicated: anterior, posterior, dorsal and ventral side (a,p,d,v).

B: In the cross section the distribution of bundles of KC I-III axons is clearly seen. The dark central core (asterisk) is surrounded by an area with KC I axons.

C, D: Note the dark zone of sprouting fibres (asterisk) and the surrounding tiny fibres with less electron dense staining. More peripheral parts (KC II area) show light extrinsic fibre (eF) profiles.

E: KC II fibre region with synapses (arrows) and a postsynaptic extrinsic fibre (eF).

F: Peripheral stalk with the larger KC III fibres. Glia (black arrow).

Scale bars: A: 60 μm ; B: 20 μm , C: 2 μm ; D: 0.3 μm ; E: 0.6 μm ; F: 0.5 μm .

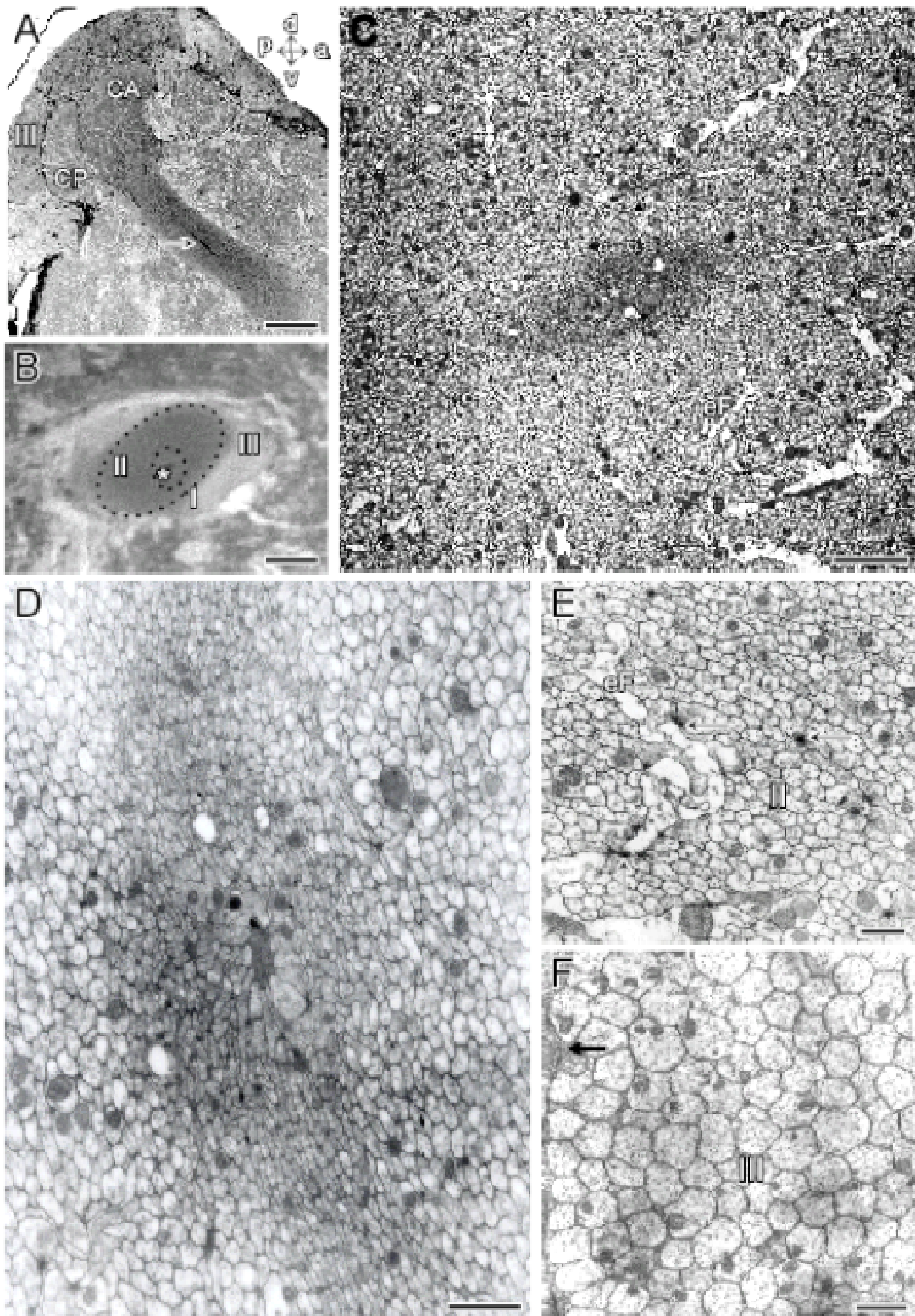


Figure 27 A-D: KC fibres in the central core of the stalk, development in the central core of the stalk, electron micrographs, serial sections.

Note the shape of dark sprouting fibres contacting the extracellular spaces; corresponding areas (1, 2).

Scale bars: A-D: 0.3 μm

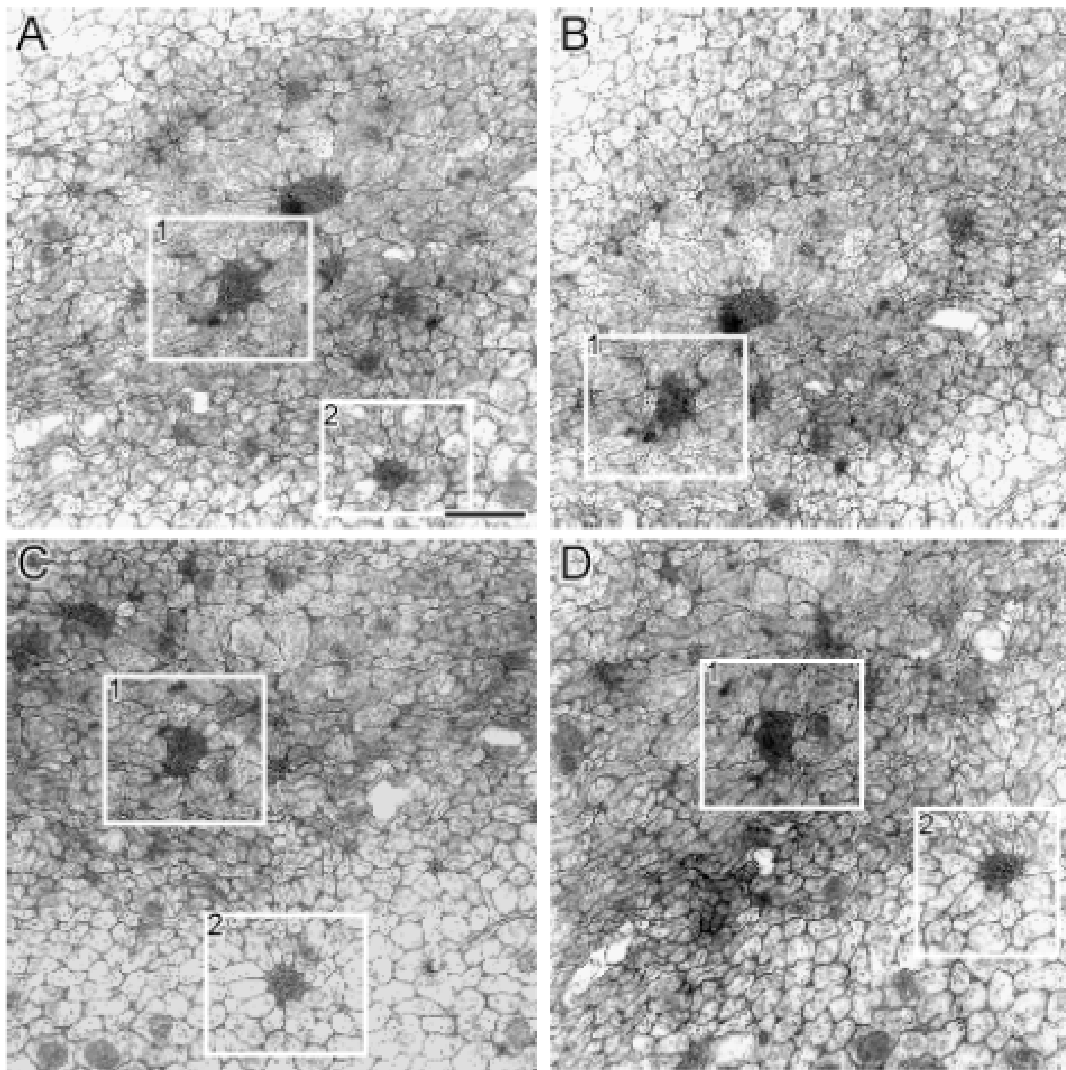


Figure 28: Alpha lobe, electron micrographs (A, B); light micrograph (C) of toluidine blue stained semithin section; section levels indicated in the scheme.

A: The central core (asterisk) at the top of the alpha lobe containing sprouting elements with irregular shape is surrounded by KC I fibres; no synapses are found in this area. The peripheral region with more mature KC fibres is invaded by extrinsic fibres (eF) and shows synaptic sites (arrows).

B: The central core with sprouting fibres (asterisk) at a more proximal level of KC fibre bundles. Electron micrograph through the medial part of the alpha lobe. In the periphery, more mature fibres of KC II type are encountered.

C: Note the differential toluidine blue staining showing the central core (asterisk) and light staining of surrounding fibres (dotted line), outer neuropil column contains KC II fibres.

Scale bars: A, B: 2 μm ; C: 20 μm

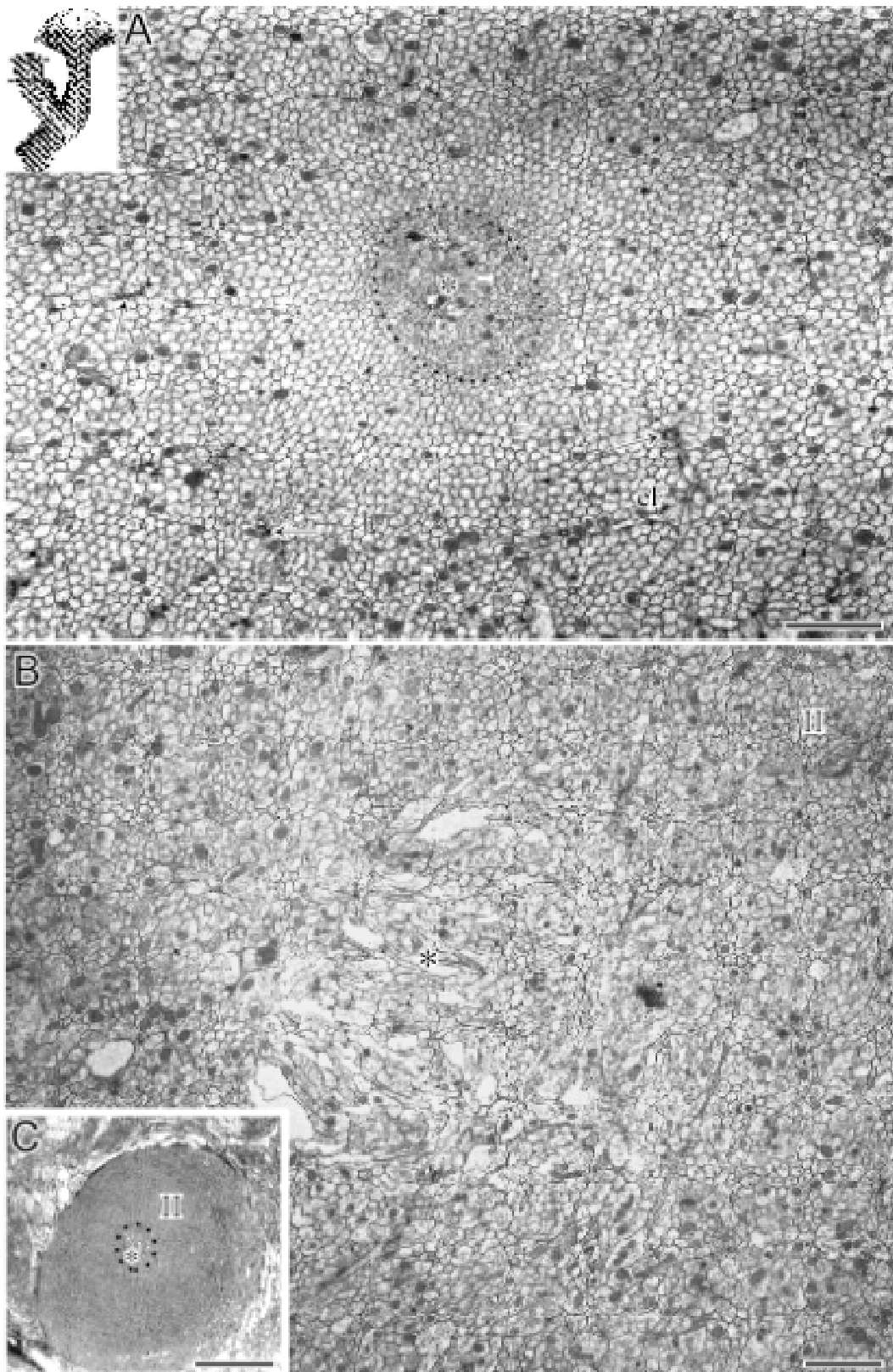


Figure 29: KC fibres in the alpha (A, B) and beta lobes (C-E), electron micrographs.

A: The central core (asterisk); sprouting fibres with centrally directed projections (arrows). Note emerging branches of tiny fibres (small arrows).

B: Tiny profiles of KC fibres with synapses (arrows) presynaptic to an extrinsic fibre (eF); area of KC II fibres.

C: The central core area with sprouting fibres (asterisk) in the beta lobe is shifted to a marginal position. As found in the stalk and alpha lobe, an adjacent area of tiny KC fibres (light staining) is surrounded by a zone of more darkly stained fibres containing abundant synapses.

D: High magnification from C showing the central core (asterisk) with sprouting fibres.

E: KC elements presynaptic to an extrinsic fibre profile (arrows); peripheral area of beta-lobe.

Scale bars: A, B: 0.5 μm ; C: 2 μm ; D, E: 0.5 μm .

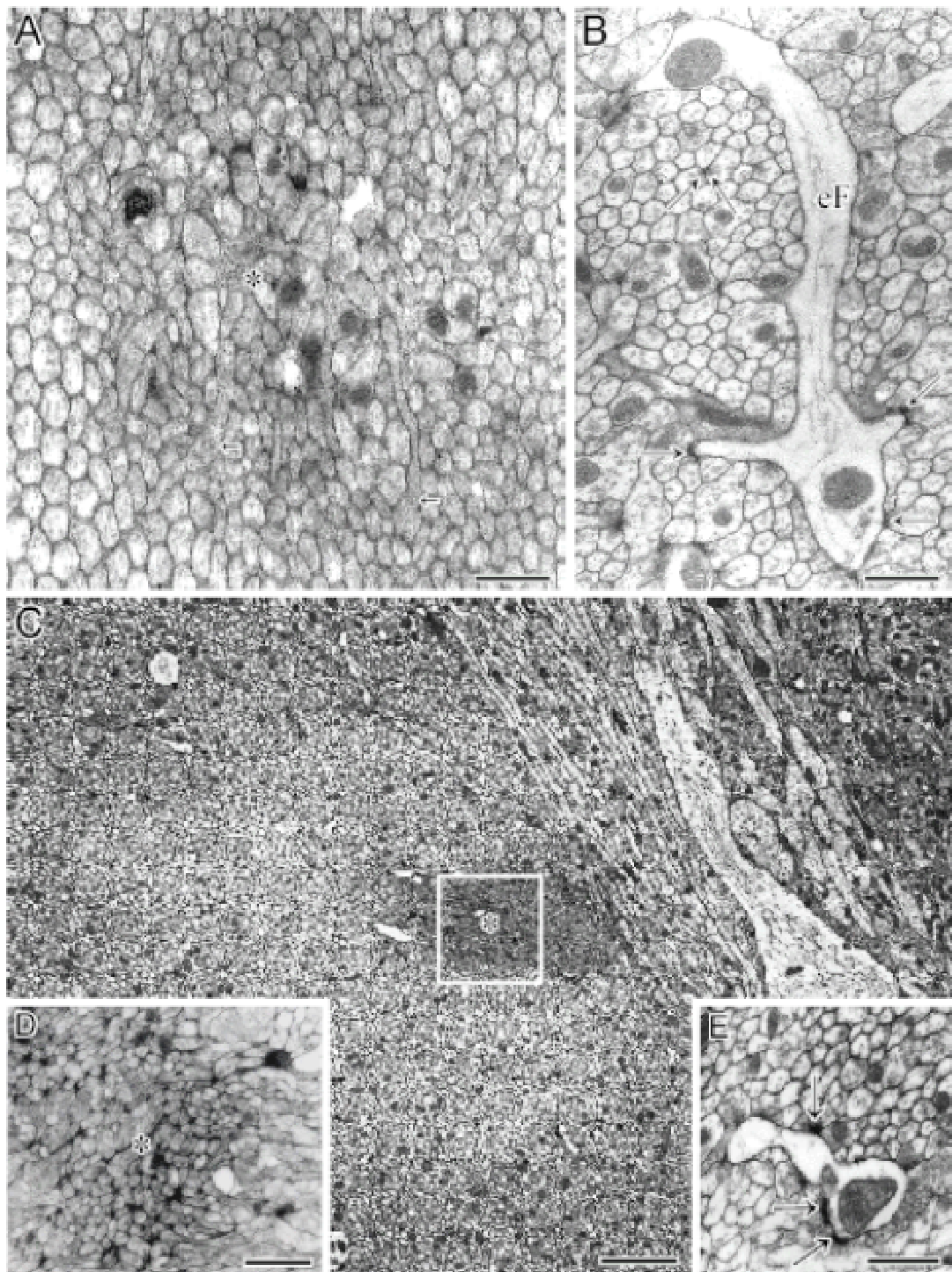


Figure 30: Fibre profiles (A, B: original micrographs; C, D: computer reconstructed fibre profiles for quantification; E: histogram of fibre profile dimensions in different stalk regions; F: histogram of tubule numbers in profiles in different stalk regions in the MB stalk (cross sections)).

A, C: Peripheral stalk area with KC III fibre profiles.

B, D: Central core with fibres of sprouting KCs.

Colour coding of fibre surface areas in C and D detected within squares of equal size ($12.25 \mu\text{m}^2$) used for measurements and counts (compare with inset in F). A series of adjacent squares from the stalk centre to its periphery (s. scheme bottom right) was analyzed.

E: Histogram showing the increase of fibre profile surfaces from the centre (arrow) to the periphery of the stalk. Note the gradual increase of mean fibre sizes along the axis from the centre to the periphery (compare with inset in F); n: number of profiles detected, error bars: \pm SE of mean profile surface area (nm^2) within a measurement square plotted versus its position along the centre to periphery stalk axis.

F: Histogram showing the distribution of tubule number per profile in different regions from the centre (arrow) to the periphery of the stalk as shown in the inset (same measurement units as in E).

Scale bar: A-D: $0.5 \mu\text{m}$

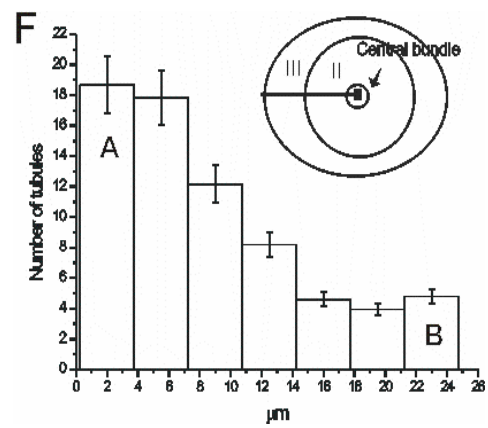
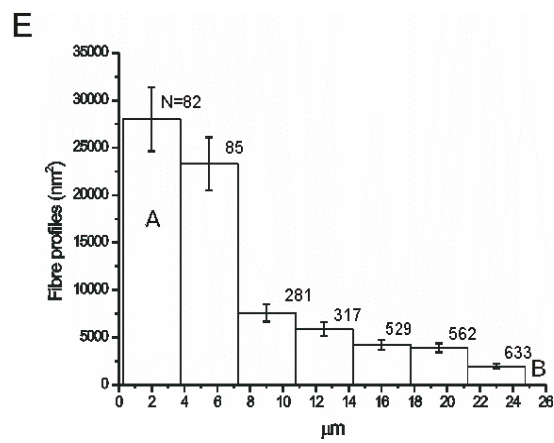
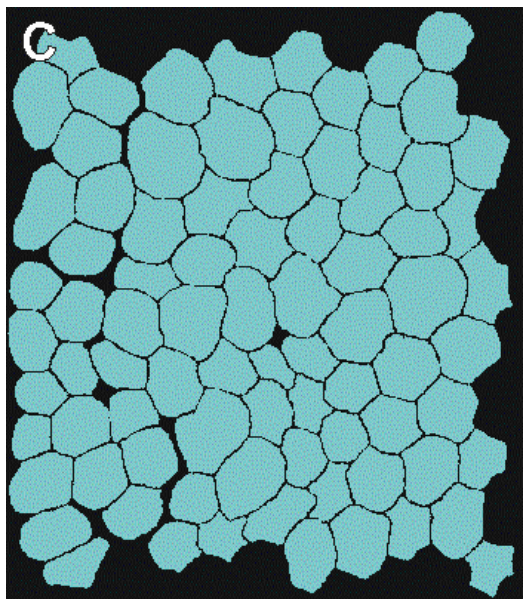
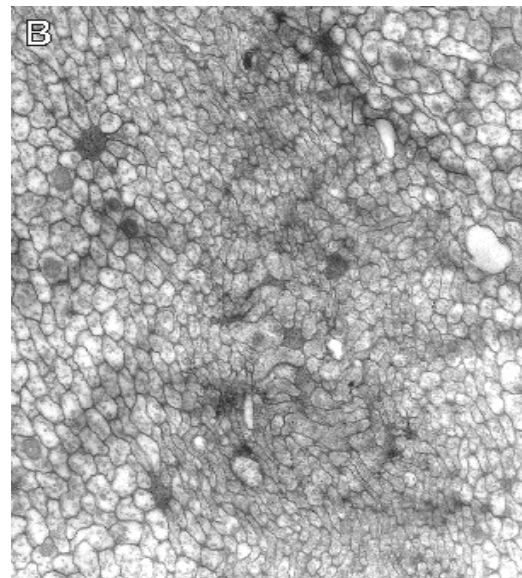
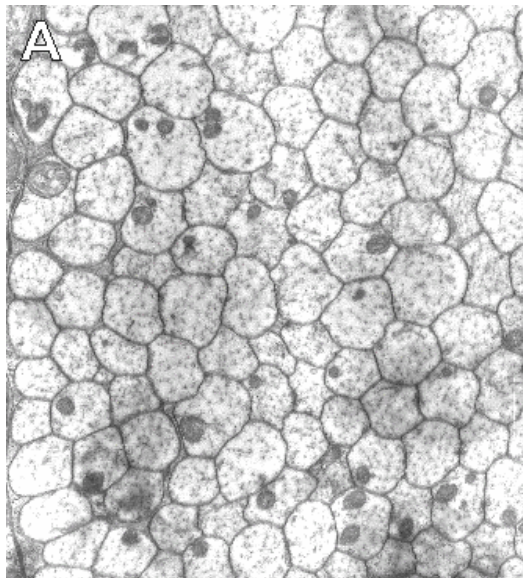


Figure 31: Fibre profiles (A, B: original micrographs; C, D: computer reconstructed fibre profiles for quantification; E: histogram of fibre profile dimensions in different alpha lobe regions (cross sections)).

A, C: Peripheral area with KC II fibre profiles and extrinsic elements in the distal alpha-lobe.

B, D: Central core with fibres of sprouting KCs.

Differential colour coding of fibre surface areas (C, D) in squares of equal size used for measurements and counts. Note the mixture of small profiles (red) and large irregularly shaped profiles of blebbed fibres filled with synaptic vesicles in B and fibre profiles with finger like projections in the central core (green colour). Samples of squares ($12.25 \mu\text{m}^2$) out of a montage of micrographs from the lobe centre to its periphery along the line given in the scheme (Fig. 30F) were used for the histogram in E.

E: Histogram showing the distribution of fibre profile surfaces from the centre (arrow) to the periphery of the alpha lobe. Note the gradual increase of mean fibre sizes along the axis from the centre to the periphery (compare inset in Fig. 30 F); n: number of profiles detected, error bars: +/- SE of mean profile surface area (nm^2) within a measurement square plotted versus its position along the centre to periphery stalk axis.

Scale bar: A-D: $0.5 \mu\text{m}$.

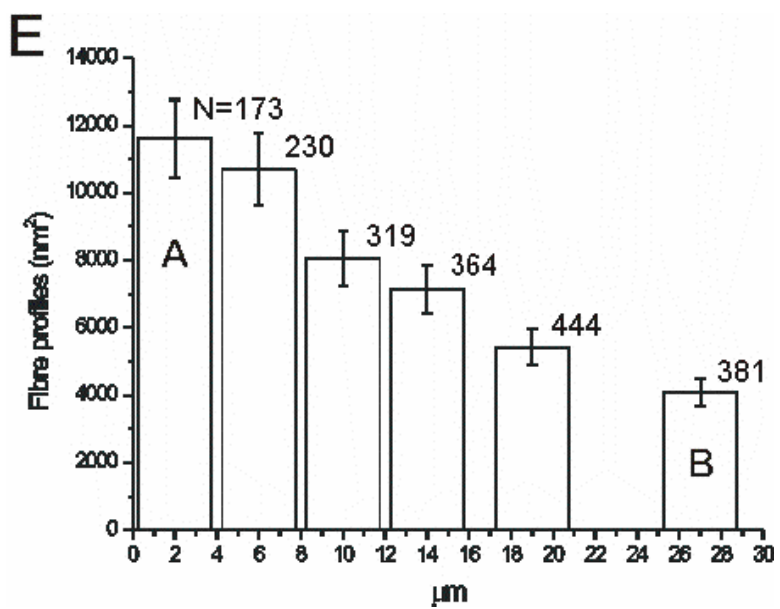
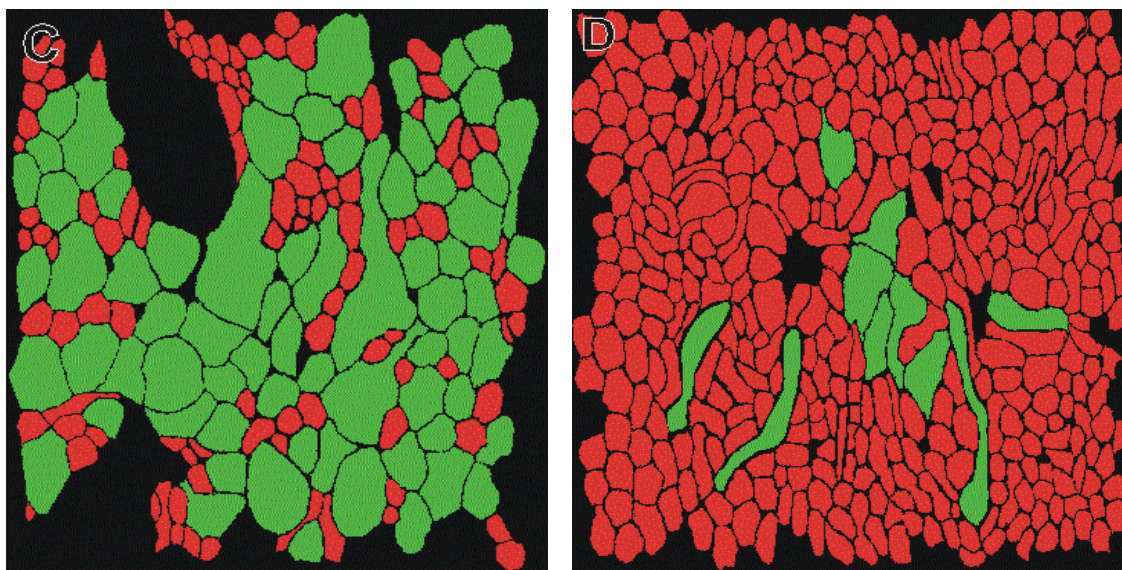
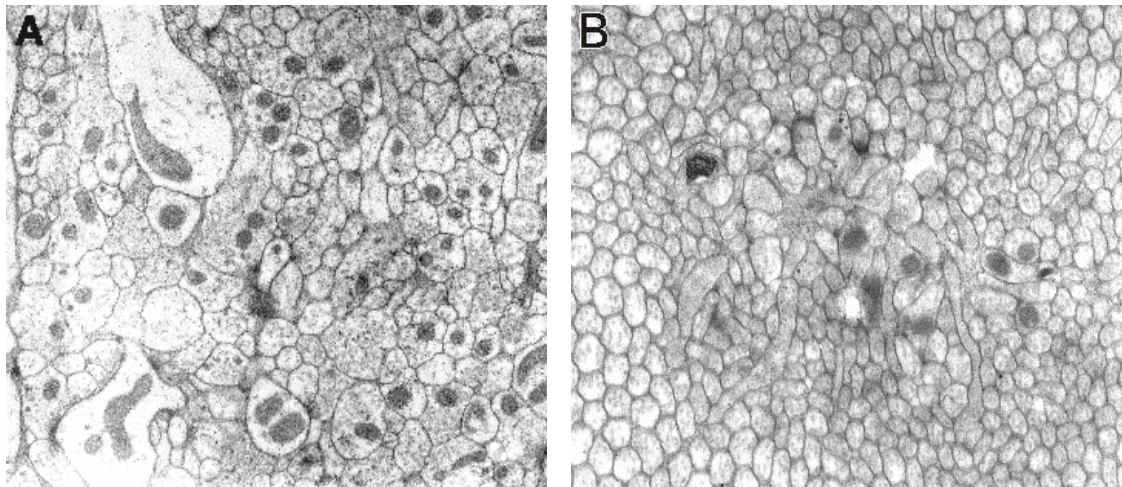


Figure 32: Differential distribution of synapses and mitochondria in MB neuropil compartments; counts from samples (squares of 9 μm^2) of a montage of micrographs along an axis from the central core to the MB periphery; cross sections of the columnar neuropil of the calyx, stalk alpha- and beta lobe; levels of sections indicated in the MB scheme, samples from one mushroom body.

A: Calyx; the central core area (arrow) is free of synapses. The numbers of synapses and mitochondria per square increase towards the periphery.

B-F: The central core area is devoid of synapses in all compartments; the amount of synapses and mitochondria is increased towards the periphery. The equipment with synapses and mitochondria varies at the different levels of sections. The counts support the view of age correlated functionalisation of KC fibres. Colour coded squares, circles and triangles indicate the numbers of synapses and mitochondria counted per square.

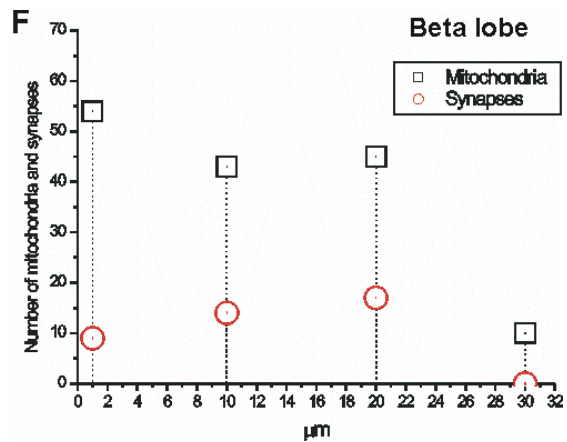
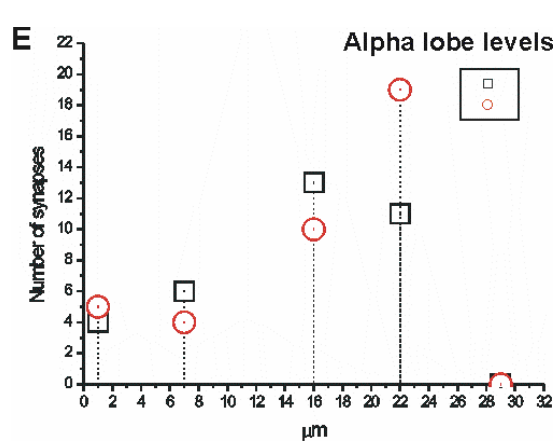
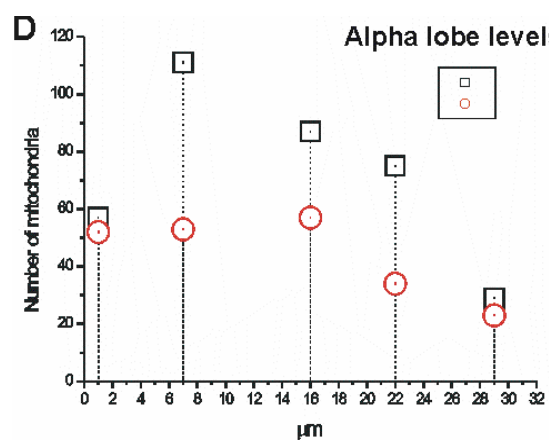
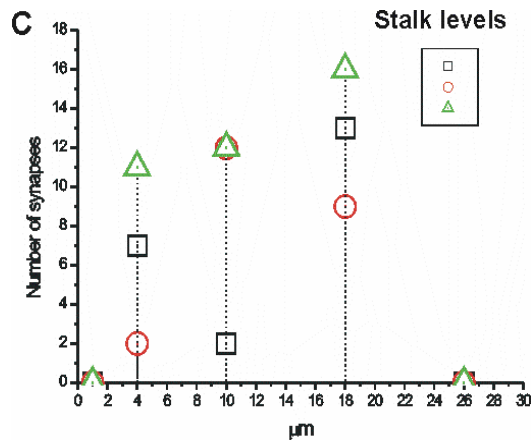
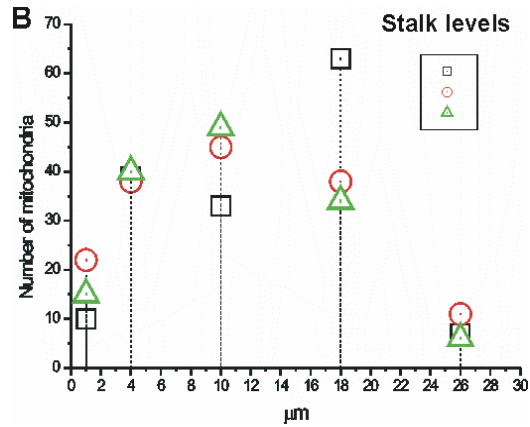
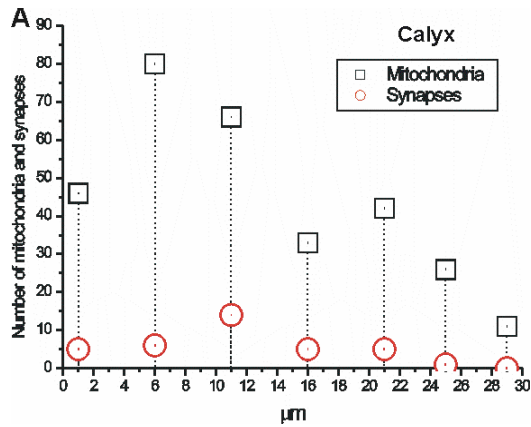
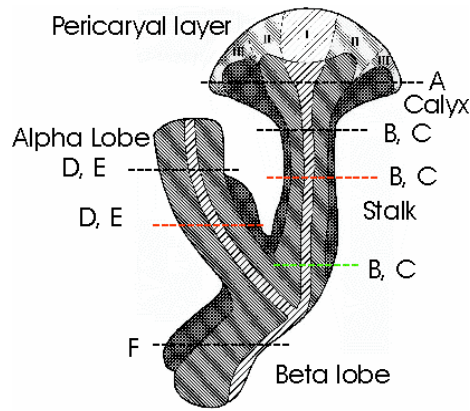


Figure 33: Degeneration in the MBs, electron micrographs (A, C-H); light micrograph of toluidine blue stained semithin section (B).

A: Degenerating KC somata (deg).

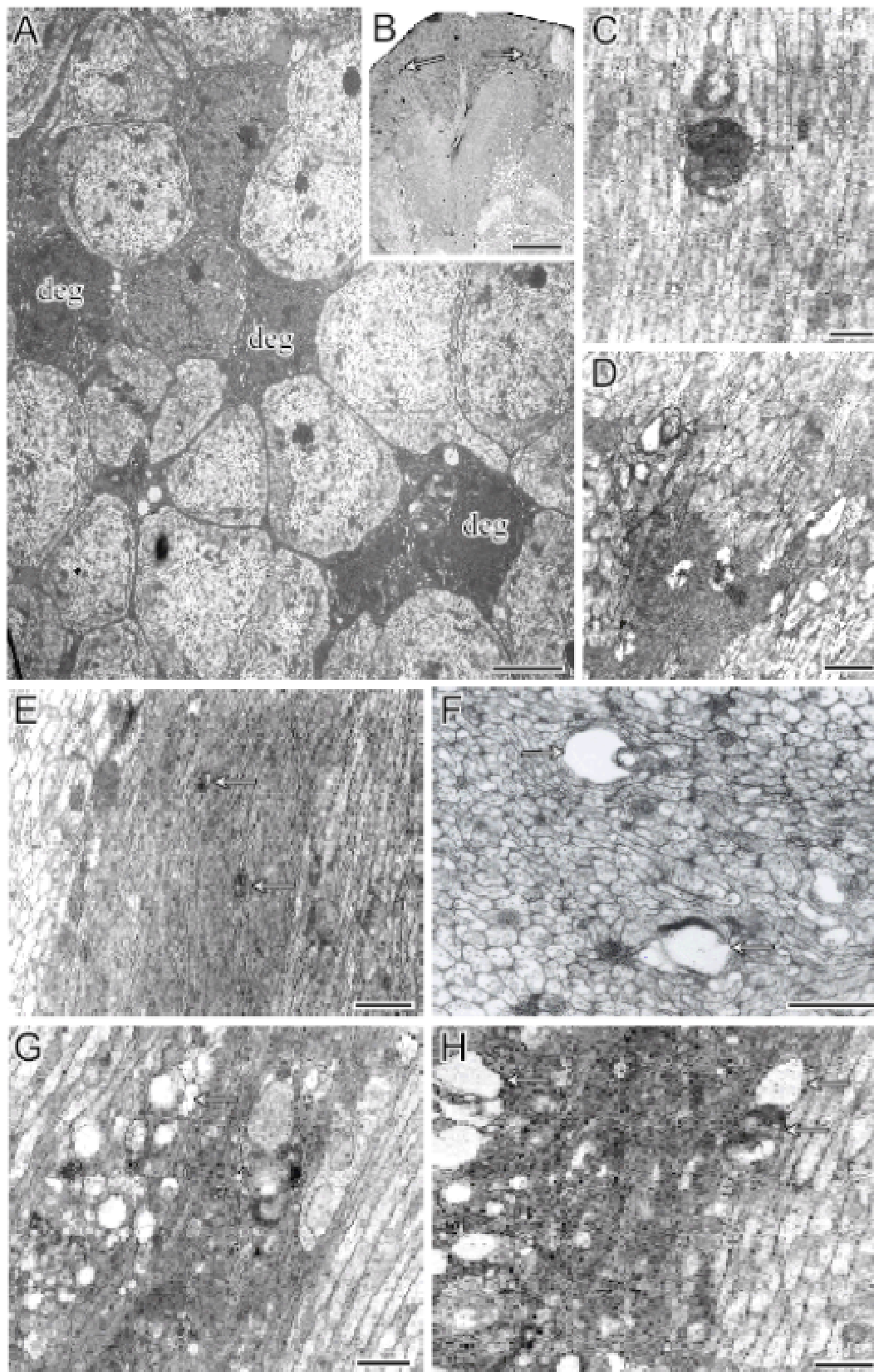
B: Degenerating KC somata (arrows) at the periphery of the anterior pericaryal rind.

C, D: Degenerating fibres (arrows) in the central core area of the anterior calyx.

E, F: Aspects of degenerating stages (arrows) in the central core of the anterior calyx.

G, H: Degeneration in the central core area of the stalk. Note empty vacuoles (arrows); sagittal sections.

Scale bars: A: 2 μm ; B: 20 μm ; C-E: 0.8 μm ; F-G: 0.5 μm .



Acknowledgments

My warmest thanks are due to my supervisor Prof. Dr. Friedrich Wilhelm Schürmann (Department of cell biology, Institute of Zoology and Anthropology, Georg-August-University, Göttingen) for the possibility to work in his department. He supported, advised and been patient with me through my study, without which this thesis would not have been possible.

I wish to thank Dr. Heribert Gras for help with confocal microscope and for writing the computer programs, which were used for quantitative study.

Thanks to Prof Dr. Michael Hörner for his help, support and encouragements.

Thanks to Prof. Dr. Dr. Detlef Schildt and Dr. Leonid Nezzlin and Mrs. Sigrid Hoyer-Fender for the opportunity to use the confocal microscopy.

Thanks to Mrs. Margret Winkler and Marion Knierim-Grenzebach for introducing electron microscopical and immunocytological methods, technical assistance as well as for advice not only concerning techniques but also for the good times in and outside the lab.

Thanks to all colleagues (Dr. Ina Frambach, Katarzyna Miskiewicz and Dr. Rolf Heblich) that I have been working with them in the department of cell biology for all help in the work and for friendship.

I like to thank my friends for their unflinching kindness and encouragements.

My parents have given me tons of love and supported me during both happy and difficult moments of my life. Special thanks also to my brother Nabel Mashaly for his support.

I dedicate this work to my wife and children who have been patient with me during the period of this work.

My special thanks to the Egyptian Government which has financed my study.

Curriculum Vitae

Name : Ashraf Mohamed Ali Mashaly
Address : Department of cell biology
Institute of Zoology and Anthropology
Berlinerstr. 28
37073 Göttingen
Date of birth : 30. Oktober 1969
Place of birth : Cairo, Egypt
Marital status : Married
Nationality : Egyptian

Education:

1987 – 1991 : B.Sc. of Entomology from the Department of Entomology, Faculty of Science, El-Zagazig University, Benha Branch, Benha, Egypt.

1994 : Diploma of Entomology from the Department of Zoology and Entomology, Faculty of Science, El-Minia University, El-Minia, Egypt

1994 - 1996 : M.Sc. from the Department of Zoology and Entomology, Faculty of Science, El-Minia University, El-Minia, Egypt (Studies on the pheromones of some myrmicine ant species).

1997 - 2000 : PhD student the Department of Zoology and Entomology, Faculty of Science, El-Minia University, El-Minia, Egypt, in the field of Insect pheromones

2000 – present : PhD student (scholarship from the Egyptian Government) at the Department of Cell Biology, Institute of Zoology and Anthropology, University of Göttingen, Göttingen, Germany.

Work experiences

1992 - 1996 : Demonstrator in the Department of Zoology and Entomology, Faculty of Science, El-Minia University, El-Minia, Egypt

1997 - present : Assistance lecturer in the same place.